The Role of Periostin in HER2/ErbB2-induced Breast Cancer

Vivian Lo

Thesis submitted to the

Faculty of Graduate and Postdoctoral Studies

in partial fulfillment of the requirements for the

Master of Science degree in Cellular and Molecular Medicine

Department of Cellular and Molecular Medicine

Faculty of Medicine

University of Ottawa

Abstract

Periostin (Postn) is a secreted cell adhesion protein that shares a structural homology to the insect axon guidance protein fasciclin 1 (FAS1). Periostin interacts with multiple cell-surface receptors, most notably integrins, which activate signaling pathways to promote cancer cell survival, angiogenesis, invasion, and metastasis. Interestingly, periostin is frequently overexpressed in numerous human cancers, including breast, lung, colon, pancreatic, and ovarian cancer. Here, we investigated the role of periostin in HER2/ErbB2-induced mammary tumorigenesis. Although periostin is primarily expressed in the stromal fibroblasts and not the epithelial cells of the mammary gland, it does not affect mammary gland outgrowth during development or pregnancy when ablated. The male FVB Postn$^{-/-}$ mice weighed less than the male FVB Postn$^{+/+}$ and Postn$^{+/-}$ mice, whereas there was no difference in weight among the female mice of all genotypes. We also demonstrate that NeuNDL Postn$^{+/-}$ mice in a mixed FVB/C57 background (Postn +/-*) did not develop tumors after 12 months, whereas NeuNDL Postn$^{+/-}$ (Postn +/-) and NeuNDL Postn$^{-/-}$ (Postn -/-) mice in a pure FVB background developed tumors by 10 months of age, similar to NeuNDL Postn$^{+/+}$ mice in a pure FVB background (Postn +/+). However, Postn +/+ tumors had a higher cellularity of tumors and appeared more dense than the cystic Postn +/- or Postn -/- tumors. *In vitro* studies with ErbB2/Neu-overexpressing primary mammary tumor epithelial cells demonstrated that the presence of periostin does not affect the cell proliferation or migration rate. In conclusion, periostin ablation affects cellularity of NeuNDL tumors and may play a role in tumor cell proliferation *in vivo*.

Table of Contents

List of Figures and Illustrations

List of Abbreviations

βig-h3	TGF-β induced gene clone 3
ABC	avidin-biotin complex
AR	amphiregulin
ATP	adenosine triphosphate
BMP	bone morphogenetic protein
bp	base pair
BTC	betacellulin
CIP	calf intestinal alkaline phosphatase
DCIS	ductal carcinoma *in situ*
ddH_2O	double distilled water
dpc	days post coitum
ECM	extracellular matrix
EGF	epidermal growth factor
EGFR	epidermal growth factor receptor
EMI	EMILIN-1
EMT	epithelial-mesenchymal transition
EPR	epiregulin
ER	estrogen receptor
FAK	focal adhesion kinase
FAS1	fasciclin 1
FVB/C57	FVB and C57Bl/6
HB-EGF	heparin-binding epidermal growth factor
HRGs	heregulins
HRP	horseradish peroxidase

LCIS	lobular carcinoma *in situ*
MAPK	mitogen-activated protein kinase
Max-Bax	marker-assisted accelerated backcrossing
MMP	matrix metalloproteinase
MMTV	mouse mammary tumor virus
NDL	Neu deletions
NRGs	neuregulins
OSF-2	osteoblast-specific factor-2
PBLs	peripheral blood lymphocytes
PCR	polymerase chain reaction
PDL	periodontal ligament
PI3K	phosphatidylinositol-3-kinase
PKB	protein kinase B
PLF	periostin-like factor
Postn	periostin
PTB	phosphotyrosine binding
PVDF	polyvinylidene fluoride
RNase	ribonuclease
RTKs	receptor tyrosine kinases
SDS	sodium dodecyl sulfate
SH2	Src homology 2
TGF-α	transforming growth factor-α
TGF-β	transforming growth factor-β
TM	transmembrane
VEGF	vascular endothelial growth factor
VEGFR	vascular endothelial growth factor receptor

Acknowledgements

This research project would not have been possible without the support of many people. First and foremost, I offer my sincerest gratitude to my supervisor, Dr. Luc Sabourin, who has helped me throughout my thesis with his invaluable knowledge, guidance, and patience. I attribute the caliber of my Masters degree to his encouragement and effort and without him this thesis, too, would not have been completed or written.

Sincere appreciation is also due to my committee chairman, Dr. Bruce McKay, and to the other member of my graduate supervisory committee, Dr. Ian Lorimer, whose knowledge and suggestions in this study helped make it a success. I am indebted to Dr. Manijeh Daneshmand for her pathology expertise and assistance, without which this project would be impossible.

A very special thank you goes out to all my colleagues, especially lab members: Marlene McKay, Roshan Sriram, Jen Quizi, Lilia Antonova, and Kyla Garbuio, for their advice and support. I would also like to thank Jeff Hamill, for his time and assistance in making the periostin adenovirus lysates.

I wish to express my love and gratitude to my beloved family for their understanding and endless love through the duration of my studies. Special thanks to my parents for supporting me and encouraging me to pursue this degree. I am grateful to all my graduate friends, especially Agnieszka, Jude, Ian, Jenn, and Matt for sharing their experience and invaluable help. Also, to all my friends who always provided support and encouragement.

Lastly, I offer my regards and blessings to all of those who supported me in any respect during the completion of the project.

1. Introduction

1.1 Breast Cancer

1.1.1 Types of Breast Cancer

Breast cancer is a clinically heterogeneous disease, the complexity of which relates to the different molecular abnormalities driving the tumor phenotype [1]. Based on distinct gene expression profiles, a novel molecular classification of breast cancer was revealed, including luminal-type (luminal A and luminal B), basal-like, normal-like, and HER2/ErbB2 positive, which all have different prognosis and therapeutic responses [2, 3]. The basal-like subgroup is mostly estrogen receptor (ER) negative, the HER2/ErbB2 positive subgroup is mostly HER2/ErbB2 amplified and ER negative, and the luminal-type subgroup is ER positive [1, 4]. The basal-like and HER2/ErbB2 positive subgroups are more aggressive, resulting in a shorter relapse-free period and a shorter overall survival than the luminal-type subgroup [1, 4]. However, in terms of treatment responsiveness, basal-like and HER2/ErbB2 positive subgroups respond better to chemotherapy, while the luminal-type subgroup is more sensitive to endocrine therapy [1, 4]. As a result, treatment should be tailored to the appropriate breast cancer subgroup [4].

The TNM classification of malignant tumors is a cancer staging system based on the extent of the tumor (T), lymph node involvement (N), and the presence of metastasis (M) [5]. Once the pathologist knows the T, N, and M characteristics, they are combined in a process called stage grouping, in which an overall stage is assigned [5]. Stage 0 is used to describe non-invasive breast cancers, such as lobular carcinoma *in situ* (LCIS) and ductal carcinoma *in situ* (DCIS). Stage I is characterized by early-stage invasive breast cancer [5]. Stage II is divided into two subcategories known as IIA and IIB, both correspond to early-stage invasive breast cancer [5]. Stage III is separated into three subcategories known as IIIA, IIIB, and IIIC, which

represent locally advanced breast cancer [5]. Inflammatory breast cancer is considered at least stage IIIB [5], is relatively rare, and is characterized by diffused erythema and edemas referred to as peau d'orange, where there is no palpable mass, poor nuclear grade, negative hormone-receptor status, and poor survival outcome [6]. Stage IV is metastatic breast cancer, in which the cancer has spread to other organs of the body, usually the lungs, liver, bone, or brain [5].

1.1.2 Treatment of Breast Cancer

Historically, the prognosis and the selection of adjuvant systemic therapy or treatment in early breast cancer has relied on risk assessment incorporating both patient-related and tumor-related prognostic factors [4]. Patient-related factors include age, menopausal status, and co-morbidities, whereas tumor-related factors include lymph node involvement, tumor size, tumor grade, and ER or HER2/ErbB2 status [4]. Tumor grades 1-3 correspond to well-differentiated, moderately-differentiated, or poorly differentiated tumors, referring from low to high grade tumors [7].

Primary or local therapy is the main treatment used to reduce or eliminate the cancer and usually includes surgery such as a mastectomy, where the whole breast is removed, or a lumpectomy, where the tumor and a small amount of the normal tissue around it is removed, and is a type of breast-conserving surgery [8]. Radiation therapy, another local therapy, is usually given after breast-conserving surgery and may be given after a mastectomy to kill cancer cells that may be left in tissues next to the breast, such as in the chest wall or nearby lymph nodes [8]. Most cancer patients with early-stage breast cancer receive adjuvant therapies, which is any treatment given after primary therapy to increase the chance of long-term disease-free survival [8]. Most adjuvant therapies are systemic and travel through the bloodstream, reaching and affecting cancer cells all over the body. These include chemotherapy, endocrine therapy, tissue-targeted therapies, or a combination of treatments [8].

They enhance local therapy, substantially decreasing cancer recurrence and disease-specific death [6].

1.1.3 Targeted Therapies for Breast Cancer

Increased understanding of the molecular events involved in cancer development has led to the identification of a large number of novel targets [9]. Targeted therapy focuses on specific molecules in the malignant cell signal transduction machinery, including crucial molecules involved in cell invasion, metastasis, apoptosis, cell cycle control, and tumor-related angiogenesis [9]. More than 50% of all major drug targets are membrane proteins [10].

The HER2/ErbB2 proto-oncogene is amplified and overexpressed in 20-30% of human breast cancers, and its overexpression is correlated with poor prognosis [11, 12]. This is due to shorter disease-free intervals with increased rates of recurrence, increased tumor aggressiveness and metastasis, increased resistance to many types of therapy, and increased mortality [11-14]. Since HER2/ErbB2 is a cell-surface protein, it is easily accessible to drugs, and as a kinase, it is amenable to targeted inhibition by small molecules [1].

One anti-HER2/ErbB2 receptor therapeutic strategy is the generation of small molecules that compete with adenosine triphosphate (ATP) for binding to the receptor kinase pocket, thus blocking receptor activation and the transduction of downstream signals. Another strategy utilizes humanized monoclonal antibodies, such as Herceptin, generated against the receptors' extracellular domain, thus blocking the dimerization with other HER/ErbB receptors and inducing receptor endocytosis and downregulation [15]. Inhibition of HER2/ErbB2 activity with antagonistic antibodies, small molecule kinase inhibitors, or inducers of HER2/ErbB2 degradation, have shown that blockage of HER2/ErbB2 signaling leads to the reversal of most HER2/ErbB2 tumorigenic features, identifying it as a potential therapeutic target [1, 16].

1.2 HER/ErbB Receptors

1.2.1 HER/ErbB Receptor Family

The HER/ErbB family of receptor tyrosine kinases (RTKs) is important in the transduction of extracellular cues into intracellular signals that allow a cell to adjust to its environment [1, 17]. They are expressed in various tissues of epithelial, mesenchymal, and neuronal origin [1, 17]. Therefore, they are essential for the embryonic development of the nervous system, cardiovascular system, gastrointestinal system, and other organ systems, as well as biological processes such proliferation, differentiation, migration, and apoptosis [1, 17, 18].

The epidermal growth factor receptor (EGFR) or HER/ErbB family of RTKs, includes four members, EGFR/HER1/ErbB1, HER2/ErbB2/Neu, HER3/ErbB3, and HER4/ErbB4. All the HER/ErbB receptors are transmembrane proteins, sharing an extracellular epidermal growth factor (EGF)-like ligand-binding domain composed of two cysteine-rich domains (II and IV) interspersed with unique domains (I and III), a single α-helix transmembrane domain, an intracellular region comprised of a well conserved tyrosine kinase domain, and a divergent number of regulatory carboxyl-terminal tyrosine residues (Figure 1) [1, 18].

Domains I and III can form a binding site for the receptor's potential ligands [19], while domains II and IV are involved in dimerization between two identical HER/ErbB receptors (homodimerization) and between two different HER/ErbB receptors (heterodimerization) [20]. Domain II contains a dimerization arm, which is generally believed to be the main contributor for dimerization [21]. It consists of a protruding short hairpin loop that can contact the dimerization arm of its partner [21].

Ligand binding activates the HER/ErbB receptor, then induces homodimerization or heterodimerization, which enables the kinase domains to cross-phosphorylate the carboxyl-terminal tyrosine residues on the dimerization partner [22, 23]. Once these residues are

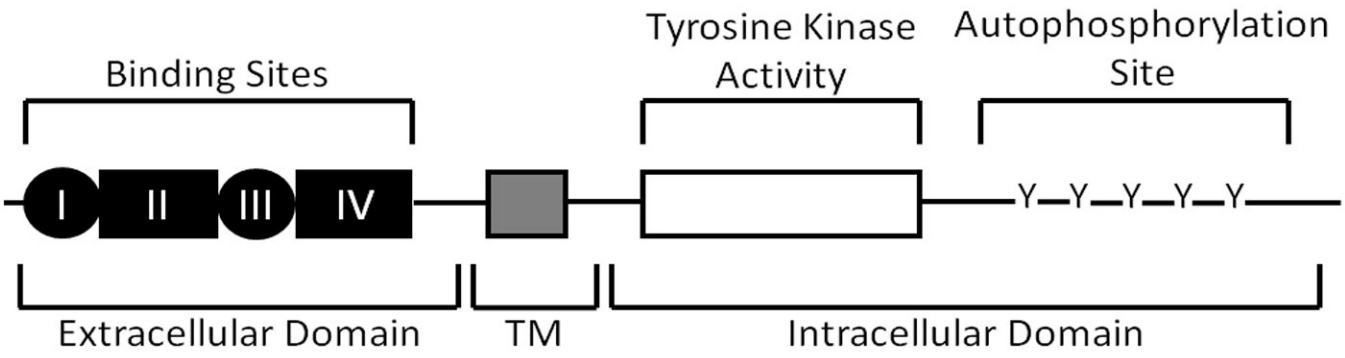
Binding Sites
Tyrosine Kinase Activity
Autophosphorylation Site
I
II
III
IV
Y
Y
Y
Y
Y
Extracellular Domain
TM
Intracellular Domain

Figure 1: Schematic representation of the receptor tyrosine kinase, *ErbB2*. At the amino-terminal is an extracellular domain (black). In the middle is a single transmembrane (TM) domain (grey) that has extensive homology to the epidermal growth factor receptor. At the carboxyl-terminal is an intracellular domain (white). The TM domain separates a catalytically active intracellular kinase domain from an extracellular ligand-binding domain. HER2/ErbB2 encodes a 185 kDa, 1255 amino acid protein. Within the extracellular domain, the roman numerals represent subdomains I-IV, the circles (domain I and III) represent potential ligand-binding domains, and the rectangles (domain II and IV) represent cysteine-rich EGF-like ligand-binding domains for heterodimerization or homodimerization. Within the intracellular domain, the Y represents the five tyrosine autophosphorylated residues, which are Y1023, Y1139, Y1196, Y1221/1222, and Y1248 [17]. Adapted from Sliwkowski, 2003.

phosphorylated, they serve as recognition sites for phosphopeptide binding adaptors and signaling proteins, whose recruitment leads to the activation of intracellular pathways, including the mitogen-activated protein kinase (MAPK) and the phosphatidylinositol-3-kinase (PI3K) pathways (Figure 2) [24].

1.2.2 HER/ErbB Receptor Ligands

Activation of the family of HER/ErbB receptors is controlled by spatial and temporal expression of its ligands, members of the EGF-related ligand growth factor family [25, 26]. There are a number of HER/ErbB-specific ligands, each of which contains an EGF-like domain that confers binding specificity [16]. These ligands can be divided into three groups. The first group includes EGF, amphiregulin (AR), and transforming growth factor-α (TGF-α), which binds specifically to EGFR/HER1/ErbB1. The second group includes betacellulin (BTC), heparin-binding EGF (HB-EGF), and epiregulin (EPR), which binds both EGFR/HER1/ErbB1 and HER4/ErbB4. The third group is composed of the neuregulins (NRGs), which are also known as heregulins (HRGs), and contains two subgroups based on their ability to bind HER3/ErbB3 and HER4/ErbB4 (NRG-1 and NRG-2) or only HER4/ErbB4 (NRG-3 and NRG-4) [16, 25, 27].

HER2/ErbB2 and HER3/ErbB3 are unique because none of the EGF family of ligands binds to HER2/ErbB2 directly, while HER3/ErbB3 does not have intrinsic kinase activity [28]. However, HER2/ErbB2 constitutively adopts an extended or active state, exposing the dimerization arm in a ligand-independent manner, making it constantly poised for interaction and the preferred heterodimerization partner for all other HER/ErbB receptors [1, 29]. These HER2/ErbB2 containing heterodimers are responsible for strong and prolonged activation of downstream signaling pathways [30, 31]

1.2.3 HER/ErbB Receptor Signaling Adaptors

Activation of the intracellular kinase domain, through the phosphorylation of carboxyl-terminal tyrosines on HER/ErbB receptors, triggers the association of specific signaling

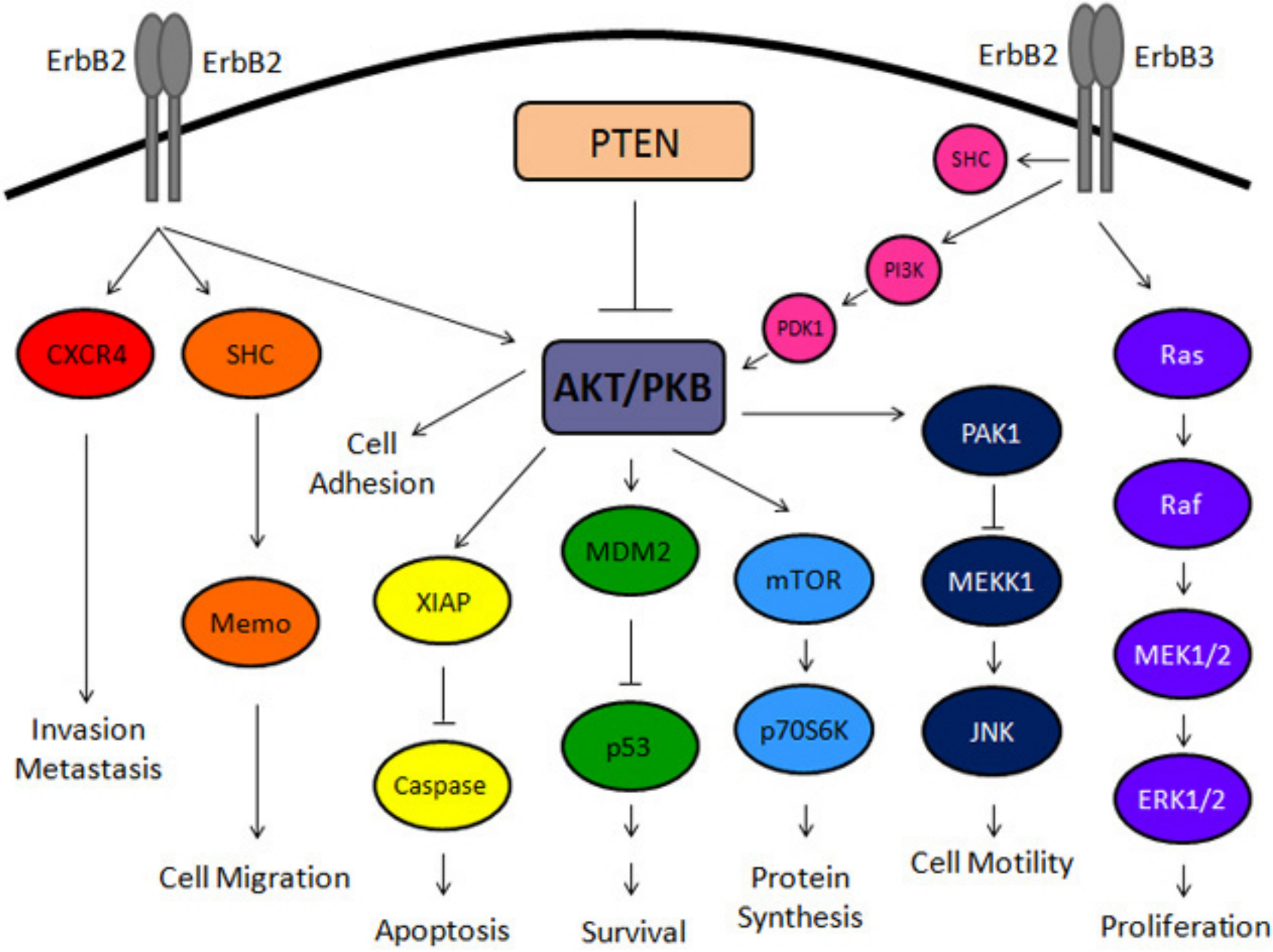
ErbB2
ErbB2
ErbB2
ErbB3
PTEN
SHC
PI3K
PDK1
CXCR4
SHC
AKT/PKB
Ras
Cell
Adhesion
PAK1
Raf
MDM2
XIAP
mTOR
MEKK1
MEK1/2
Memo
p53
p70S6K
JNK
ERK1/2
Invasion
Metastasis
Caspase
Cell Migration
Apoptosis
Survival
Protein
Synthesis
Cell Motility
Proliferation

Figure 2: The signaling of ErbB2 is activated through homodimerization and heterodimerization, which transmits growth factor activation signals to multiple downstream signaling pathways. The HER/ErbB receptors are well known mediators of cell proliferation, migration, differentiation, apoptosis, and metastasis. HER2/ErbB2 is often overexpressed, amplified, or mutated in cancers, making it an important therapeutic target. Adapted from Yarden Y, Shilo BZ, 2007.

molecules, whose binding initiates downstream signaling events [32]. Each of the four HER/ErbB receptors has a different set of phosphorylation sites and recruits different combinations of signaling molecules, such as Src homology 2 (SH2) and phosphotyrosine binding (PTB) domain-containing molecules [17, 24, 27, 33]. Known SH2 and PTB domain-containing proteins that interact with HER/ErbB receptors include adaptor proteins (Crk, Gab1, Grb2, Grb7, and Shc), protein and lipid kinases (Src and PI3K), protein phosphatases (SHP1 and SHP2), and phospholipase Cγ [17]. Only HER3/ErbB3 efficiently activates PI3K due to multiple coupling sites on HER3/ErbB3 for the PI3K regulatory subunit, p85, but this depends on heterodimerization of HER3/ErbB3 with the constitutively active HER2/ErbB2 [34, 35].

1.2.4 HER/ErbB Receptor Signaling Pathways in Cancer

Cancer cells evade contact inhibition, cell cycle checkpoints, and apoptosis [36]. The transforming capacity of HER2/ErbB2 is associated with its overexpression, generally due to gene amplification [16]. Overexpression of HER2/ErbB2 disrupts the regulators of the G1/S transition and other cell cycle checkpoints to increase cell proliferation of tumor cells through HER2/ErbB2-dependent pathways, such as Ras/Erk, p38 MAPK, and PI3K [1]. Overexpression of HER2/ErbB2 has been shown to occur in a significant portion of breast [37], ovarian [38], bladder [39], gastric [40], and other human malignancies.

Avoiding cell death is an essential trait acquired during the malignant process [41]. A main effector of HER/ErbB signaling, the PI3K/Akt/protein kinase B (PKB) signaling pathway is particularly important in mediating cell survival since several Akt/PKB substrates directly control various apoptotic processes [32]. For growth beyond a certain size, the primary tumor must improve its oxygen and nutrient supply through the formation of new blood vessels in a process known as angiogenesis. HER/ErbB receptors have been associated with tumor cell production of proangiogenic factors, the most significant being vascular endothelial growth factor (VEGF) [42]. Breast and lung cancer cell lines with constitutive HER2/ErbB2 activation show elevated

VEGF mRNA levels, and the addition of heregulin to these cultures further increases VEGF transcription in a MAPK-dependent manner [43-45]. Furthermore, treatment of HER2/ErbB2-overexpressing tumor cells with a monoclonal antibody that interferes with the HER2/ErbB2 receptor decreases expression of proangiogenic factors, including VEGF and TGF-α, resulting in a dramatic change in the tumor vasculature and a decrease in tumor size [46].

The final step of cancer progression involves tumor cells leaving the site of primary growth and forming metastases. For tumors to metastasize, the cells must possess certain characteristics, including the ability to migrate and invade the surrounding basement membrane and distant tissues. The functional inactivation of HER2/ErbB2 blocks EGF-, BTC-, and HRG-induced breast cancer cell migration [47]. HER2/ErbB2-containing heterodimers promote strong activation of the MAPK and PI3K pathways known to have important roles in promoting cell migration.

Motile cancer cells must also have the ability to invade the surrounding basal membrane to acquire full metastatic potential, a process requiring proteolytic activity [16]. HER2/ErbB2 cooperates with hepatocyte growth factor [48] and TGF-β [49, 50] to promote an invasive phenotype. HRG treatment of breast cancer cells demonstrated an increase expression of matrix metalloproteinase (MMP)-9 [51], as well as serine protease uPA and its receptor [52], leading to increased invasion. HER2/ErbB2 can also contribute to several distinct capabilities required to complete tumorigenesis [41].

Interestingly, EGFR/HER1/ErbB1 is a target for mutations and deletions in the extracellular or intracellular domain, some of which promote constitutive kinase activity in the absence of ligands to drive tumor cell proliferation [16, 53]. TGF-α is frequently co-expressed with EGFR/HER1/ErbB1 in non-small cell lung cancer [54], prostate cancer [55], gastrointestinal stromal tumors [56] and significantly correlates to worse patient prognosis in invasive breast carcinomas [57].

1.3 Mouse Models for Studying Breast Cancer

1.3.1 NeuNT: An Activated Neu Point Mutant

Transgenic mice represent a useful model with which to assess the tissue-specific action of oncogenes *in vivo* [58-62]. Researchers have used the mouse mammary tumor virus (MMTV) promoter/enhancer to target high level expression of several oncogenes in the ductal and alveolar luminal epithelial cells and myoepithelial cells of the mammary epithelium at all stages of mammary gland differentiation (Figure 3) [58, 60, 63, 64].

The *Neu* oncogene was first identified in transfection experiments using genomic DNA isolated from chemically induced rat neuroblastomas [65, 66]. Oncogenic activation of *Neu*, the rat homologue of mouse *ErbB2* and human *HER2*, occurs as a result of high level overexpression [67-69], deletion of the extracellular domain [70], or a single point mutation in the transmembrane domain [71, 72], causing an increase in ligand-independent tyrosine kinase activity [73-76].

To study the role of Neu in mammary tumorigenesis and tumor progression *in vivo*, several strains of transgenic mice for *Neu* under the control of the MMTV promoter/enhancer have been engineered to recapitulate the initial events of HER2/ErbB2-induced mammary tumorigenesis [77-82]. The first transgenic mouse model to express an activated form of rat *Neu* (NeuNT) consisted of a single amino acid substitution in the transmembrane domain, which converts a valine residue to glutamic acid (MMTV-*NeuNT*) [72, 80]. The mammary gland-specific expression of the activated *Neu* transgene in female mice initially resulted in a lactation defect. In every transgenic mouse, male and female, there was also the spontaneous appearance of mammary tumors as a result of rapid conversion of the epithelium to a malignant phenotype within 3 months [79, 80].

In addition, pulmonary metastases were observed in transgenic mice carrying the MMTV-*NeuNT* transgene [80]. However, metastasis in these mice was relatively infrequent

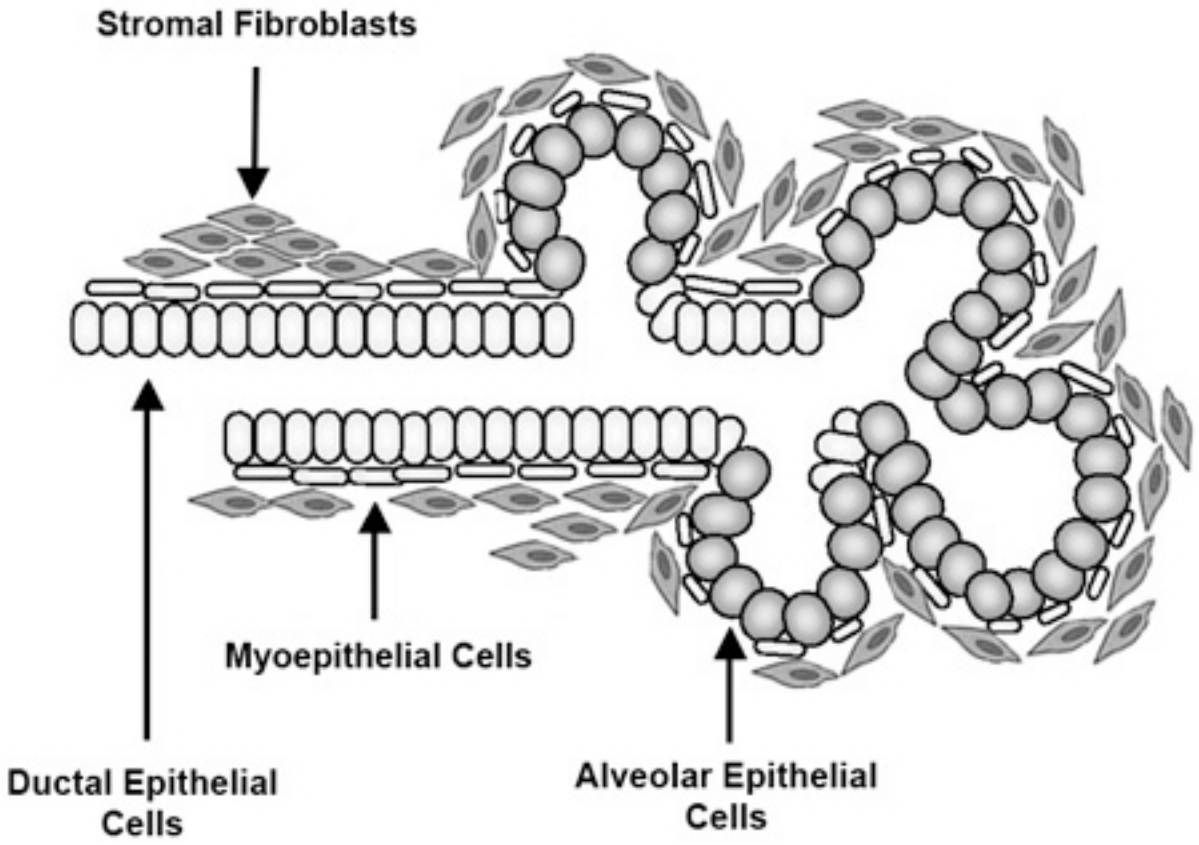
Stromal Fibroblasts
Myoepithelial Cells
Ductal Epithelial Cells
Alveolar Epithelial Cells

Figure 3: Schematic view of the ductal and alveolar epithelial cells during midpregnancy. The ducts are surrounded by a basal layer of overlapping myoepithelial cells, whereas the alveolar cells are surrounded by a basket-like layer of myoepithelial cells. Stromal fibroblasts surround the epithelial cells. Adapted from Woodward et al., 2005.

because these activated *Neu* tumors involved the entire mammary epithelium and this considerably shortens the animals' survival, preventing metastasis from occurring [78].

Histological analysis of these MMTV-*NeuNT* tumors and surrounding tissues revealed the complete absence of any morphologically normal mammary epithelium [80]. Therefore, overexpression of activated *Neu* is sufficient to efficiently transform mammary epithelial cells in transgenic mice [58]. Although increased mammary gland-specific expression of activated *Neu* is sufficient to induce mammary tumorigenesis in mice, there was no evidence for comparable activating mutations in primary human HER2/ErbB2-positive breast cancers [79, 83].

1.3.2 Neu: A Wildtype Neu

In order to determine whether the overexpression of the wildtype *Neu* proto-oncogene would also promote mammary tumorigenesis, MMTV-*Neu* transgenic mice were established [78]. These mice developed focal mammary tumors with a latency period of 7 months [78]. Histological examinations of the tumors revealed focal mammary carcinomas surrounded by hyperplastic mammary epithelium [78]. In MMTV-*Neu* mice, the expression of wildtype *Neu* in the mammary epithelium leads to the development of metastatic disease, as evidenced by the development of lung metastases [78]. Upon further analysis, most of the mammary tumors harbored in-frame deletions or insertions of cysteine residues within the *Neu* extracellular domain, resulting in constitutive dimerization through the formation of intermolecular disulphide bridges [84, 85].

The tumor progression of mice carrying the MMTV-*NeuNT* transgene were different from those carrying the MMTV-*Neu* transgene [78]. Mammary gland-specific expression of the activated *Neu* oncogene in this strain was associated with the rapid and synchronous development of multifocal mammary tumors and an absence of normal mammary epithelium [80]. The expression of activated *Neu* was sufficient for mammary tumorigenesis, but the expression of wildtype *Neu* is not since normal mammary epithelium adjacent to the tumors also

expresses significant levels of the wildtype Neu protein [78]. It is likely that differences in the activity of the *Neu* tyrosine kinase in transgenic mice, either the activated or wildtype *Neu* transgene, account for this phenotypic variation [58].

1.3.3 NeuNDL: An Activated Neu Deletion Mutant

The mammary epithelial expression of activated *Neu* receptors, which harbored distinct in-frame *Neu* deletions (NDL) within the extracellular domain, under the control of the MMTV promoter (MMTV-*NeuNDL*), resulted in the rapid induction of mammary tumors within the fat pad [86]. Quantitative phosphorimager analysis revealed that the major sites of transgene expression in female carriers included the mammary and salivary glands, while lower levels were also observed in the lungs and ovaries [86]. In male carriers, transgene expression was detected in the salivary glands and reproductive organs, such as the epididymis, seminal vesicles, and testes [86].

The MMTV-*NeuNDL* transgenic mice developed mammary tumors faster than observed in the MMTV-*Neu* mice [86]. Histologically, these tumors are similar to those described for both point mutation activated [80] and wildtype *Neu* expressing mice [78], appearing as nodular masses amongst hyperplastic and dysplastic tissue [86]. Furthermore, mammary gland tumors from MMTV-*NeuNDL* virgin female mice expressed HER2/ErbB2 protein that was constitutively tyrosine phosphorylated and active [86]. However, the penetrance of this phenotype was incomplete, with approximately 80% of NDL transgene carriers developing mammary tumors prior to one year of age [86]. Mammary epithelial-specific expression of these activated in-frame deletions of *Neu* resulted in the efficient induction of metastatic mammary carcinomas [86]. MMTV-*NeuNDL* females showed lung metastases which originated from the mammary gland [86]. Interestingly, several studies have reported the expression of an alternatively spliced human HER2/ErbB2 isoform, encoding a 16 amino acid in-frame deletion in the juxtamembrane

domain that closely resembles the in-frame deletion in the *Neu* transgene-derived somatic mutations [86, 87].

Two other HER/ErbB family members, EGFR/HER1/ErbB1 and HER3/ErbB3, are overexpressed in MMTV-*NeuNDL* derived mammary tumors [86]. HER3/ErbB3 is overexpressed in both invasive and non-invasive HER2/ErbB2-positive human breast tumors [88]. Therefore, heterodimerization of HER2/ErbB2 with EGFR/HER1/ErbB1 and HER3/ErbB3 is likely to represent an additional mechanism for activating the HER2/ErbB2 receptor tyrosine kinase in HER2/ErbB2-positive breast cancers [58].

Current transgenic mouse models of HER2/ErbB2-positive breast cancer have significantly advanced our understanding of how HER2/ErbB2 contributes to disease progression and poor prognosis [58]. These MMTV-based *Neu* transgenic mouse models have identified many target genes that control cell cycle and survival, which function downstream of, or in concert with, HER2/ErbB2 to promote breast cancer progression [58]. These genes can be used both as diagnostic tools and for the development of new adjuvant therapeutics to better combat the disease and increase patient survival [58]. In addition, transgenic mouse models have helped to develop and test the efficacy of current drug therapies and tumor vaccines in the treatment of breast cancer [58].

1.4 Periostin

1.4.1 Structure and Expression

Periostin (Postn), also designated osteoblast-specific factor-2 (OSF-2), is a disulfide-linked, secreted cell adhesion protein that was originally isolated as an osteoblast- and mesenchyme-specific factor, and is believed to be involved in osteoblast recruitment, attachment, and spreading [89, 90]. Its structure consists of a typical amino-terminal secretory signal sequence, a cysteine-rich domain, four internal homologous repeat regions, and a carboxyl-terminal hydrophilic domain (Figure 4) [89]. It lacks a typical transmembrane domain

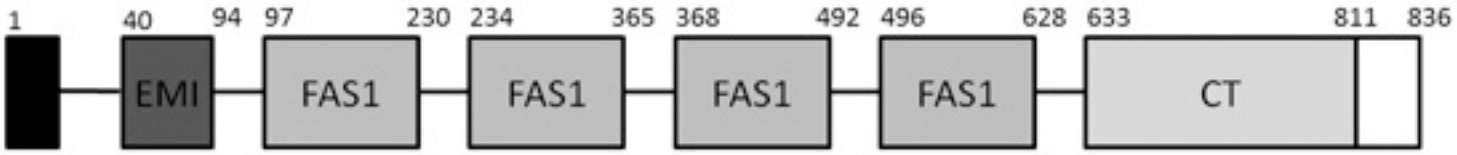
1
40
94
97
230
234
365
368
492
496
628
633
811
836
EMI
FAS1
FAS1
FAS1
FAS1
CT

Figure 4: Schematic structure of *periostin*. At the amino-terminal is the signal peptide (black) and at the end of the carboxyl-terminal is the heparin binding motif (white). The EMILIN-1 (EMI) domain is a small cysteine-rich domain, which is followed by four fasciclin 1 (FAS1) domains. CT represents the carboxyl-terminal domain. Adapted from Kudo et al., 2007.

[89]. The four internal repeat regions in *periostin* are homologous to the insect axon guidance protein fasciclin 1 (FAS1) [89]. Thus, periostin belongs to the family of fasciclin genes, which also includes βig-h3 (TGF-β induced gene clone 3), MBP-70, Algal CAM, periostin-like factor (PLF), stabilin-1, and stabilin-2 [91, 92].

The murine and human periostin genes are located on chromosome 3 and chromosome 13q, respectively [93]. Murine *periostin* has four different isoforms, while human *periostin* has five different isoforms due to alternative splicing that occurs within the carboxyl-terminal domain resulting in in-frame deletions or insertions [89]. Murine and human *periostin* display an homology of 89.2% over the entire protein and 90.1% for the mature form [89]. As a result, *periostin* is highly conserved between the two species, suggesting that their function is likely to be conserved.

Periostin is primarily expressed in collagen-rich fibrous connective tissues that are subjected to constant mechanical stresses, such as in the periosteum and periodontal ligaments, where it functions in the formation and structural maintenance of bones and teeth [89, 90]. Periostin mRNA is expressed in a wide range of normal tissues, but is negligible in peripheral blood lymphocytes (PBLs) and spleen, and is very low in salivary gland and thymus [94]. In normal breast and skin tissue samples, the expression of periostin varies significantly, but is characterized as high [94]. In general, tissues with low fibroblast content, including PBLs, spleen, pancreas, or liver, show reduced periostin expression compared to fibroblast-rich tissues like skin or breast [94]. Therefore, fibroblasts may be the source of periostin expression.

Supporting this observation, the level of periostin expression was often undetectable in immortalized cell lines derived from normal mammary epithelial cells [95]. In breast tumor tissues, known to contain both epithelial cancer cells and cancer-associated fibroblasts or tumor stromal cells, periostin was highly expressed in the stromal cells immediately surrounding the tumor, but not within the breast cancer cells themselves [37]. Interestingly, periostin is also overexpressed in various types of human cancer, including breast cancer [95], colon cancer

[96], head and neck cancer [97], nasopharyngeal carcinoma [98], neuroblastoma [99], non-small cell lung carcinoma [100], ovarian cancer [101], pancreatic ductal adenocarcinoma [102], and thyroid carcinoma [103]. Surprisingly, serum periostin levels are elevated in breast cancer patients with bone metastasis, but not in lung cancer patients with bone metastasis [37].

1.4.2 Periostin and Development

The integrity of the extracellular matrix (ECM) is essential for maintaining the normal structure and function of connective tissues [104]. The ECM is secreted locally by cells and organized into a complex meshwork providing physical support to cells, tissues, and organs [104]. Matricellular proteins are a class of ECM-related molecules that modulate cell-matrix interactions [104]. They are expressed at high levels during development, but typically only appear in postnatal tissue during wound repair or disease, where their levels increase substantially [104]. Periostin is a matricellular protein because of its expression pattern and function during development as well as in wound repair [104]. It directly binds many ECM proteins such as collagen, fibronectin, tenascin-C, and periostin itself [105]. It also acts as a ligand for several integrins such as $\alpha_v\beta_3$ and $\alpha_v\beta_5$ to mediate cell adhesion and migration [89, 105].

As a developmental factor, periostin is involved in bone, cartilage, skin, and cardiac development [104, 106, 107]. It is re-expressed in adults after myocardial [106, 108, 109], vascular [110], and skeletal muscle [111] injuries or bone fractures [112]. It participates in the remodeling of damaged cardiac tissue after acute myocardial infarction [113], which may provide a target for innovative strategies to treat heart failure. Periostin deficiency does not result in embryonic lethality, although approximately 14% of periostin-null mice die postnatally before weaning [114]. The remaining periostin-null mice exhibit severe growth retardation, incisor enamel defects, and an early-onset periodontal disease-like phenotype [114]. These

results suggest that periostin is critically required for maintenance of the integrity of the periodontal ligament in response to mechanical stresses [114].

Furthermore, periostin knock-out mice show reduced collagen fibril diameters in skin dermis, signifying an indication of aberrant collagen I fibrillogenesis, and a lower collagen denaturing temperature, reflecting a reduction in the level of collagen cross-linking [91]. Hence, periostin appears to regulate collagen I fibrillogenesis by directly interacting with collagen I and thereby serves as an important mediator of the biomechanical properties of fibrous connective tissues [91].

1.4.3 Periostin and Cancer

Periostin has been linked to invasion, cellular survival, angiogenesis, and metastasis in epithelial tumors, suggesting a role for periostin in tumor progression (Figure 5) [105]. Invasion through the extracellular matrix is a three-step process involving adhesion, migration, and the expression of proteases [102]. Periostin, an adhesion molecule, is able to promote the attachment and cell migration of epithelial cells without inducing expression of proteases [102]. Through interaction with $\alpha_6\beta_4$ integrin, it activates focal adhesion kinase (FAK) and Akt phosphorylation, resulting in the stimulation of the PI3K pathway [102].

In addition, periostin expression is significantly increased by transforming growth factor-β (TGF-β) and bone morphogenetic protein (BMP)-2, which promotes epithelial-mesenchymal transition (EMT) and tumor metastasis [90]. Thus, periostin can induce cell invasive activity through EMT [115].

Tumor growth is determined by the balance of cell proliferation and programmed cell death [41]. Cell proliferation is regulated by mitogenic growth and anti-proliferative signals that converge on regulators of the cell cycle [41, 116]. It has been demonstrated that the proliferation rate of periostin-producing cells was slower than that of the control cells in culture, suggesting that periostin does not promote proliferation of tumor cells *in vitro* [95]. In addition, periostin

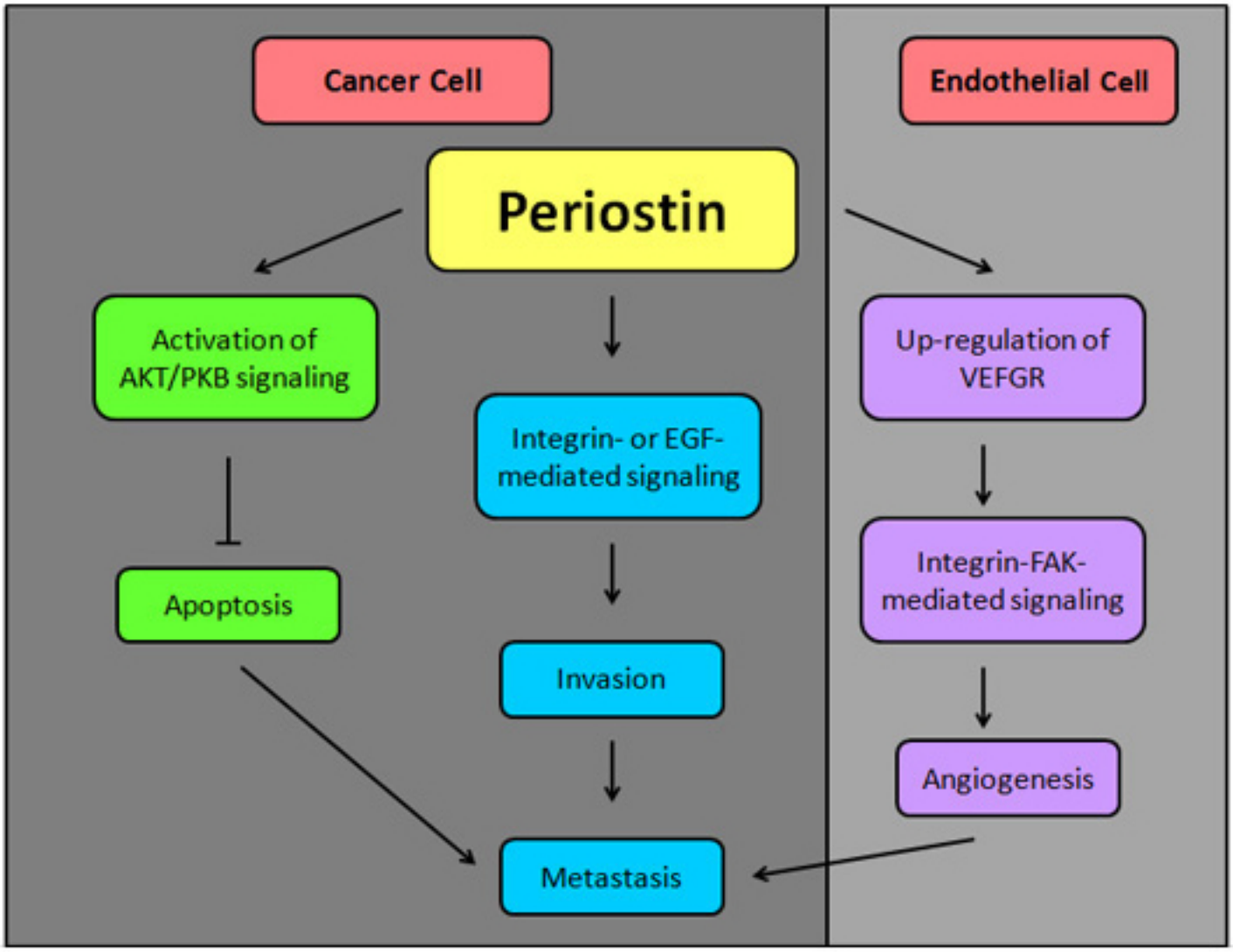
Cancer Cell
Endothelial Cell
Periostin
Activation of AKT/PKB signaling
Integrin- or EGF-mediated signaling
Up-regulation of VEFGR
Apoptosis
Invasion
Integrin-FAK-mediated signaling
Angiogenesis
Metastasis

Figure 5: Schematic model of periostin stimulated pathways in cancer. Once cancer cells secrete periostin, it binds to integrins in cancer cells and endothelial cells inducing cellular survival through the activation of Akt/PKB pathway via $\alpha_v\beta_3$ integrin. Interactions between periostin and integrins also promote invasion through the activation of intracellular signal as well as angiogenesis in endothelial cells. In the end, invasion, cellular survival and angiogenesis all contribute to metastasis. Adapted from Kudo et al. 2007.

overexpression does not appear to be associated with cell proliferation in head and neck cancer cell lines [97]. Periostin producing cells also show fewer apoptotic cells, due to the activation of the Akt/PKB pathway via the $\alpha_v\beta_3$ integrin, which enhances growth by promoting cellular survival [96] and resistance to hypoxia and serum starvation [102]. It also promotes cellular survival by inducing Akt phosphorylation through binding of $\alpha_6\beta_4$ integrin and activation of the PI3K pathway [102]. Therefore, promoting cell survival by evading apoptosis might be one key mechanism of periostin-enhanced tumor growth [117].

Unrestricted growth of tumors is dependent upon angiogenesis [41, 118]. There are many molecules that can promote angiogenic signaling cascades [119]. VEGF, which acts through its membrane tyrosine kinase receptors, VEGF receptor 1 (VEGFR-1 or Flt-1) and receptor 2 (VEGFR-2 or Flk-1/KDR), is one of the most potent angiogenic molecules [117]. Angiogenesis, which occurs during the late stages of tumorigenesis, can be induced by periostin through the up-regulation of VEGFR-2 via an integrin $\alpha_v\beta_3$-FAK-mediated signaling pathway [95]. Overexpression of periostin in human breast cancers leads to a significant enhancement of angiogenesis and a growth advantage of breast tumors *in vivo* by altering the microenvironment [117].

Integrins are transmembrane heterodimeric receptors involved in both cell-cell and cell-ECM interactions [120]. They play a role in cell adhesion and the activation of cytosolic signaling cascades to mediate cell proliferation, cell survival, and cell migration [121, 122]. The periostin-integrin interaction may inhibit the ECM-integrin interaction and trigger the intracellular signaling and activation of certain cells that are involved in tumor progression [105]. Supporting this, periostin has been shown to enhance migration and invasion of cancer cells through integrins or the EGF signaling pathway [115]. Periostin also promotes tumor metastasis in breast, lung, colon, and gastric cancer, as well as melanoma, head and neck squamous cell carcinoma, thymoma, and neuroblastoma [117]. Clinicopathological studies have revealed that periostin

overexpression is well correlated with metastasis and poor prognosis in various human cancers [96, 100], making it a potential therapeutic and diagnostic target for various human cancers.

1.5 Purpose of Research

1.5.1 Rationale

Integrin signaling regulates diverse functions in tumor cells, including migration, invasion, proliferation, and survival. In several tumor types, the expression of particular integrins correlates with increased disease progression and decreased patient survival. Tumor cell expression of the integrin $\alpha_6\beta_4$ increases tumor size and grade and decreases survival while integrin $\alpha_v\beta_3$ increases bone metastasis, both of which can be correlated with breast cancer progression [123]. Periostin interacts with $\alpha_v\beta_3$, $\alpha_6\beta_4$, and $\alpha_v\beta_5$ integrins to mediate endothelial cell adhesion and migration, promoting tumor development and progression [101, 102]. One report has shown that secreted periostin triggers co-activation of integrin $\alpha_v\beta_5$ and EGFR/HER1/ErbB1 signaling pathways, promoting EMT, resulting in tumor invasion and metastasis [115].

Interestingly, EGFR/HER1/ErbB1 associates and forms a complex with $\alpha_2\beta_1$ integrin [124]. Blocking β1 integrin binding activity in human breast cancer cells was shown to downregulate EGFR/HER1/ErbB1 signaling [125]. Furthermore, targeted disruption of β1 integrin in a MMTV-PyV MT transgenic mouse model of human breast cancer reveals an essential role for β1 integrin in mammary tumor induction [126]. Moreover, β4 integrin signaling promotes mammary tumor cell proliferation and invasion, suppresses apoptosis, and amplifies HER2/ErbB2 signaling to promote mammary tumorigenesis [127]. Therefore, periostin signaling through the various integrins may amplify HER2/ErbB2 signaling to promote mammary tumorigenesis.

1.5.2 Hypothesis

We hypothesized that periostin enhances HER2/ErbB2-induced tumorigenesis and metastasis in a transgenic mouse model, and that periostin increases cell proliferation and cell migration of mammary epithelial cells *in vitro*.

1.5.3 Objectives

The objective of my research was to generate Postn$^{-/-}$ mice in a NeuNDL background. Subsequently, it was to determine if the absence of periostin affects mammary gland development and overall growth in Postn$^{-/-}$ mice, and mammary tumorigenesis in NeuNDL Postn$^{-/-}$ mice *in vivo*. Lastly, it was to observe the effects of periostin on primary ErbB2/Neu-overexpressing primary mammary tumor epithelial cell proliferation and migration *in vitro*.

2. Materials and Methods

2.1 Generation of Targeted Mutant and Transgenic Mice in a FVB Background

2.1.1 Periostin *lacZ* Knock-in

Mice carrying two periostin knock-in alleles where the DNA encoding the translational start site, all of the first exon, and approximately 300 bp of the first intron of both periostin genes were replaced with the bacterial β-galactosidase/*lacZ* reporter gene ($Postn^{-/-}$) (obtained from Dr. Simon Conway) in a C57Bl/6 background were backcrossed to FVB mice for 2 generations. After which the DNA from the $Postn^{+/-}$ offspring were sent for advanced speed congenics genotyping called Marker-Assisted Accelerated Backcrossing (MAX-BAX®), which facilitates the rapid production of congenic strains of knock-out or transgenic animals through the use of microsatellite analysis. This pioneering process selects individuals with preferred genetic content, in this case FVB, and greatly reduces the number of generations needed to produce a congenic research model. The $Postn^{+/-}$ mice from the 2nd generation with the highest FVB contribution (~85%) from MAX-BAX® analysis was backcrossed with a FVB to generate the 3rd generation $Postn^{+/-}$ mice. DNA from the $Postn^{+/-}$ offspring from the 3rd generation were sent for MAX-BAX® analysis and resulted in approximately 95% FVB contribution for these mice. The generation of $Postn^{+/-}$ mice in a relatively pure FVB background is shown in figure 6. The generation of $Postn^{-/-}$ mice in a pure FVB background and maintenance of periostin mice in a pure FVB background is illustrated in figure 7.

2.1.2 NeuNDL Periostin *lacZ* Knock-in

When setting up the matings, two new mouse lines were generated. One of the NeuNDL periostin mouse lines was generated in a mixed FVB and C57Bl/6 (FVB/C57) background, whereas the other NeuNDL periostin mouse line was generated in a pure FVB background.

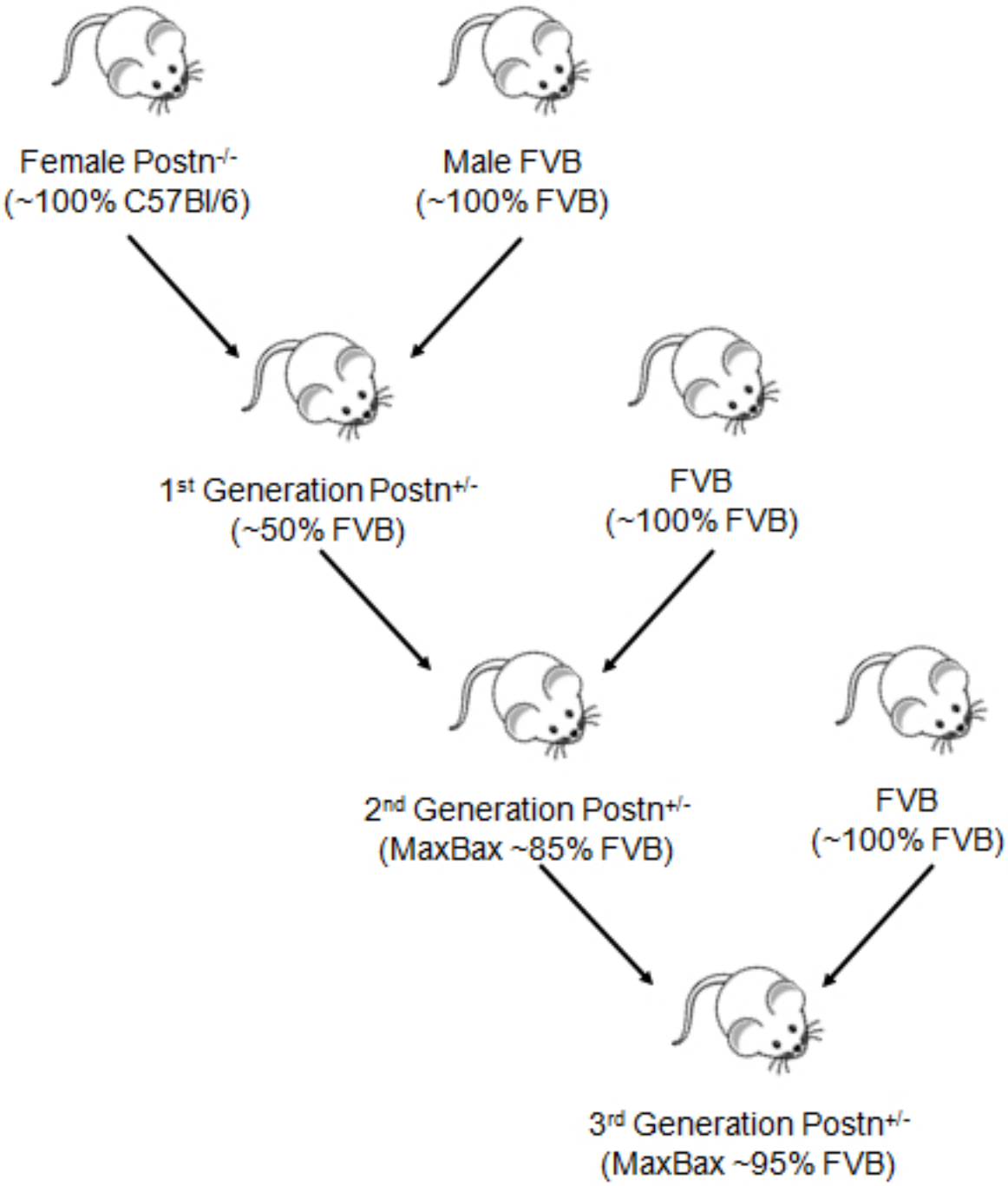
Female Postn-/-
(~100% C57Bl/6)
Male FVB
(~100% FVB)
1st Generation Postn+/-
(~50% FVB)
FVB
(~100% FVB)
2nd Generation Postn+/-
(MaxBax ~85% FVB)
FVB
(~100% FVB)
3rd Generation Postn+/-
(MaxBax ~95% FVB)

Figure 6: Generation of Postn$^{+/-}$ mice in a relatively pure FVB background.

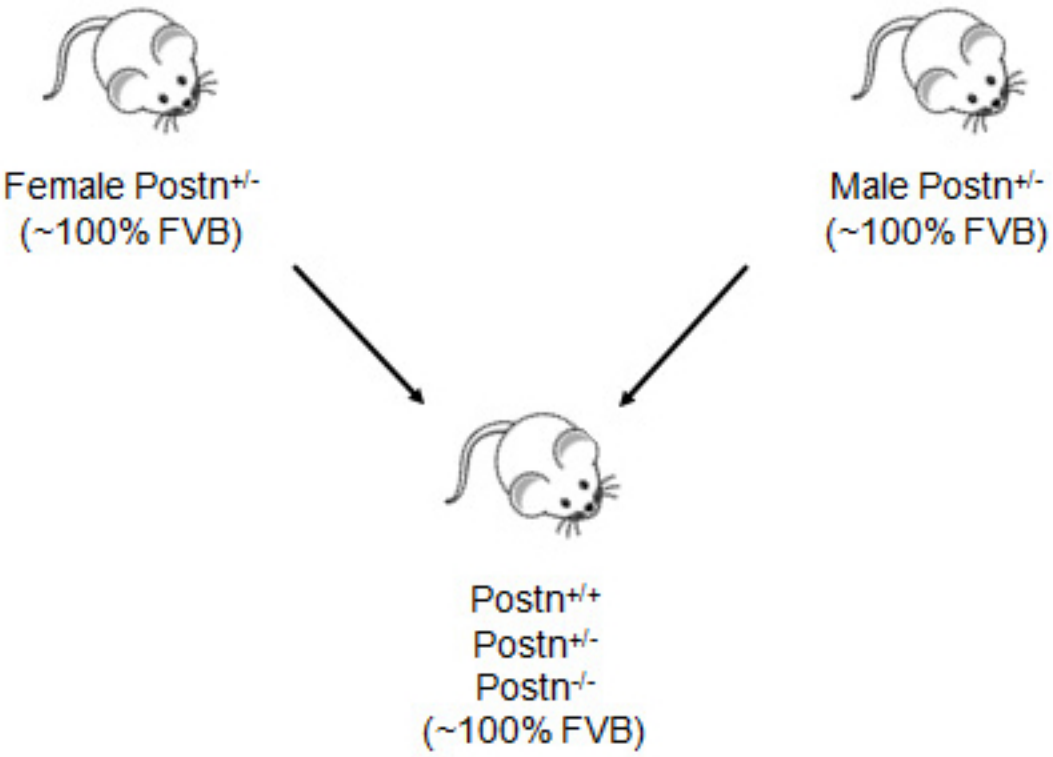
Female Postn+/-
(~100% FVB)
Male Postn+/-
(~100% FVB)
Postn+/+
Postn+/-
Postn-/-
(~100% FVB)

Figure 7: Generation of Postn$^{-/-}$ mice in a pure FVB background.

2.1.2.1 NeuNDL Periostin lacZ Knock-in in a Mixed Background

In order to generate a NeuNDL periostin mouse line in a mixed FVB and C57Bl/6 (FVB/C57) background, a male MMTV-*NeuNDL* mouse (NeuNDL) (obtained from Dr. William Muller) already in a FVB background was mated with a female Postn$^{-/-}$ mouse that was in a C57Bl/6 background, generating NeuNDL Postn$^{+/-}$ mice in a mixed FVB/C57 background. One of these male NeuNDL Postn$^{+/-}$ mice was later mated with a female Postn$^{+/-}$ mouse from a mating between a FVB mouse with a C57Bl/6 Postn$^{-/-}$ mouse. These NeuNDL Postn$^{+/+}$, NeuNDL Postn$^{+/-}$, and NeuNDL Postn$^{-/-}$ mice are classified as still being in a mixed FVB/C57 background. The generation of the NeuNDL periostin mouse line in a mixed FVB/C57 background is shown in figure 8.

2.1.2.2 NeuNDL Periostin lacZ Knock-in in a FVB Background

In order to generate a NeuNDL periostin mouse line in a pure FVB background, a male NeuNDL Postn$^{+/-}$ mouse in a pure FVB background was mated with a female Postn$^{+/-}$ mouse in a pure FVB background. These NeuNDL Postn$^{+/+}$, NeuNDL Postn$^{+/-}$, and NeuNDL Postn$^{-/-}$ mice are classified as being in a pure FVB background. The generation of the NeuNDL periostin mouse line in a pure FVB background is illustrated in figure 9.

2.2 Genotyping of Mice

Mice were genotyped by polymerase chain reaction (PCR) analysis. Mouse DNA was extracted from mouse ear clippings and purified using the DNeasy® blood and tissue kit (Qiagen) and the animal tissue spin-column protocol.

For genotyping periostin mice, three primers were used. Primer one: 5’ – AGTGTGCAGATGTTTGCTTG – 3’, primer two: 5’ – ACGAAATACAGTTTGGTAATCC – 3’, and primer three: 5’ – CAGCGCATCGCCTTCTATCG – 3’. Primers one and two results in a 300 base pair (bp) wildtype periostin band, while primers one and three amplify a 700 bp targeted mutant periostin band. Each PCR sample includes 0.4 µM of final primer concentration, 0.2 mM

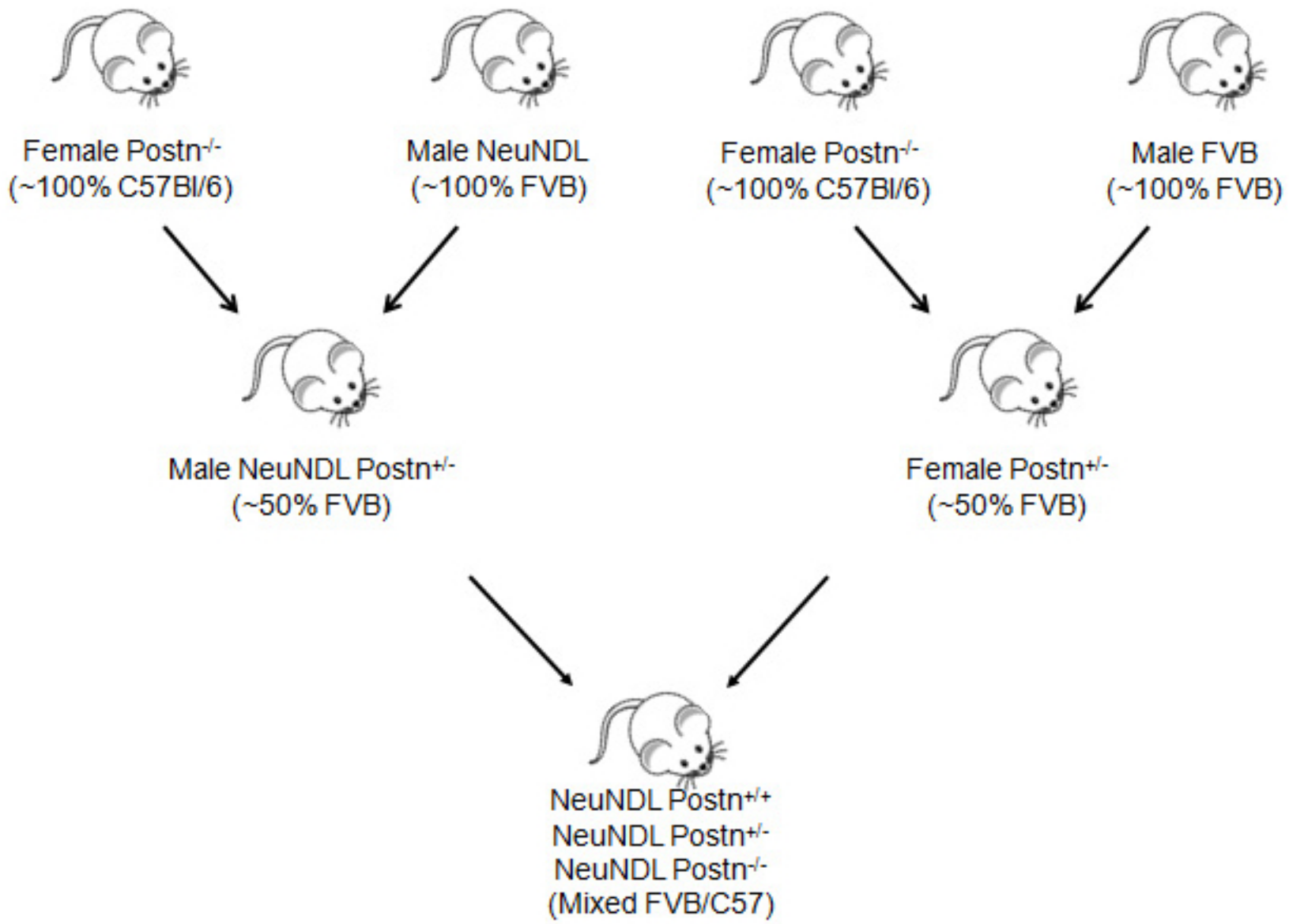
Female Postn-/-
(~100% C57Bl/6)
Male NeuNDL
(~100% FVB)
Female Postn-/-
(~100% C57Bl/6)
Male FVB
(~100% FVB)
Male NeuNDL Postn+/-
(~50% FVB)
Female Postn+/-
(~50% FVB)
NeuNDL Postn+/+
NeuNDL Postn+/-
NeuNDL Postn-/-
(Mixed FVB/C57)

Figure 8: Generation of the NeuNDL periostin mouse line in a mixed FVB/C57 background.

Female Postn$^{+/-}$
(~100% FVB)

Male NeuNDL Postn$^{+/-}$
(~100% FVB)

NeuNDL Postn$^{+/+}$
NeuNDL Postn$^{+/-}$
NeuNDL Postn$^{-/-}$
(~100% FVB)

Figure 9: Generation of the NeuNDL periostin mouse line in a pure FVB background.

dNTPs (dCTP, dATP, dGTP, dTTP), 0.25 µl Taq polymerase, 2.5 mM Mg^{2+}, 1 µl of DNA template, and enough double distilled water (ddH_2O) to make the final volume up to 25 µl. The PCR conditions for both wildype and mutant *periostin* is 94°C for 5 minutes, 94°C for 30 seconds, 55°C for 30 seconds, 72°C for 40 seconds, for 40 cycles, and 72°C for 10 minutes. The PCR samples were then analyzed on a 0.8% agarose gel at 100 V until the bands could be resolved.

For genotyping NeuNDL mice, two primers were designed. Primer one (5' – GTTTCCTGCAGCAGCCTACGC – 3') and primer two (5' – TTCCGGAACCCACATCAGGCC – 3') detects a 700 bp band when the mouse harbors the NDL transgene. Each PCR sample includes 0.4 µM of final primer concentration, 0.2 mM dNTPs, 0.25 µl Taq polymerase, 1 µl of DNA template, and enough ddH_2O to make the final volume up to 25 µl. The PCR conditions for *NeuNDL* is 94°C for 1 minute, 92°C for 30 seconds, 57°C for 30 seconds, 72°C for 1 minute, for 30 cycles, and 72°C for 5 minutes. The PCR samples were then analyzed on a 0.8% agarose gel at 100 V until the bands could be resolved.

2.3 Weight Measurement of Periostin Mice

$Postn^{+/+}$, $Postn^{+/-}$, and $Postn^{-/-}$ mice in a pure FVB background were weighed with a scale twice a week for 9 weeks to establish a growth curve. The weight of the mice was separated based on gender and genotype. The two different weights for each mouse were averaged after each week to establish weekly averages. Weekly averages were averaged for mice with the same gender and genotype to generate the data points.

2.4 Tumor Detection in NeuNDL Mice

NeuNDL $Postn^{+/-}$ mice in a mixed FVB/C57 background as well as NeuNDL $Postn^{+/+}$, NeuNDL $Postn^{+/-}$, and NeuNDL $Postn^{-/-}$ mice in a pure FVB background were followed for tumor development to establish a survival curve. These mice were palpated once a week, every week

starting at 4 months of age. A large tumor (~1.0 cm) was deemed as end point, as per the Canadian Council on Animal Care guidelines, for the animal.

2.5 Generation of Periostin Adenovirus Construct

pDC316, a shuttle plasmid, and periostin cDNA were digested with EcoR1 (New England Biolabs) for an hour at 37°C. The EcoR1 cut pDC316 and periostin cDNA were purified with the QIAquick® PCR purification kit (Qiagen). The EcoR1 digested and purified pDC316 DNA was further treated with 0.5 U of calf intestinal alkaline phosphatase (CIP) in 1X CIP buffer for 30 minutes at 37°C to remove terminal phosphate groups. The purified DNA was ligated in the following reaction at room temperature for 1.5 hours: 1.5 µl 10X T4 DNA ligase buffer, 400 U T4 DNA ligase, 1 µl of pDC316 DNA, and 9.5 µl periostin DNA. The ligated DNA was heat killed by incubating at 70°C for 10 minutes. The ligated reaction was then transformed into DH5α by heat shock. Transformations were plated on a LB-ampicillin plate and incubated at 37°C overnight.

The next day (approximately 16 hours later), colonies were then selected and placed into 3 ml of LB with ampicillin (50 µg/ml). Colonies were screened by rapid boiling mini prep using HindIII. The 20 µl digests were analyzed on a 0.8% agarose gel to confirm the positive clones. Crude adenovirus lysates were generated by Jeff Hamill (Dr. McKay) according to the protocol described by Ng and Graham [128]. This protocol includes cell culture of low-passage 293 cells followed by co-transfection of 293 cells with a shuttle plasmid and an adenovirus genomic plasmid by site-specific recombination. The transfected cells were then overlayed with a solution of 1% agarose and 2X maintenance medium. Plaques were picked and transferred to PBS^{2+} supplemented with 10% glycerol. Once the plaques have been isolated, they were expanded for extraction of vector DNA for analysis. The crude adenovirus was used to infect primary mammary tumor epithelial cell cultures.

2.6 Primary Mammary Tumor Epithelial Cell Cultures

Tumor-bearing FVB NeuNDL mice were sacrificed and mammary tumors were collected. The tumors were placed into a Falcon tube with sterile PBS and then transferred to a 100 mm cell culture plate in the tissue culture hood where they were washed 3-5 times with sterile PBS. The tissue was minced with a scalpel for 10 minutes and resuspended in 10 ml of collagenase B at 3 mg/ml in plain DMEM (Hyclone) media. The suspension was incubated at 37ºC, 5% CO_2 for an hour. The digested tumors were transferred from the 100 mm plate into a 50 ml Falcon tube. The volume was brought up to 30 ml with mammary tumor epithelial media (1:1, DMEM:F12 (GIBCO), 10% fetal bovine serum (NorthBio Inc), 1% mammary epithelial growth supplement (GIBCO), 0.1 mM non-essential amino acid, 1 nM cholera toxin, 5% penicillin and streptomycin mixture, and 0.25 µg/ml fungizone). The sample was spun at 700 rpm for 2 minutes, the supernatant, which contains fibroblasts, red blood cells, and haematopoietic cells, was removed, and the pellet was resuspended in 10 ml of PBS. The cells were washed with PBS 5-8 times to limit the amount of fibroblasts in the cultures. These cells were then plated in 100 mm plates and incubated at 37ºC, 5% CO_2 in mammary tumor epithelial media.

The mammary tumor epithelial cells were grown in mammary tumor epithelial media and the media was changed every two days. These cells were maintained at 37°C, 5% CO_2 and used in migration as well as proliferation experiments.

2.7 Periostin Adenovirus Infection

Media was replaced on primary mammary tumor epithelial cells with 3 ml of serum-free DMEM for a 100 mm plate. Periostin adenovirus (1:100 of crude lysates) was directly pipetted into the plate. The cells were incubated for 1.5 hours at 37°C, 5% CO_2 after which, the media was changed to mammary tumor epithelial media and left overnight at 37°C, 5% CO_2. The next day, the cells were trypsinized and used in the various assays described below.

2.8 Proliferation Assay

Mammary tumor epithelial cells (3 x 10^5) were initially plated in each of the wells of a 12-well cell culture plate. On day 3, 5, 7, and 9, these cells were trypsinized, resuspended in 1 ml of mammary tumor epithelial media, and counted in triplicates using the Vi-Cell™ XR cell viability analyzer (Beckman Coulter). The cells were either previously infected with periostin adenovirus and plated on non-coated plates, or uninfected and plated on 5 µg/ml periostin-, 10 µg/ml collagen-, or 5% BSA-coated plates.

2.9 Scratch Induced Migration Assay

Mammary tumor epithelial cells were grown to 90% confluency in 12-well plates prior to a scratch induced migration assay. A single scratch was performed on a monolayer of cells with a 200 µl pipette tip to induce cell migration for each of the three treatments: 5 µg/ml periostin-, 10 µg/ml collagen-, or 5% BSA-coated plates; each treatment was done in quadruplicates. Three pictures of each wound were taken. For every picture, three measurements between the migrating fronts were performed at 0 and 24 hours. The migration was quantified by calculating the percent wound closure.

2.10 Protein Expression Analysis

Mammary tumors and mammary glands were crushed in liquid nitrogen with a mortar and pestle into a powder. It was then transferred to an Eppendorf tube and lysed in RIPA buffer (50 mM Tris-HCl [pH 7.5], 150 mM NaCl, 1.0% Triton-X, 1.0% Nonidet P-40, 0.5% sodium dideoxycholate, 0.1% sodium dodecyl sulfate (SDS), 2 mM EDTA), containing 10 mM NaF, 1 mM DTT, 10 µg/ml leupeptin, 10 µg/ml aprotinin, 0.1 mM benzamidine, 10 mM β-glycerol phosphate, 1 mM PMSF, 0.25 mM Na_3VO_4, and 10 µg/ml pepstatin. The samples were vortexed, sonicated, and spun at 13000 RPM for 5 minutes to remove any debris. The

supernatant was transferred to a new Eppendorf tube. Protein concentrations were established using the BioRad protein assay dye reagent and the absorbance at A_{595}.

Samples containing 20 µg of protein were resolved by 8% SDS-PAGE and transferred to polyvinylidene fluoride (PVDF) membrane (PerkinElmer). Membranes were then probed with various antibodies and washed six times for 10 minutes each with 1X TBST (5 mM Tris-HCl [pH 7.4], 15 mM NaCl, 0.1% Tween 20, 1.7 mM KCl). The primary antibodies were detected using conjugated horseradish peroxidase (HRP)-labeled secondary antibodies (1:4000) and visualized using Western Lightning® Plus-ECL enhanced chemiluminescence substrate (PerkinElmer) according to the manufacturers' directions. Western blots were subsequently followed by exposure to, and development of X-ray film.

2.11 Immunohistochemical Analysis

2.11.1 ABC Method for Paraffin-Embedded Sections

Mammary glands and mammary tumors were excised and fixed with 10% formalin buffer overnight at room temperature. The samples were then sent to the Department of Pathology at the University of Ottawa where they were paraffin-embedded and sectioned onto microscope slides. The mammary gland and mammary tumor sections were deparaffinized in 3 separate xylene washes and rehydrated in 5 graded alcohol washes (100%, 100%, 95%, 95%, and 80%) at room temperature for 5 minutes each. The sections were then rinsed in ddH_2O and washed with 1X PBS at room temperature for 5 minutes.

Heat-mediated antigen retrieval was performed using standard heat treatment with citrate buffer in a microwave. The sections were place in a container with 10 mM sodium citrate buffer, which was heated in the microwave for 5 minutes and allowed to cool at room temperature for 5 minutes. The sections were then heated again for another 5 minutes and allowed to cool for 20 minutes. Then, the sections were washed in ddH_2O, and the endogenous peroxidase activity was quenched with 3% H_2O_2 in ddH_2O at room temperature for 15 minutes.

The sections were washed three times in 1X PBS at room temperature for 5 minutes each, followed by blocking with 1.5% normal goat serum diluted in PBS for an hour, followed by incubation with a primary antibody in 1.5% normal goat serum at 4°C overnight in a humidified chamber.

The sections were then washed three times in 1X PBS at room temperature for 5 minutes each and then incubated with biotin-conjugated secondary antibody diluted in 1.5% normal goat blocking serum at room temperature for 30 minutes. Sections were washed and incubated with avidin-biotin complex (ABC) at room temperature for 30 minutes. Slides were then incubated with DAB peroxidase substrate in ddH_2O at room temperature for 7 minutes. The reaction was stopped, and sections were stained with hematoxylin at room temperature for 2 minutes, washed with tap water, and rinsed with ddH_2O. Sections were destained with 0.5% acid alcohol for 5 seconds, rinsed with ddH_2O, and dipped three times in ammonia water. They were dehydrated in 5 graded alcohol washes (80%, 95%, 95%, 100%, and 100%) and 3 separate xylene washes at room temperature for 5 minutes each. Mounting media (Fisher-Protocol) was added and sections were covered with a cover slip. Immunohistochemical analysis of paraffin-embedded sections was viewed and imaged using the ScanScope (Aperio).

2.11.2 Envision Plus Method for Paraffin-Embedded Sections

This method was identical to the ABC method for paraffin-embedded sections with minor changes. Following blocking with 1.5% normal goat serum diluted in PBS for an hour, the sections were incubated with a primary antibody in 1.5% normal goat serum at 4°C overnight in a humidified chamber. The secondary antibody was Envision Plus anti-mouse reagent.

2.11.3 Dako Method for Paraffin-Embedded Sections

This method was identical to the ABC Method for paraffin-embedded sections with the following changes. After the peroxidase activity was quenched with 3% H_2O_2 in ddH_2O, the sections were washed three times in 1X PBS at room temperature for 5 minutes each followed

by blocking with Dako protein block serum free reagent at room temperature for 10 minutes. Further blocking was performed with Dako biotin blocking system where the tissue sections were incubated with avidin solution for 10 minutes, rinsed off with 1X PBS, then incubated with biotin solution for 10 minutes and rinsed again with 1X PBS. The Ki-67 primary antibody was diluted 1:25 in Dako antibody diluent and incubated with the sections at 4°C overnight in a humidified chamber. The secondary antibody was a biotinylated rabbit anti-rat immunoglobulin antibody (1:200), followed by streptavidin HRP (1:200).

2.12 Mammary Gland Whole Mount

The #4 mammary gland was excised, as well as the maximum amount of connective tissue around the fat pad to facilitate the spreading of the mammary gland on the microscope slide. The mammary gland was then allowed to dry for 30 minutes at room temperature. It was then placed in a Coplin jar at room temperature containing 100% acetone overnight to de-fat the gland. The next day, a second microscope slide was used to press down on the mammary gland to help remove the excess fat before being placed back into 100% acetone for another 3 hours. The mammary gland was stained in a container of hematoxylin for 4 hours and then transferred to 70% ethanol with 0.5% HCl (acid alcohol) to destain overnight. The next day, the destained mammary gland was placed in 100% ethanol for an hour to completely dehydrate it. Subsequently, the gland was placed in 100% xylene overnight. Mammary glands were then mounted between two microscope slides with mounting media, being careful not to introduce any air bubbles and also making sure that enough mounting solution was added to completely cover the gland.

3. Results

3.1 Characterization of Periostin *lacZ* Knock-in Mice

To determine whether periostin (Postn) is required for mammary gland development and tumorigenesis *in vivo*, we obtained mice carrying a periostin knock-in allele where the DNA encoding the translational start site, all of the first exon, and approximately 300 bp of the first intron of the periostin gene was replaced with the bacterial β-galactosidase/*lacZ* reporter gene (Figure 10). Previously, it has been shown that heterozygotic intercrosses of $Postn^{+/-}$ mice produce viable $Postn^{+/+}$ (wildtype), $Postn^{+/-}$ (periostin heterozygous), and $Postn^{-/-}$ (periostin-null) offspring with roughly Mendelian ratios and an average litter size of 6.9 [114]. Homozygous embryos carrying two copies of the *lacZ-neo* cassette are null for the periostin gene. Genotyping of the offspring was determined by PCR analysis of genomic DNA to detect the wildtype or the targeted periostin mutant allele. Targeted deletion of *periostin* in $Postn^{+/-}$ and $Postn^{-/-}$ mice can be demonstrated by PCR analysis (Figure 11A) and confirmed by Western blot analysis of mammary gland lysates (Figure 11B). PCR analysis shows a mutant and a wildtype periostin band in $Postn^{+/-}$ mice, whereas only a mutant or a wildtype periostin band is observed in $Postn^{-/-}$ and $Postn^{+/+}$ mice, respectively. Western blot analysis shows the multiple periostin isoforms which range from 86 to 93 kDa, as previously documented, in $Postn^{+/+}$ and $Postn^{+/-}$ mice [92].

The cell type-specific expression of periostin was investigated using immunohistochemical analysis of paraffin-embedded mammary gland sections. Examination of the mammary epithelium derived from $Postn^{+/+}$ and $Postn^{+/-}$ mice revealed that periostin is expressed in the stromal cells of the lobules, but not in the epithelial cells of the mouse mammary gland (Figure 12). In mammary glands prepared from $Postn^{-/-}$ mice, periostin could no longer be detected (Figure 12), validating the specificity of our antibody.

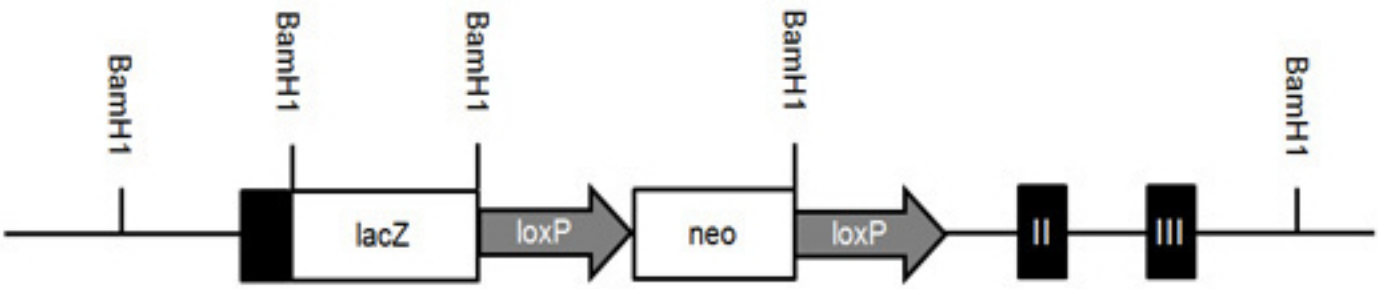
BamH1
BamH1
BamH1
BamH1
BamH1
lacZ
loxP
neo
loxP
II
III

Figure 10: Schematic representation of the targeted periostin allele. A promoterless *IRES-lacZ-neo-loxP* cassette was inserted into exon 1 in the mouse wildtype periostin locus resulting in the targeted allele as shown. The roman numerals represent the exon number.

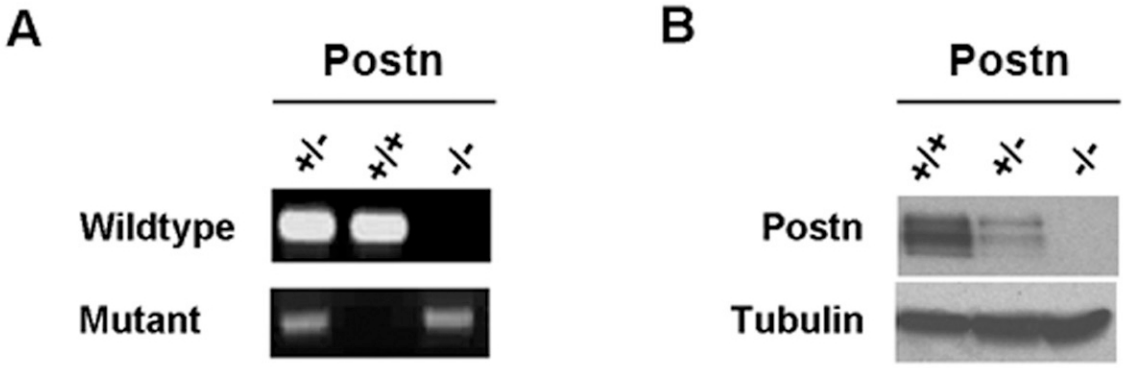
A
Postn
+/-
+/+
-/-
Wildtype
Mutant
B
Postn
+/+
+/-
-/-
Postn
Tubulin

Figure 11: Targeted deletion of periostin in the mouse mammary gland epithelium. A) PCR analysis of DNA from $Postn^{+/-}$ (lane 1), $Postn^{+/+}$ (lane 2), and $Postn^{-/-}$ (lane 3) mice in a FVB background, confirming *lacZ* insertion into the periostin allele in $Postn^{+/-}$ and $Postn^{-/-}$ mice. B) Western blot analysis of periostin expression in mammary gland lysates from $Postn^{+/+}$ (lane 1), $Postn^{+/-}$ (lane 2), and $Postn^{-/-}$ (lane 3) mice, confirming the decrease and absence of periostin expression in $Postn^{+/-}$ and $Postn^{-/-}$ mice, respectively. Gamma-tubulin was used as a loading control.

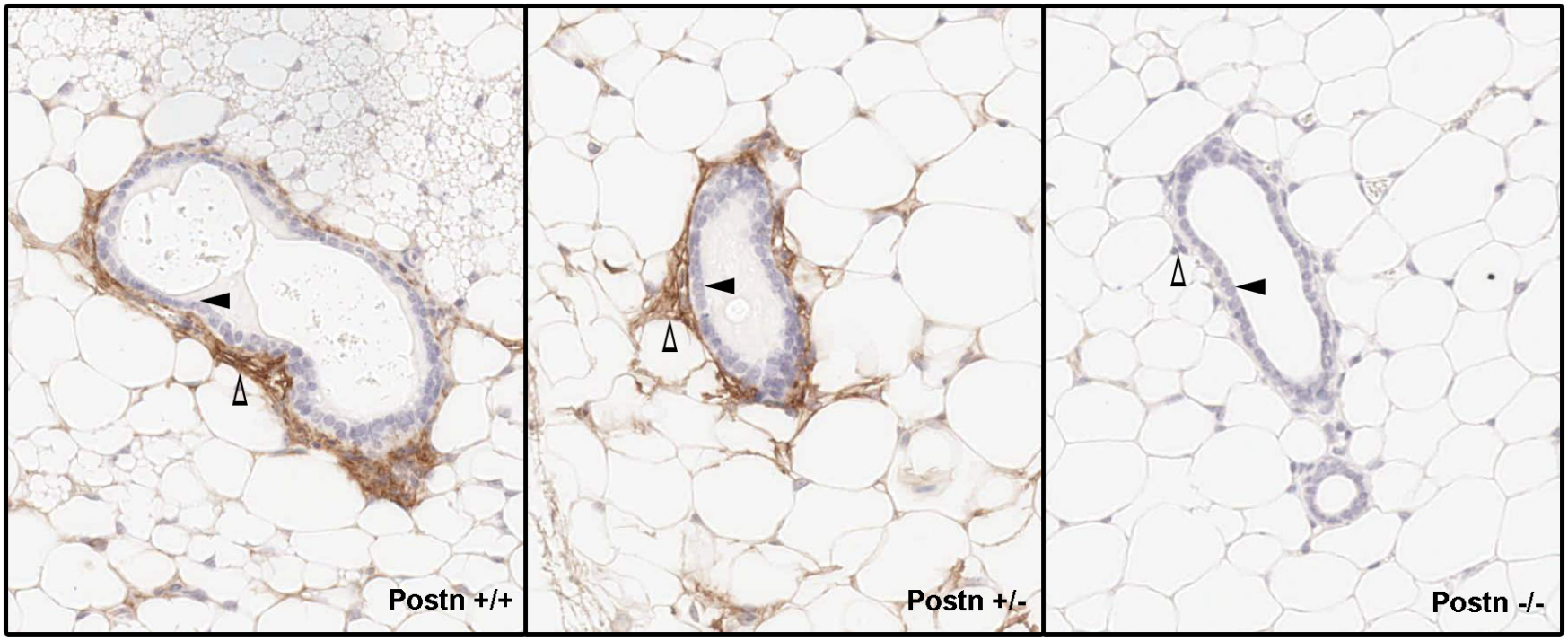
Postn +/+
Postn +/-
Postn -/-

Figure 12: Periostin is expressed in the stromal fibroblasts and not the epithelial cells of the mammary gland. ScanScope images of immunohistochemical analysis of periostin expression (brown) in FVB $Postn^{+/+}$, $Postn^{+/-}$, and $Postn^{-/-}$ mice. Hematoxylin counterstained sections appear blue. Note the absence of periostin protein (brown) in the $Postn^{-/-}$ mammary gland, compared to the $Postn^{+/+}$ and $Postn^{+/-}$ mammary glands. The black arrows show the mammary epithelial cells while the white arrows show the stromal fibroblasts.

3.2 Ablation of Periostin Does Not Interfere with Mammary Ductal Outgrowth

Prior to the introduction of this periostin *lacZ* knock-in allele into a mouse mammary tumor model, it was necessary to determine whether targeted ablation of periostin was compatible with normal mammary gland development. For this purpose, mammary gland whole mounts and paraffin-embedded sections were analyzed. Mammary gland sections from 8-week old nulliparous and 14.5 days post coitum (dpc) pregnant $Postn^{+/-}$ and $Postn^{-/-}$ female mice were stained with hematoxylin and eosin and compared to $Postn^{+/+}$ female mice (Figure 13). Examination of mammary glands from $Postn^{+/-}$ and $Postn^{-/-}$ mice revealed normal mammary ductal outgrowth, indistinguishable from that of control $Postn^{+/+}$ mice. Similarly, mammary glands from pregnant $Postn^{+/-}$ and $Postn^{-/-}$ females showed extensive outgrowth and arborization that was similar to $Postn^{+/+}$ mice (Figure 13).

It was previously shown that C57Bl/6 $Postn^{-/-}$ males were fertile while females were not [114]. Interestingly, we observed that FVB $Postn^{-/-}$ female mice were able to lactate and produce viable litters through multiple rounds of pregnancy (data not shown). Interestingly, male wildtype FVB matings with female FVB $Postn^{+/+}$, $Postn^{+/-}$, and $Postn^{-/-}$ mice, had average litter sizes of 9.2 ± 1.48, 10.5 ± 1.56, and 4.8 ± 1.47 offspring, respectively (data not shown). Litter sizes from female FVB $Postn^{-/-}$ mice were significantly smaller than from female FVB $Postn^{+/+}$ ($P < 0.005$) and FVB $Postn^{+/-}$ ($P < 0.001$) mice, suggesting that the periostin phenotype still affects $Postn^{-/-}$ females albeit with reduced penetrance. Consistent with this finding, genetic background has been shown to affect various phenotypes [129, 130].

3.3 Effect of Periostin Deletion on Overall Growth

Since targeted ablation of periostin was compatible with normal mammary gland development in nulliparous and pregnant mice, the postnatal overall growth of periostin mice was followed. It has been previously shown that 4-month-old C57Bl/6 $Postn^{-/-}$ mice were ~15 to

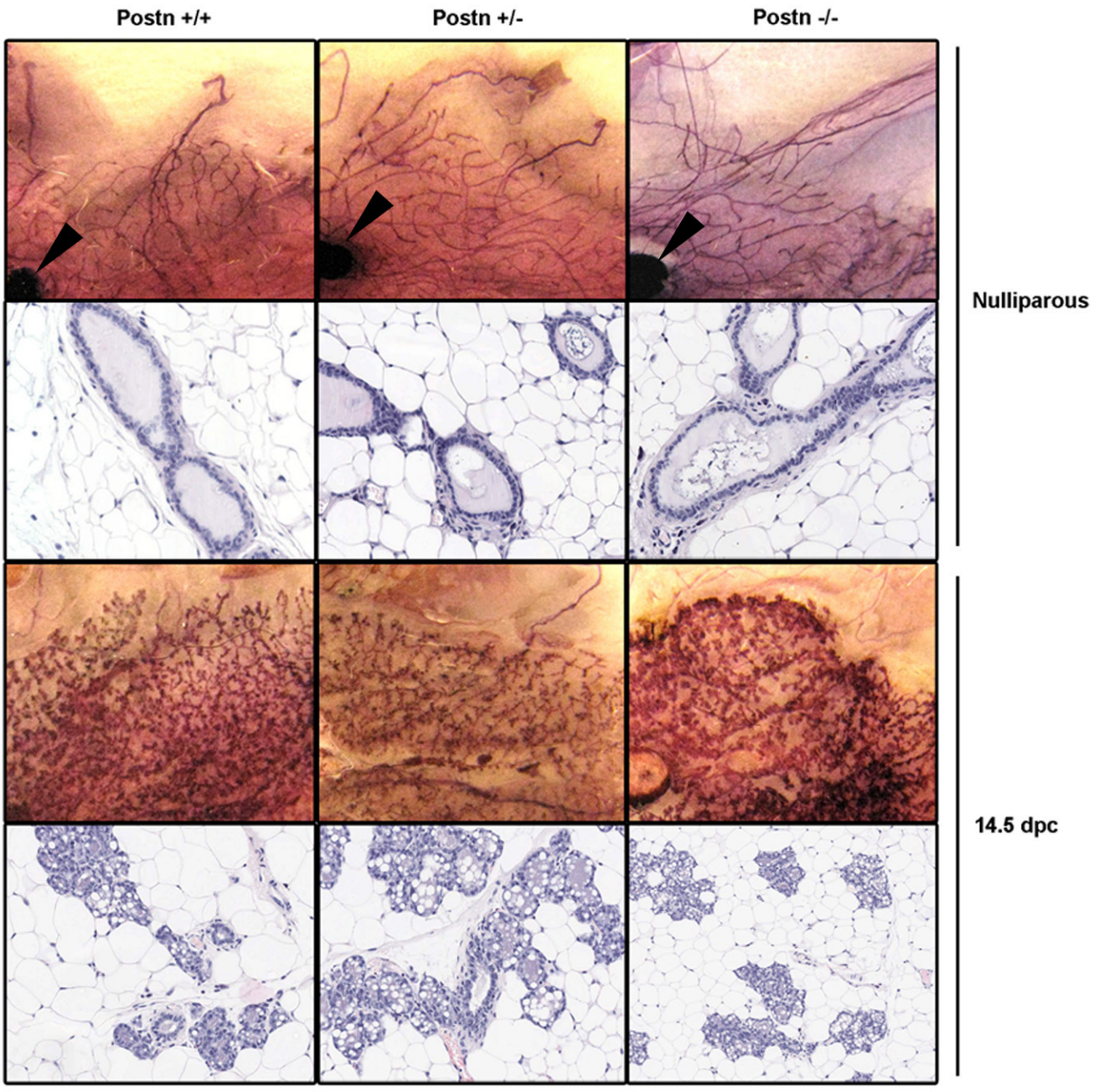
Postn +/+
Postn +/-
Postn -/-
Nulliparous
14.5 dpc

Figure 13: Targeted deletion of periostin does not impair mammary gland outgrowth during development or pregnancy. Representative images of mammary gland whole mounts and ScanScope images of paraffin-embedded sections from nulliparous and pregnant FVB $Postn^{+/+}$, $Postn^{+/-}$, and $Postn^{-/-}$ mice at 8 weeks and 14.5 days post coitum (dpc), respectively. The paraffin-embedded sections were stained with hematoxylin and eosin. The arrows indicate the lymph node within the nulliparous mammary gland. The thin, branched epithelial ducts that are characteristic of non-pregnant mammary glands undergo dramatic alterations in pregnancy when new types of epithelial structures, such as the milk-producing alveoli or lobules, emerge.

30% smaller and weighed approximately 50% less than C57Bl/6 Postn$^{+/+}$ littermates [114]. This growth retardation was detectable as early as 3 to 4 weeks after birth [114]. In order to investigate the role of periostin on postnatal growth, the weight of FVB Postn$^{+/+}$, Postn$^{+/-}$, and Postn$^{-/-}$ male (Figure 14A) and female (Figure 14B) mice was surveyed for 9 weeks. At 9-weeks of age, the average weight of male FVB Postn$^{+/+}$, Postn$^{+/-}$, and Postn$^{-/-}$ mice was 25.4 ± 0.49 g, 24.9 ± 0.16 g, and 22.8 ± 0.71 g, respectively. Statistical analysis showed that male FVB Postn$^{-/-}$ mice were significantly lighter than both male FVB Postn$^{+/+}$ ($P < 0.02$) and Postn$^{+/-}$ mice ($P < 0.008$). This observation is consistent with earlier studies on Postn$^{-/-}$ mice in a C57Bl/6 background.

However, at 9-weeks of age, no significant differences in weight were observed between female FVB Postn$^{-/-}$ mice and either female FVB Postn$^{+/+}$ or Postn$^{+/-}$ mice. The average weight of female FVB Postn$^{+/+}$, Postn$^{+/-}$, and Postn$^{-/-}$ mice was 19.5 ± 0.33 g, 20.6 ± 0.12 g, and 19.8 ± 0.56 g, respectively. Interestingly, the weight of female FVB Postn$^{+/+}$ mice were significantly different from the female FVB Postn$^{+/-}$ mice ($P < 0.02$). Contrary to the dwarfism phenotype of female C57Bl/6 Postn$^{-/-}$ mice that has been observed by other researchers, the female FVB Postn$^{-/-}$ mice in this study did not display any form of growth retardation.

3.4 Role of Periostin on Mammary Tumorigenesis

Periostin has multiple roles in tumor progression through activation of pathways involved in invasion, cellular survival, angiogenesis, and metastasis [105]. Therefore, to determine if periostin expression was required for the induction of mammary gland tumors, the in-frame Neu deletion transgene under the MMTV promoter [86] was introduced into mice with the *lacZ* knock-in periostin allele (NeuNDL Postn). This generated two mouse lines, one in a mixed FVB and C57Bl/6 (FVB/C57) background and the other in a pure FVB background (see Materials and Methods). NeuNDL Postn$^{+/-}$ mice in a mixed FVB/C57 background as well as NeuNDL Postn$^{+/+}$, NeuNDL Postn$^{+/-}$, and NeuNDL Postn$^{-/-}$ mice in a pure FVB background were

A

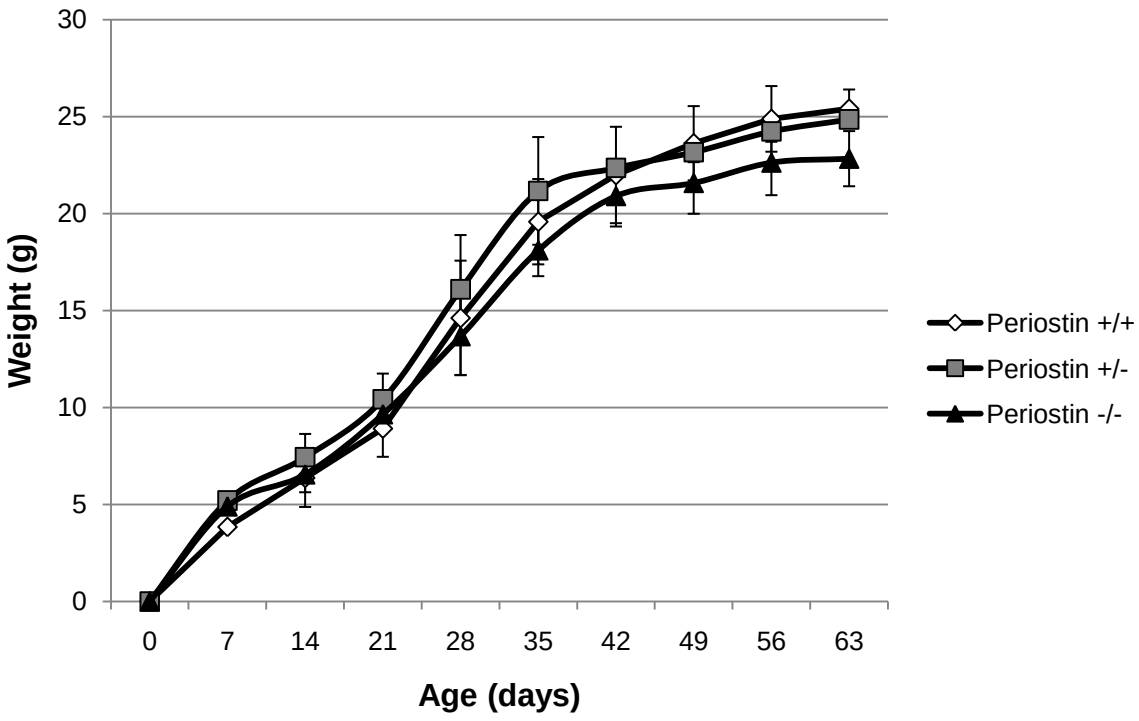
30
25
20
15
10
5
0
Weight (g)
0
7
14
21
28
35
42
49
56
63
Age (days)
Periostin +/+
Periostin +/-
Periostin -/-

B

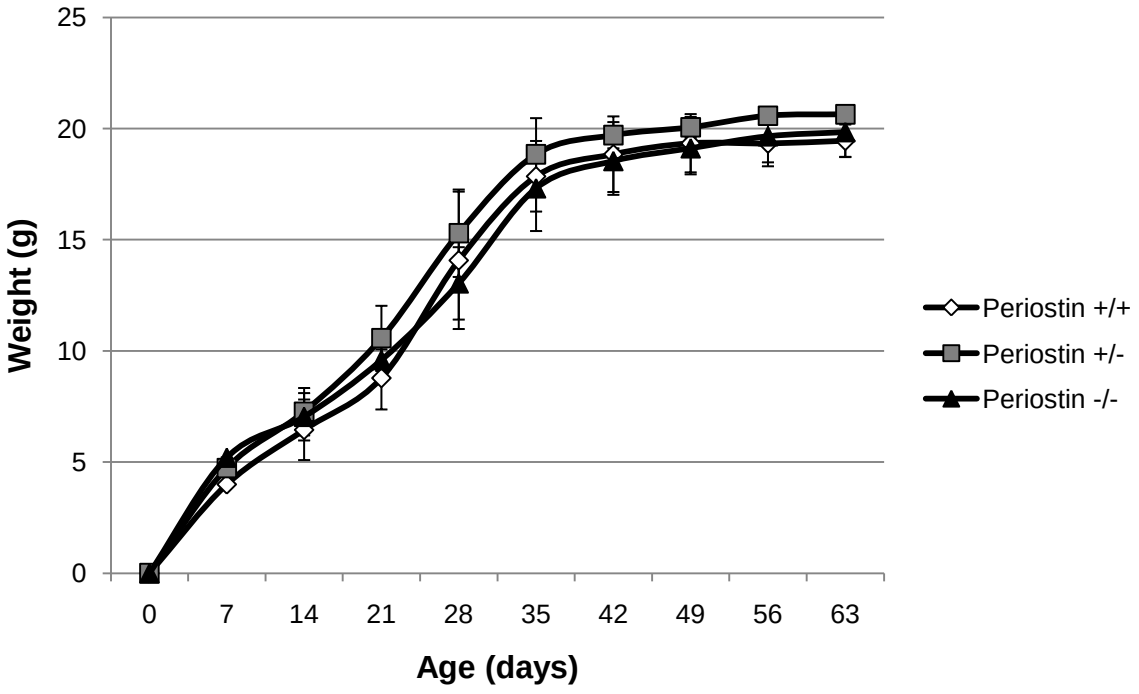
25
20
15
10
5
0
Weight (g)
0
7
14
21
28
35
42
49
56
63
Age (days)
Periostin +/+
Periostin +/-
Periostin -/-

Figure 14: Male FVB Postn$^{-/-}$ mice weighed less whereas the female FVB Postn$^{-/-}$ mice are similar in weight to FVB Postn$^{+/+}$ mice. The growth curve of male (A) and female (B) FVB periostin offspring is shown. Male FVB Postn$^{+/+}$ (n = 16), Postn$^{+/-}$ (n = 6), and Postn$^{-/-}$ (n = 4) as well as female FVB Postn$^{+/+}$ (n = 12), Postn$^{+/-}$ (n = 10), and Postn$^{-/-}$ (n = 8) mice were weighed twice a week and the two weights of the offspring for each gender and genotype was averaged at the end of the week for 9 weeks.

monitored until they developed palpable tumors at which point they were sacrificed and analyzed (Figure 15).

Virgin NeuNDL Postn$^{+/+}$ and Postn$^{+/-}$ female mice in a pure FVB background had palpable tumors that could be detected as early as 20 weeks of age. By contrast, mammary gland tumors could not be detected in NeuNDL Postn$^{+/-}$ mice in a mixed FVB/C57 background for up to one year of age. Consistent with these observations, 100% of NeuNDL Postn$^{+/-}$ mice in a mixed FVB/C57 background survived beyond one year whereas all of the NeuNDL Postn$^{+/+}$ and Postn$^{+/-}$ mice in a pure FVB background developed mammary tumors by 9 and 10 months of age, respectively (Figure 16). As a result, the overall survival of NeuNDL Postn$^{+/+}$ and Postn$^{+/-}$ mice in a FVB background was similar. Therefore, the survival of NeuNDL Postn$^{+/-}$ mice in a mixed FVB/C57 background was greatly increased when compared to NeuNDL Postn$^{+/+}$ and Postn$^{+/-}$ mice in a FVB background. Currently, the long-term data for the NeuNDL Postn$^{-/-}$ mice in a pure FVB background is incomplete. However, thus far, nine NeuNDL Postn$^{-/-}$ mouse has developed mammary gland tumors by the age of 10 months (Figure 16).

Consistent with these findings, different genetic backgrounds have been known to affect the penetrance of the expected phenotype. Specifically, the genetic background has been shown to affect the penetrance of the phenotype induced by oncogenes. In fact, FVB x C57Bl/6 (F1) MMTV-*Neu* mice had tumor latencies greater than 18 months of age compared to the FVB MMTV-*Neu* mice, which developed tumors between 7 and 12 months of age [130]. Therefore, *Neu* proto-oncogene overexpression in FVB mice leads to mammary tumors much sooner than in a mixed FVB/C57 background [130]. As a result, preliminary data suggests that periostin ablation does not prevent tumorigenesis. However, there is a significant delay in the onset of tumorigenesis among the mice in a mixed FVB/C57 background compared to a pure FVB background.

In addition, comparison of whole mount analysis of female virgin NeuNDL Postn$^{+/-}$ mice in a mixed FVB/C57 background revealed dramatic differences compared to the NeuNDL

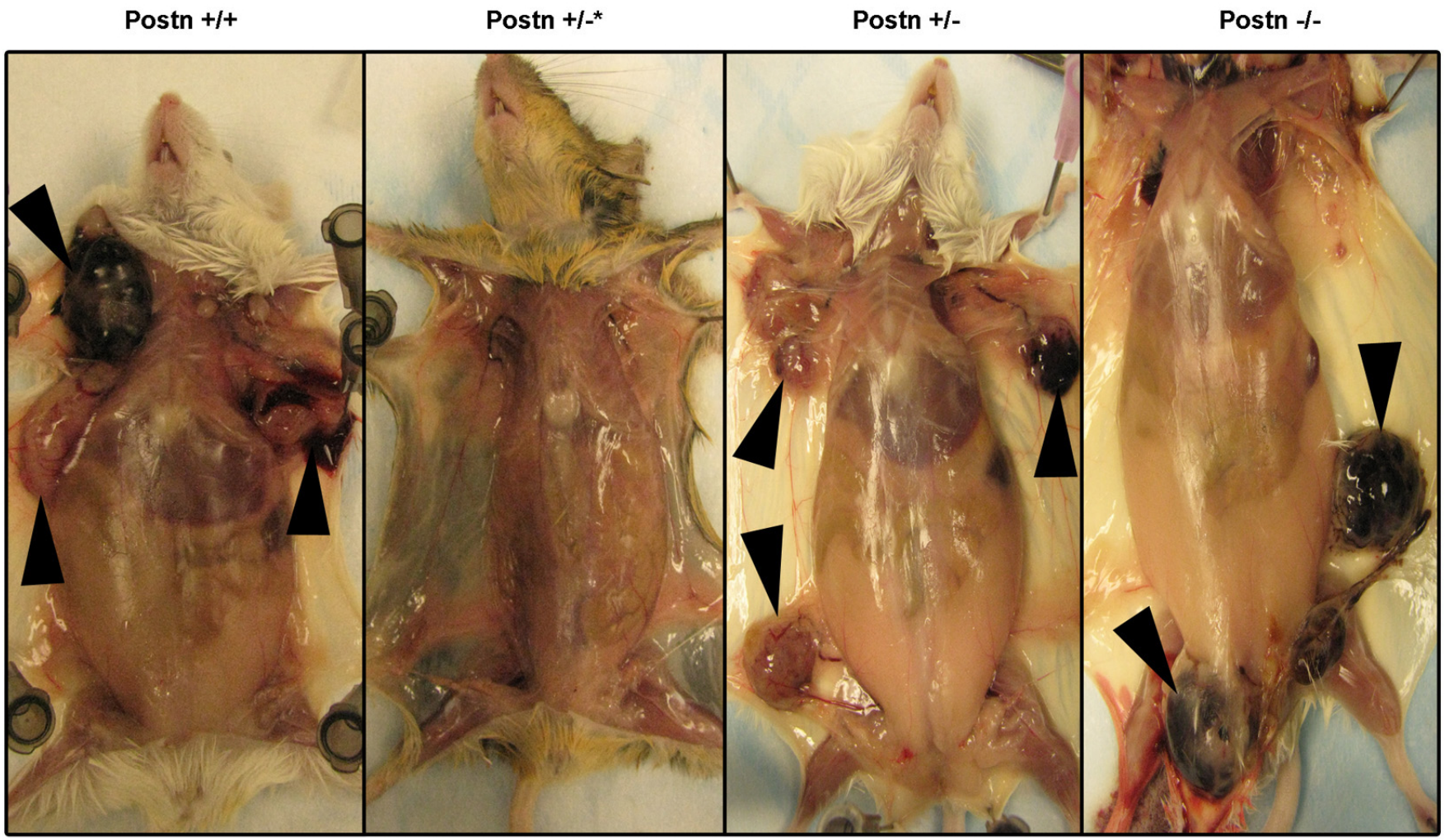
Postn +/+
Postn +/-*
Postn +/-
Postn -/-

Figure 15: Development of mammary gland tumors in FVB, but not in mixed FVB/C57 background mice. Representative digital camera images of a 6-month old NeuNDL Postn$^{+/+}$ (Postn +/+), a 6-month old NeuNDL Postn$^{+/-}$ (Postn +/-), and an 8-month old NeuNDL Postn$^{-/-}$ (Postn -/-) mouse in a FVB background are shown. A 12-month old NeuNDL Postn$^{+/-}$ mouse (Postn +/-*) in a mixed FVB/C57 background is also shown for comparison. The black arrows indicate the location of the mammary tumors.

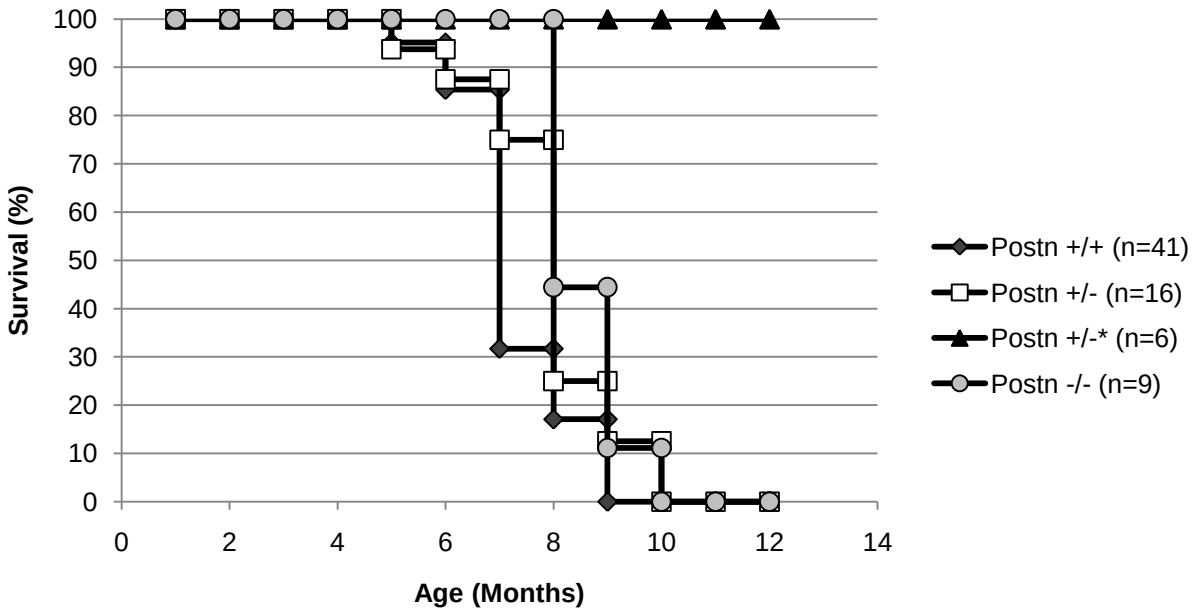
100
90
80
70
60
50
40
30
20
10
0
Survival (%)
0
2
4
6
8
10
12
14
Age (Months)
Postn +/+ (n=41)
Postn +/- (n=16)
Postn +/-* (n=6)
Postn -/- (n=9)

Figure 16: Periostin status and genetic background effect on mammary gland tumorigenesis. The Kaplan-Meier analysis of tumor onset illustrates the percent survival of NeuNDL transgenic mice. The percent survival of NeuNDL Postn$^{+/+}$ (Postn +/+) (n = 41), NeuNDL Postn$^{+/-}$ (Postn +/-) (n = 16), and NeuNDL Postn$^{-/-}$ (Postn -/-) (n = 9) mice in a FVB background as well as NeuNDL Postn$^{+/-}$ (Postn +/-*) (n = 6) mice in a mixed FVB/C57 background is shown. End point was the presence of a large tumor, which determined the age of the mouse's survival.

control mice in a pure FVB background. The mammary gland whole mounts revealed a marked reduction in the number of lesions among the 12-month old NeuNDL Postn$^{+/-}$ mice in a mixed FVB/C57 background compared to the 6-month old NeuNDL Postn$^{+/+}$ and Postn$^{+/-}$ mice in a pure FVB background (Figure 17). However, in a pure FVB background, tumor onset and the number of hyperplastic nodules were similar between the NeuNDL Postn$^{+/+}$ and NeuNDL Postn$^{+/-}$ mice. This suggests that the latency of mammary tumor development in NeuNDL Postn$^{+/-}$ mice in a mixed FVB/C57 background relative to NeuNDL Postn$^{+/-}$ and NeuNDL Postn$^{+/+}$ mice in a pure FVB background can be attributed to differences in the genetic background.

3.5 Reduced Cellularity in NeuNDL Postn$^{+/-}$ Tumors and Hyperplasias

In order to further characterize the mammary gland tumors and hyperplastic lesions, tumors and mammary glands were excised from the NeuNDL mice, paraffin-embedded, and sectioned. The sections were then stained with hematoxylin and eosin. Latency issues were further illustrated when paraffin-embedded mammary gland sections of 6-month old NeuNDL Postn$^{+/+}$ and Postn$^{+/-}$ mice in a FVB background and 12-month old NeuNDL Postn$^{+/-}$ mice in a mixed FVB/C57 background were analyzed (Figure 18A). Following staining, the number of hyperplastic lesions greater than 10^4 μm^2 in these mice was counted (Figure 18B). The number of these hyperplastic lesions were found to be 34.0 ± 1.68, 2.8 ± 0.75, and 33.0 ± 2.83 in FVB NeuNDL Postn$^{+/+}$, mixed FVB/C57 NeuNDL Postn$^{+/-}$, and FVB NeuNDL Postn$^{+/-}$ mice, respectively. These observations suggest that differences in genetic background may influence HER2/ErbB2-induced mammary tumorigenesis.

In the tumors of NeuNDL Postn$^{+/+}$, Postn$^{+/-}$, and Postn$^{-/-}$ mice in a FVB background, another marked histological difference was noticed. Further analysis of the tumors showed that the NeuNDL Postn$^{+/-}$ and Postn$^{-/-}$ tumors had a spongy appearance and more eosin staining due to significantly more cystic formation and bleeding compared to the solid appearance of the NeuNDL Postn$^{+/+}$ tumor (Figure 19). This increase in blood in the tumors from NeuNDL Postn$^{+/-}$

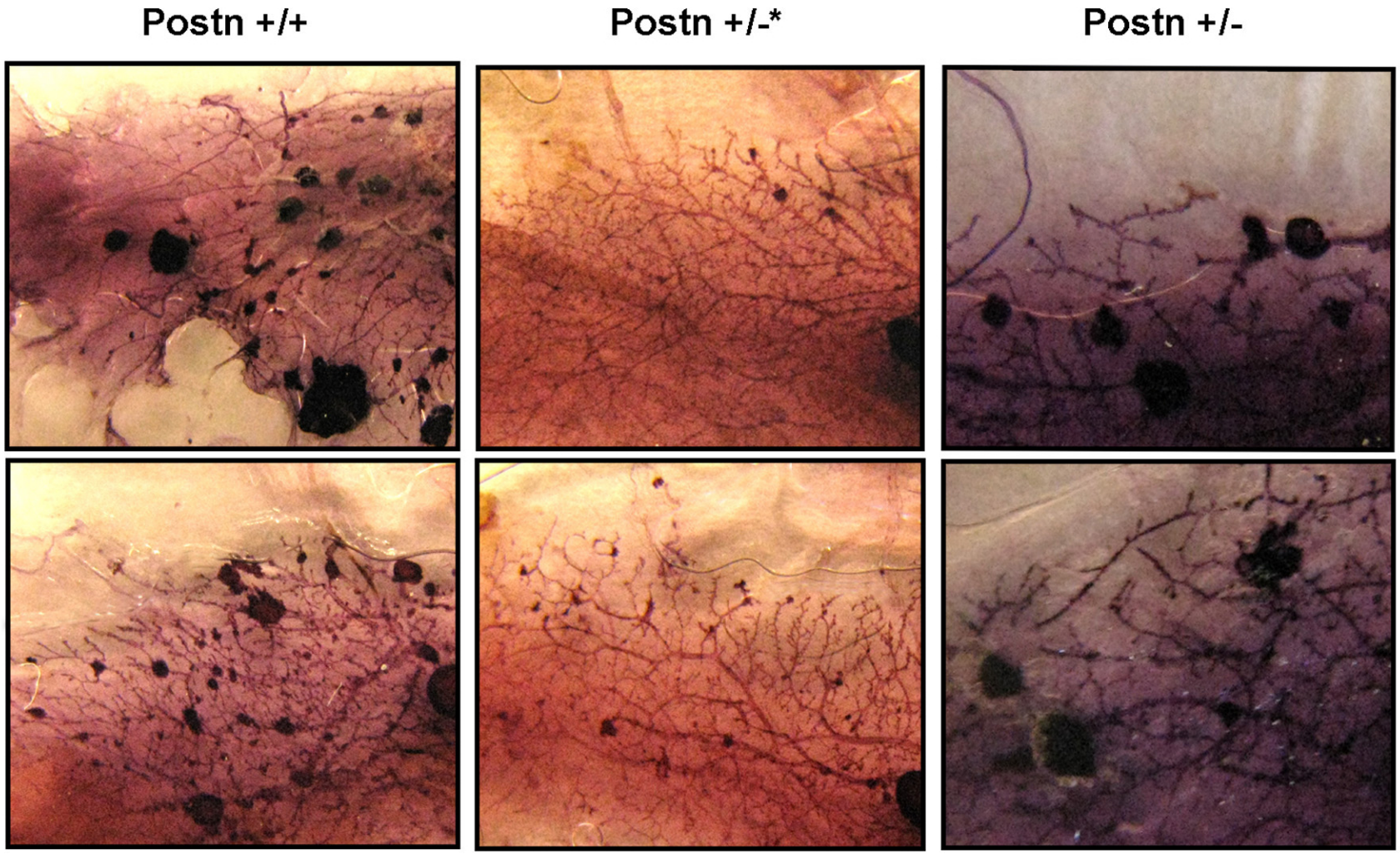
Postn +/+
Postn +/-*
Postn +/-

Figure 17: Mammary tumorigenesis in NeuNDL Postn$^{+/-}$ mice. Digital camera images of two representative hematoxylin-stained mammary gland whole mounts for each genotype are shown. Development of hyperplastic lesions within the mammary glands of 6-month old NeuNDL Postn$^{+/+}$ (Postn +/+) and 6-month old NeuNDL Postn$^{+/-}$ (Postn +/-) mice in a FVB background was readily apparent. The absence of tumorigenesis and a reduced number of hyperplastic lesions was observed in the 12-month old NeuNDL Postn$^{+/-}$ mice (Postn +/-*) in a mixed FVB/C57 background.

A

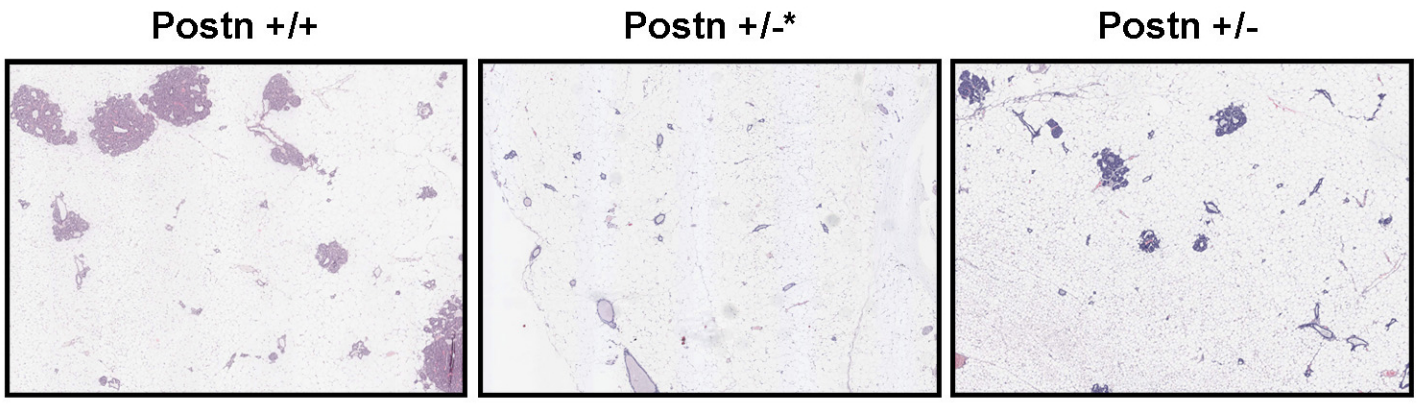
Postn +/+
Postn +/-*
Postn +/-

B

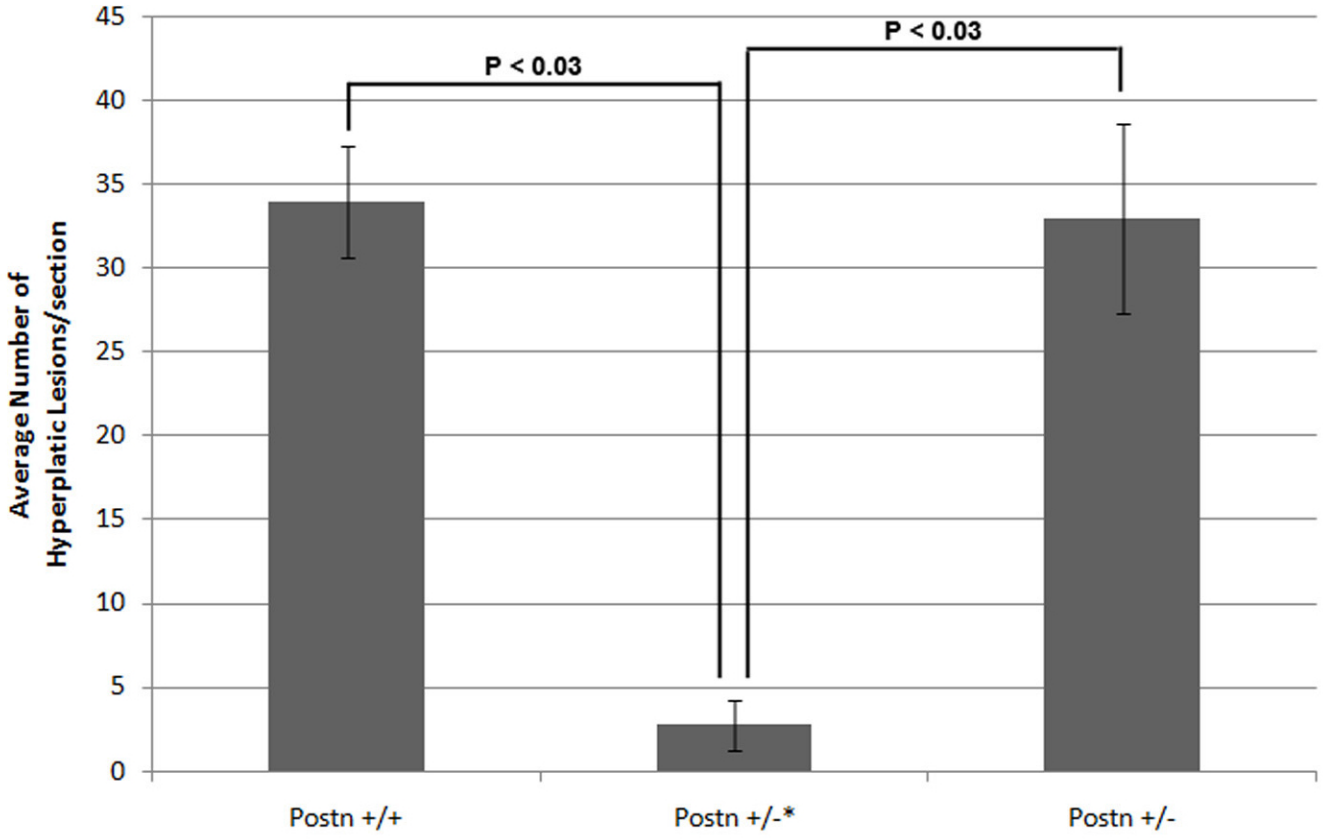
P < 0.03
P < 0.03
Average Number of Hyperplatic Lesions/section
45
40
35
30
25
20
15
10
5
0
Postn +/+
Postn +/-*
Postn +/-

Figure 18: NeuNDL Postn$^{+/-}$ mice in a mixed FVB/C57 background developed significantly fewer hyperplastic lesions in their mammary glands compared to NeuNDL Postn$^{+/+}$ and Postn$^{+/-}$ mice in a pure FVB background. A) Representative ScanScope images of hematoxylin and eosin stained paraffin-embedded mammary gland sections from a 12-month old NeuNDL Postn$^{+/-}$ mouse (Postn +/-*) in a mixed FVB/C57 background and a 6-month old NeuNDL Postn$^{+/-}$ (Postn +/-) mouse in a FVB background. A mammary gland section of a 6-month old NeuNDL Postn$^{+/+}$ (Postn +/+) mouse in a FVB background is shown for comparison. B) Quantification of the number of hyperplastic lesions that was greater than 10^4 µm^2 in Postn +/+, Postn +/-*, and Postn +/- mice (n = 4 for each genotype). All the mice are NeuNDL transgenic.

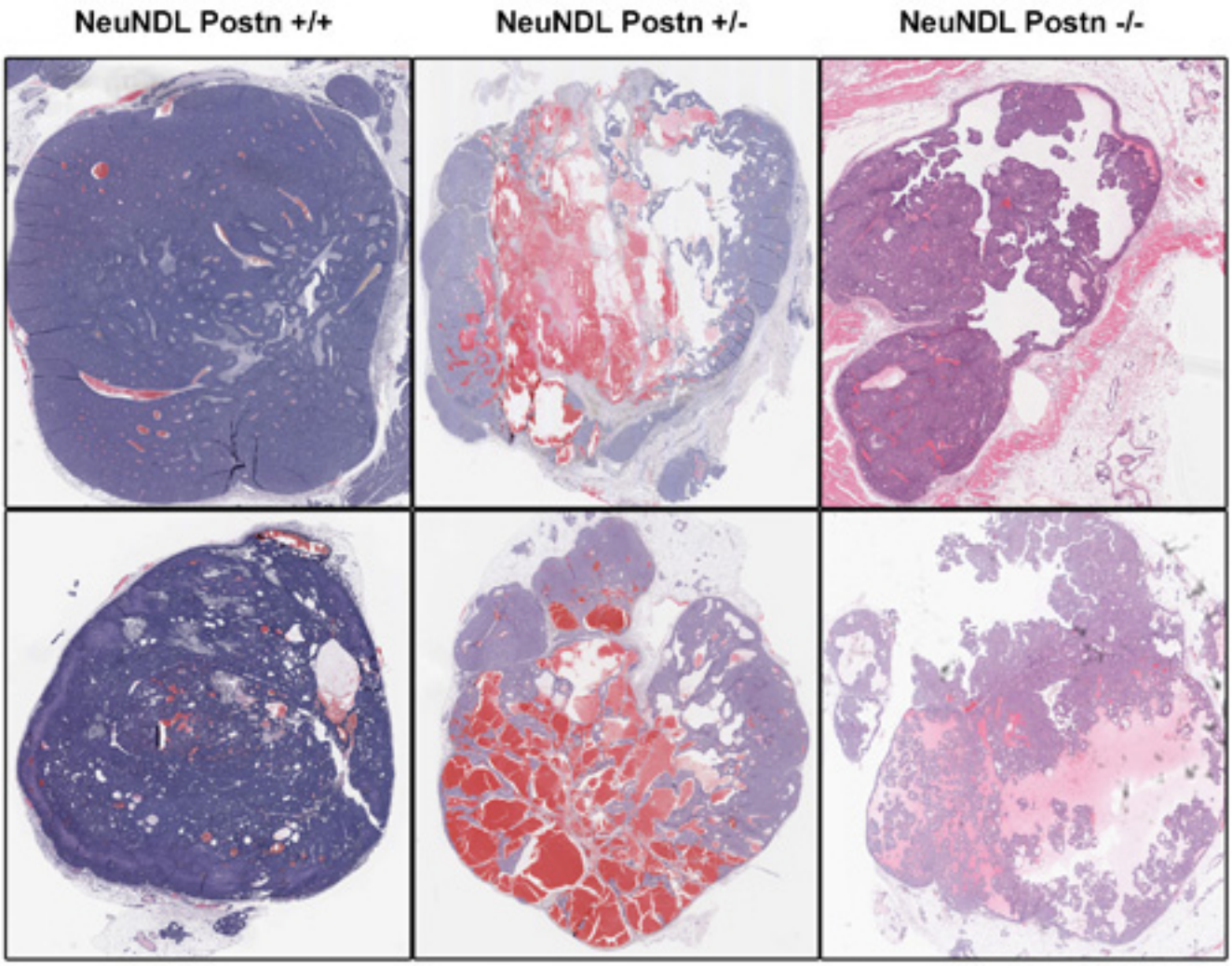
NeuNDL Postn +/+
NeuNDL Postn +/-
NeuNDL Postn -/-

Figure 19: Tumors from NeuNDL Postn$^{+/-}$ and Postn$^{-/-}$ mice in a FVB background are more cystic and less solid than tumors from NeuNDL Postn$^{+/+}$ mice in a FVB background. ScanScope images of two representative paraffin-embedded, hematoxylin and eosin stained mammary gland tumors from virgin NeuNDL Postn$^{+/+}$, Postn$^{+/-}$, and Postn$^{-/-}$ female mice in a FVB background at end point.

and Postn$^{-/-}$ mice compared to NeuNDL Postn$^{+/+}$ mice was unexpected as overexpression of periostin in human breast cancers leads to a significant enhancement of angiogenesis [95]. Based on these results, it cannot be concluded that the NeuNDL Postn$^{+/-}$ and Postn$^{-/-}$ tumors are hypervascularized compared to the NeuNDL Postn$^{+/+}$ tumors, but only that they are hyperemic.

Upon pathological analysis of NeuNDL Postn$^{+/+}$, Postn$^{+/-}$, and Postn$^{-/-}$ tumors from mice in a FVB background, it was determined that the type of tumor does not change. However, morphologically, NeuNDL Postn$^{+/-}$ and Postn$^{-/-}$ tumors are less solid and more cystic compared to NeuNDL Postn$^{+/+}$ tumors (Figure 19). A regular myoepithelial layer was also absent among all these tumors. Based on human pathology characteristics, these tumors are compatible with intracystic/encapsulated intraductal papillary carcinomas. This means that although these tumors are less cellular, they are not necessarily less invasive or aggressive.

In addition to the more cystic nature of tumors from the NeuNDL Postn$^{+/-}$ mice in the FVB background, there appears to be a reduction in tumor cell number. Due to this difference observed among NeuNDL tumors in FVB mice, the hyperplastic lesions of 6-month old NeuNDL Postn$^{+/+}$ and Postn$^{+/-}$ mice in a FVB background were analyzed for the cellularity of hyperplasia.

The surface area composed of cancer cells in mammary gland lesions was quantified by calculating the hyperplastic cell area of the lesions. The ratio of the area composed of cancer cells to the entire hyperplastic lesion was then calculated. In the NeuNDL Postn$^{+/+}$ mice, 91.7% of the hyperplastic lesions (22/24) had more than 90% cellularity compared to only 20.8% of the hyperplastic lesions (5/24) from NeuNDL Postn$^{+/-}$ mice (Figure 20A). It is also important to note that 20.8% of the hyperplastic lesions (5/24) from NeuNDL Postn$^{+/-}$ mice had less than 70% cellularity (Figure 20A). Overall, there was a significant difference in the cellularity of hyperplasias of 6-month old NeuNDL Postn$^{+/+}$ and Postn$^{+/-}$ mice in a FVB background.

Similarly, the surface area composed of cancer cells in mammary gland tumors was quantified by calculating the tumor cell area of the tumor. The ratio of the area composed of cancer cells to the entire tumor was then calculated. In the NeuNDL Postn$^{+/-}$ and Postn$^{-/-}$ tumors,

A

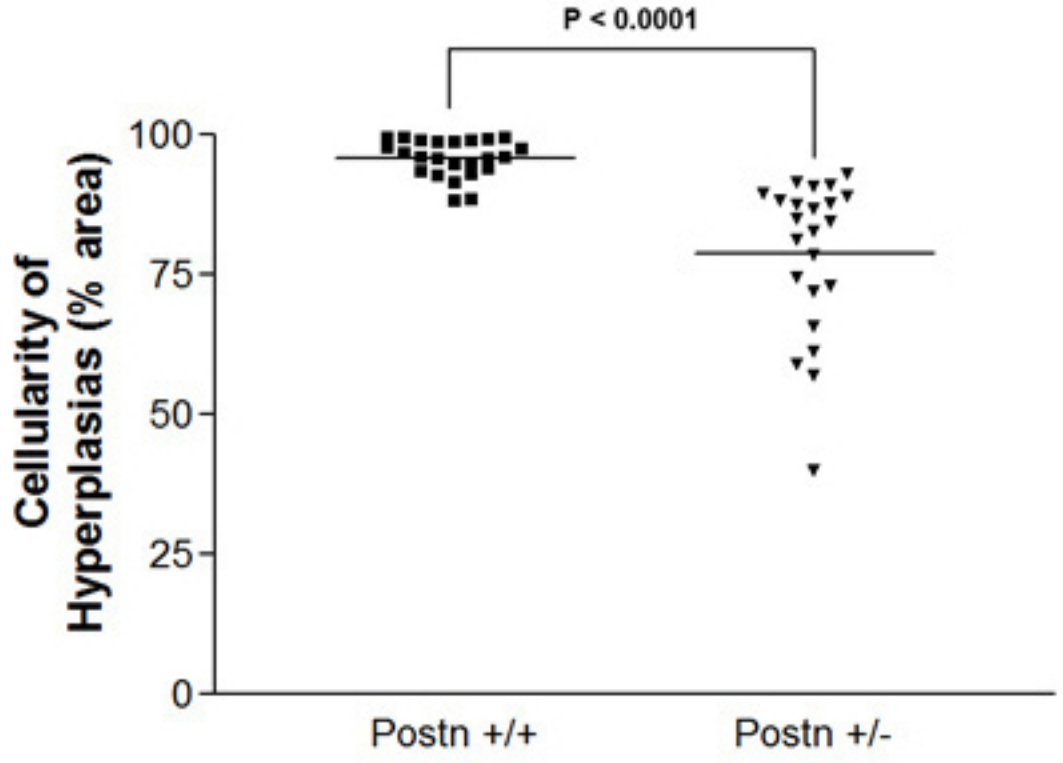
P < 0.0001
Cellularity of Hyperplasias (% area)
100
75
50
25
0
Postn +/+
Postn +/-

B

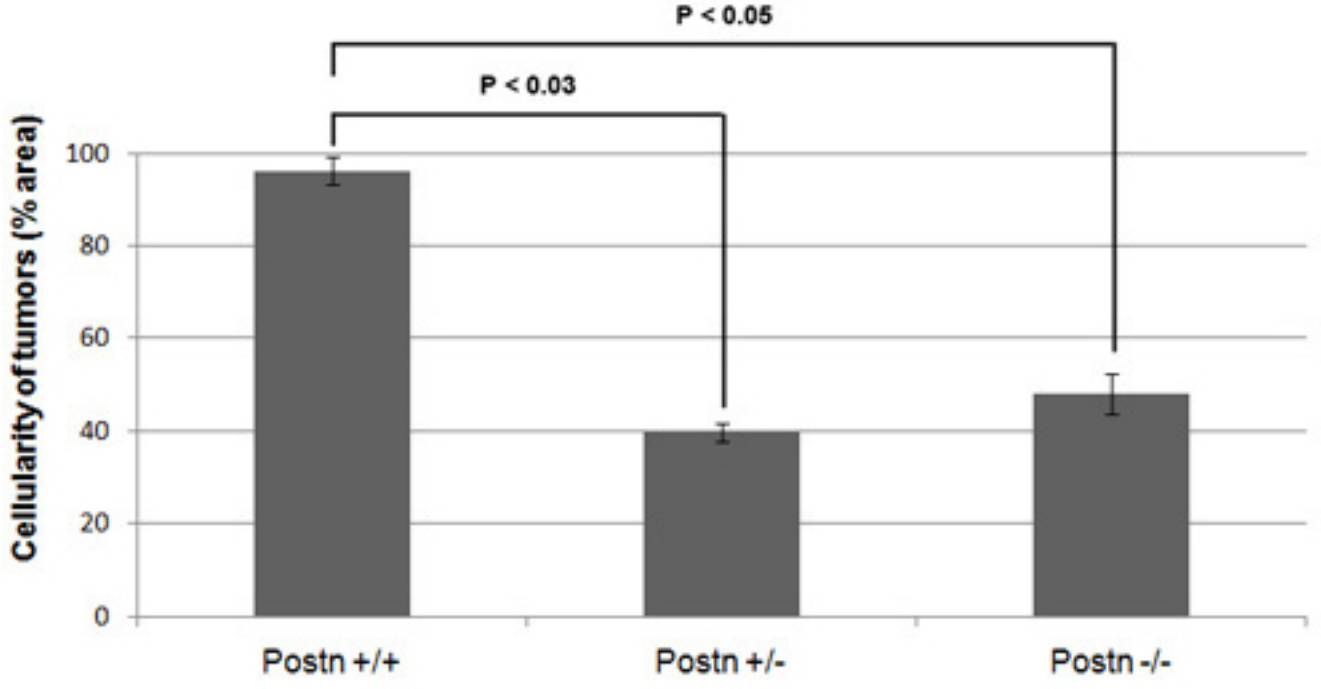
P < 0.05
P < 0.03
Cellularity of tumors (% area)
100
80
60
40
20
0
Postn +/+
Postn +/-
Postn -/-

Figure 20: Cellularity of hyperplasias and tumors in NeuNDL mice. A) Cellularity of hyperplasias in NeuNDL Postn$^{+/-}$ (Postn +/-) hyperplastic lesions compared to that of NeuNDL Postn$^{+/+}$ (Postn +/+) hyperplastic lesions. The ratio of cancer cell area to the entire hyperplastic lesion was calculated for 6-month old NeuNDL Postn$^{+/+}$ and NeuNDL Postn$^{+/-}$ mice in a FVB background. B) Cellularity of tumors in NeuNDL Postn$^{+/-}$ (Postn +/-) and NeuNDL Postn$^{-/-}$ (Postn -/-) tumors compared to that of NeuNDL Postn$^{+/+}$ (Postn +/+) tumors. The ratio of cancer cell area to the entire tumor was calculated for 2 tumors in 6-month old Postn +/+, 6-month old Postn +/-, and 8-month old Postn -/- mice in a FVB background.

there was about a 2-fold decrease in cellularity of tumors when compared to the NeuNDL Postn$^{+/+}$ tumors (Figure 20B). Taken together, these results suggest that the tumor cellularity of NeuNDL Postn$^{+/+}$ is higher than of NeuNDL Postn$^{+/-}$ and Postn$^{-/-}$ mice since the majority of NeuNDL Postn$^{+/+}$ tumors are occupied by tumor cells whereas the majority of NeuNDL Postn$^{+/-}$ and Postn$^{-/-}$ tumors are occupied by cystic cavities.

3.6 Periostin-Deficient Mice Retain ErbB2/Neu Expression

In human breast tumor tissues, periostin was reported to be highly expressed in the stromal cells immediately surrounding the tumor, but not within the breast tumor itself [37]. Supporting this is our immunohistochemical analysis of periostin. FVB NeuNDL Postn$^{+/+}$ and Postn$^{+/-}$ mammary glands and tumors show periostin expression in the stromal fibroblasts of the mammary glands and around the epithelial mammary tumors (Figure 21A). It was undetectable in the epithelial cells of the mammary glands or within the epithelial mammary tumor cells (Figure 21A). Importantly, periostin is not expressed in the stromal cells of the mammary gland or the surrounding epithelial tumor of FVB NeuNDL Postn$^{-/-}$ mice (Figure 21A). On the other hand, immunohistochemical analysis of ErbB2/Neu in FVB NeuNDL Postn$^{+/+}$, Postn$^{+/-}$, and Postn$^{-/-}$ mammary glands and tumors demonstrates that ErbB2/Neu expression is maintained and is primarily detected in the epithelial cells of the mammary tumors (Figure 21A).

NeuNDL Postn$^{+/+}$, Postn$^{+/-}$, and Postn$^{-/-}$ mice in a FVB background are apparently capable of developing mammary gland tumors regardless of the level of periostin. We were interested in comparing the level of ErbB2/Neu expression in FVB NeuNDL Postn$^{+/+}$, Postn$^{+/-}$, and Postn$^{-/-}$ tumors. Our immunohistochemical analysis demonstrated that ErbB2/Neu expression is retained even in FVB NeuNDL Postn$^{-/-}$ tumors. ErbB2/Neu Western blot analysis shows that the expression of ErbB2/Neu is similar among FVB NeuNDL Postn$^{+/+}$, Postn$^{+/-}$, and Postn$^{-/-}$ tumors (Figure 21B). Therefore, periostin ablation does not alter ErbB2/Neu expression in the mammary gland tumors of NeuNDL transgenic mice.

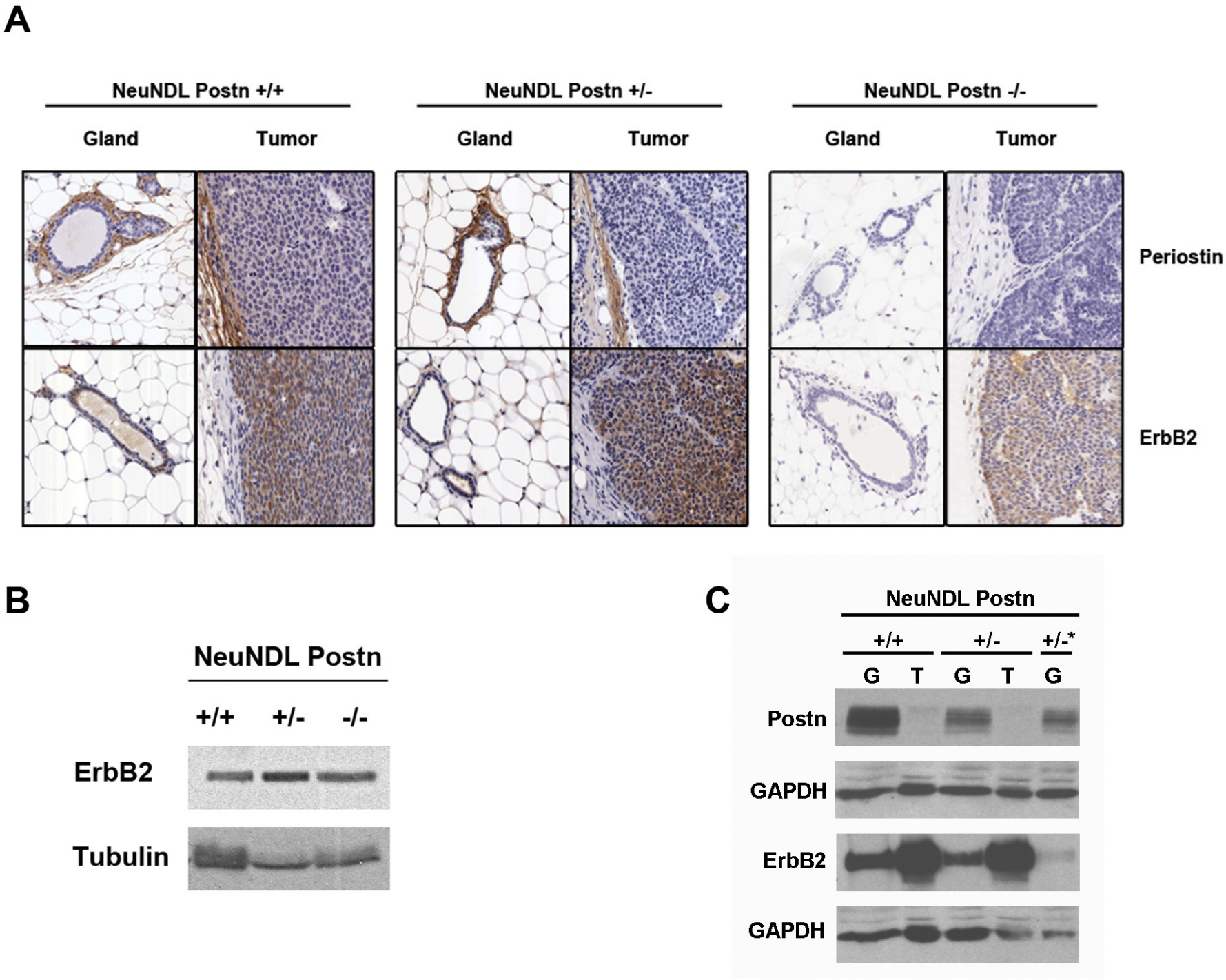
A
NeuNDL Postn +/+
NeuNDL Postn +/-
NeuNDL Postn -/-
Gland
Tumor
Gland
Tumor
Gland
Tumor
Periostin
ErbB2
B
NeuNDL Postn
+/+
+/-
-/-
ErbB2
Tubulin
C
NeuNDL Postn
+/+
+/-
+/-*
G
T
G
T
G
Postn
GAPDH
ErbB2
GAPDH

Figure 21: Periostin and ErbB2/Neu expression in FVB NeuNDL whole mammary glands and tumors. A) ScanScope images of immunohistochemical analysis of periostin and ErbB2/Neu expression (brown) of paraffin-embedded mammary gland and tumor sections from FVB NeuNDL Postn$^{+/+}$, Postn$^{+/-}$, and Postn$^{-/-}$ mice. The sections were subsequently counterstained with hematoxylin (blue). B) Western blot analysis of ErbB2/Neu expression in FVB NeuNDL Postn$^{+/+}$, Postn$^{+/-}$, and Postn$^{-/-}$ tumors. Gamma-tubulin was used as a loading control. C) Western blot analysis of periostin and ErbB2/Neu expression in FVB NeuNDL mammary glands (G) and tumors (T). The mammary gland of a NeuNDL Postn$^{+/+}$ and Postn$^{+/-}$ in a FVB background was compared to the mammary gland of a NeuNDL Postn$^{+/-}$ (+/-*) in a mixed FVB/C57 background. GAPDH was used as a loading control.

Supporting the immunohistochemistry data, Western blot analysis of periostin shows higher expression in the mammary gland compared to the tumor samples (Figure 21C). In contrast, ErbB2/Neu is expressed higher in the mammary tumor samples when compared to the mammary gland samples (Figure 21C). Together, this data suggests that ErbB2/Neu is predominately expressed in the epithelium of mammary tumors and that periostin is primarily expressed in the stromal compartment of mammary glands and not upregulated in the tumor epithelium.

Antigen Ki-67 is a nuclear protein for which the expression has been correlated with cellular proliferation. The fraction of Ki-67-positive tumor cells is often also correlated with cancer progression. The reduced cellularity of tumors of periostin-deficient tumors prompted us to examine the proportion of Ki-67 positive cells. Mammary tumor sections of NeuNDL $Postn^{+/+}$, $Postn^{+/-}$, and $Postn^{-/-}$ mice in a pure FVB background was stained for Ki-67 using immunohistochemical analysis (Figure 22A). Ki-67 expression and positivity was significantly decreased in NeuNDL $Postn^{+/-}$ and $Postn^{-/-}$ tumors relative to NeuNDL $Postn^{+/+}$ tumors (Figure 22B). This suggests that periostin is required *in vivo* for HER2/ErbB2-induced cell proliferation. Interestingly a threshold level of periostin appears to be necessary since $Postn^{+/-}$ tumors present with a similar Ki-67 phenotype.

Cyclins are a family of proteins that control the progression of cells through the cell cycle by activating cyclin-dependent kinases [131]. They are named so because their concentration varies in a cyclical fashion during the cell cycle; they are produced or degraded as needed in order to drive the cell through the different stages of the cell cycle [131]. There are two main groups of cyclins: G1/S cyclins and G2/M cyclins, which are essential for the control of the cell cycle at the G1/S transition and the G2/M transition (mitosis), respectively [131]. Cyclin D is a member of the G1/S cyclins that is involved in regulating cell cycle progression. The synthesis of cyclin D is initiated during G1 and drives the G1/S phase transition.

A

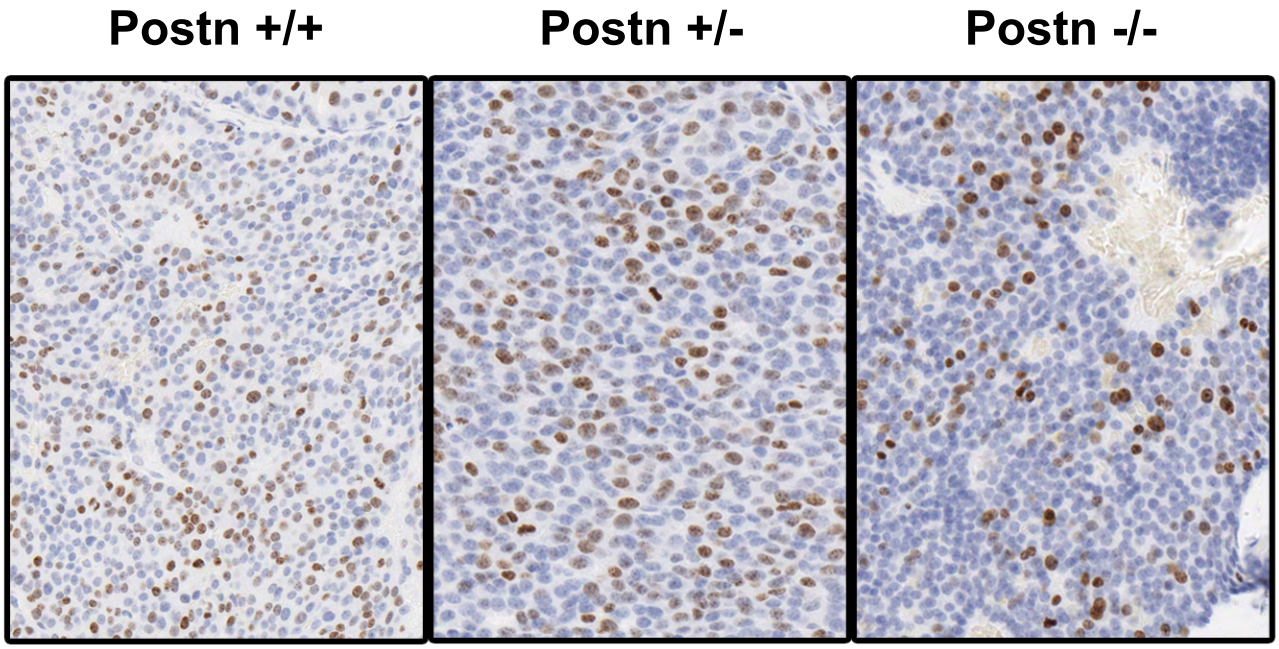
Postn +/+
Postn +/-
Postn -/-

B

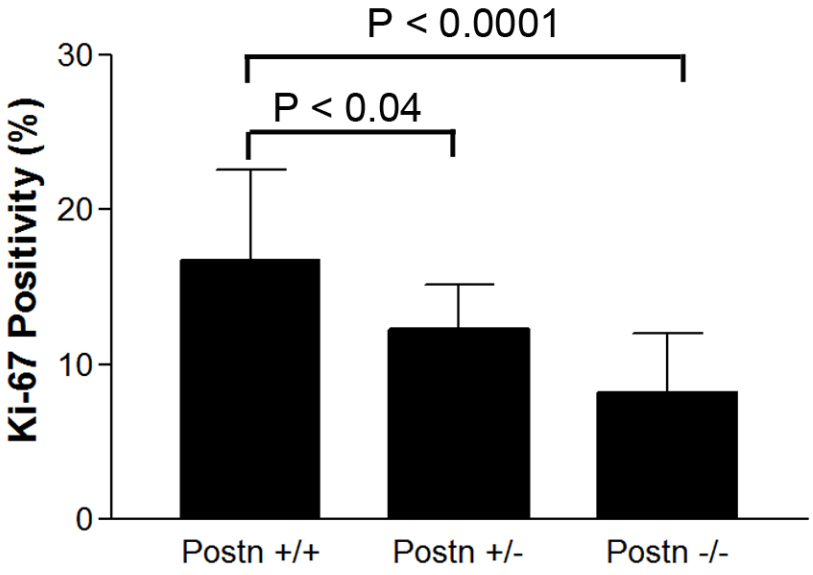
P < 0.0001
P < 0.04
Ki-67 Positivity (%)
30
20
10
0
Postn +/+
Postn +/-
Postn -/-

C

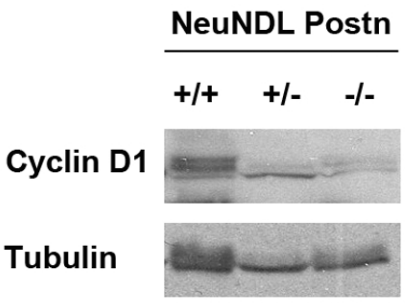
NeuNDL Postn
+/+
+/-
-/-
Cyclin D1
Tubulin

Figure 22: Ki-67 expression and positivity in tumors of NeuNDL Postn$^{+/+}$, Postn$^{+/-}$, and Postn$^{-/-}$ mice in a pure FVB background. A) Representative ScanScope images of immunohistochemical analysis of Ki-67 expression (brown) of paraffin-embedded tumor sections of NeuNDL Postn$^{+/+}$, Postn$^{+/-}$, and Postn$^{-/-}$ mice in a pure FVB background. The sections were subsequently stained with hematoxylin (blue). B) Quantification of Ki-67 expression in tumors of NeuNDL Postn$^{+/+}$, Postn$^{+/-}$, and Postn$^{-/-}$ mice in a pure FVB background. To calculate Ki-67 positivity, the total number of positive pixels (brown) was divided by the total number of pixels (positive and negative). C) Western blot analysis of cyclin D1 expression in FVB NeuNDL Postn$^{+/+}$, Postn$^{+/-}$, and Postn$^{-/-}$ tumors. Gamma-tubulin was used as a loading control.

Cyclin D1, a G1/S-specific protein, is expressed in most proliferating cells and the relative amounts expressed differs in various cell types [132]. Therefore, a Western blot analysis of cyclin D1 was performed on tumors from NeuNDL Postn$^{+/+}$, Postn$^{+/-}$, and Postn$^{-/-}$ mice in a FVB background to validate our Ki-67 immunohistochemistry data (Figure 22C). Overall, cyclin D1 expression seems to be decreased in NeuNDL Postn$^{+/-}$ and Postn$^{-/-}$ tumors, which corresponds to the Ki-67 positivity data. The cyclin D1 Western blot analysis showed multiple bands. An explanation is that the cyclin D1 antibody recognizes or cross reacts with cyclin D2 and cyclin D3, which is 34 and 33 kDa, respectively as well as isoforms of cyclin D1.

3.7 Effect of Periostin on Cell Proliferation and Migration *In Vitro*

Periostin, an adhesion molecule, is able to promote the attachment and migration of epithelial cells [117]. Angiogenesis can regulate tumor growth and periostin can induce up-regulation of VEGFR-2 [95]. Periostin can also stimulate cell survival through evasion of apoptosis. However, the role of periostin on cell proliferation depends on the microenvironment, whether *in vitro* or *in vivo*.

In order to look at the effect of periostin stimulation *in vitro*, tumor-bearing FVB NeuNDL mice were sacrificed and primary mammary tumor epithelial cell cultures were established. These cells were seeded on plates coated with BSA (5%), collagen (10 µg/ml), or periostin (5 µg/ml) prior to the proliferation assay. Initially, 3 x 10^5 cells were plated on the various substrates and monitored for proliferation over time. Surprisingly, after 9 days, the various substrate-coated cell culture plates each had a similar number of cells (Figure 23). This suggests that the presence of periostin or collagen alone does not affect the proliferation of mammary tumor epithelial cells *in vitro* compared to the BSA control (Figure 23).

To test the role of periostin on epithelial cell migration, primary mammary tumor epithelial cells were infected with a periostin adenovirus and plated on non-coated plates. Also, uninfected primary mammary tumor epithelial cells were plated on non-coated plates as well as

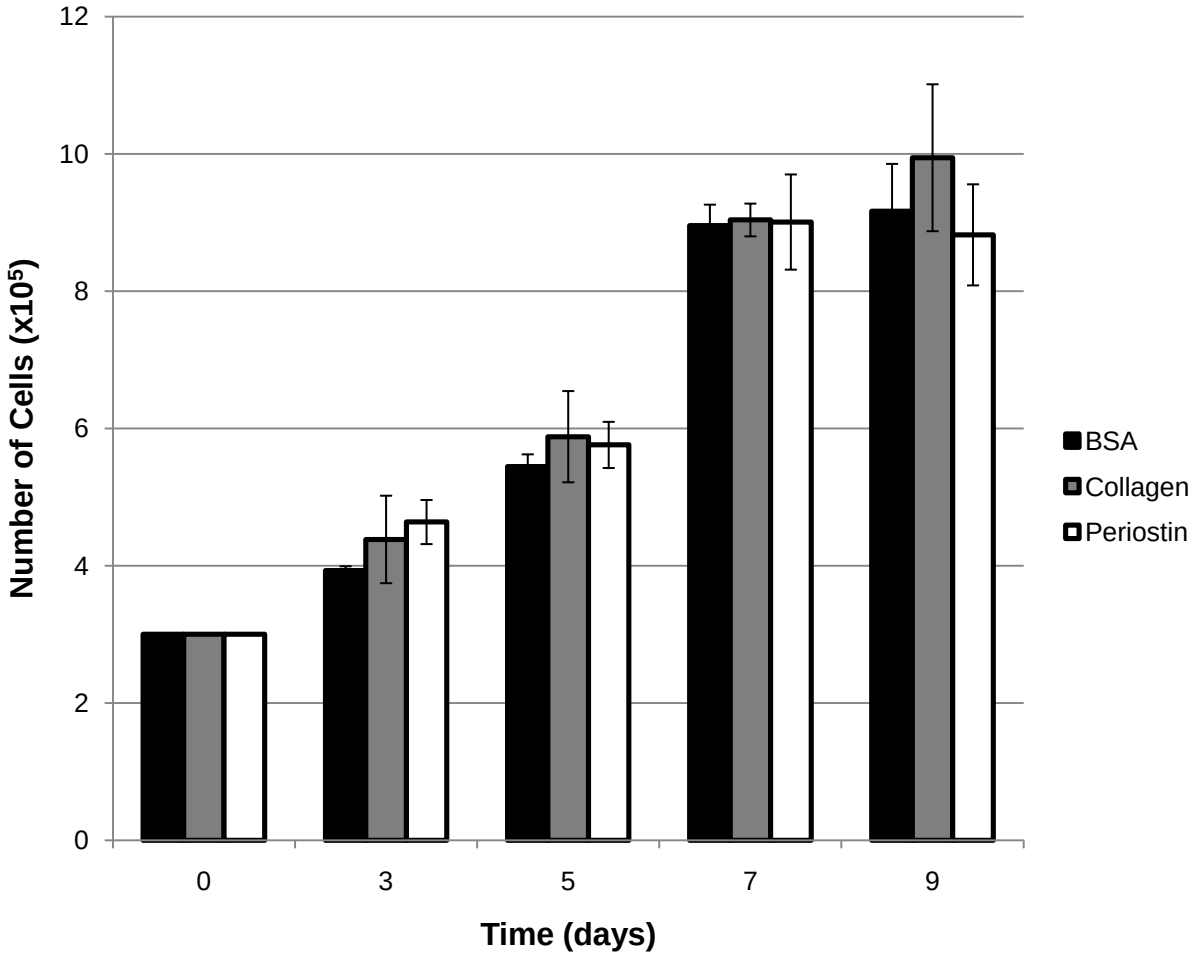
12
10
8
6
4
2
0
Number of Cells (x10⁵)
0
3
5
7
9
Time (days)
BSA
Collagen
Periostin

Figure 23: Presence of periostin or collagen does not affect the proliferation of ErbB2/Neu-overexpressing mammary tumor epithelial cells *in vitro*. *In vitro* proliferation assay of mammary tumor epithelial cells in the presence of periostin (5 µg/ml), collagen (10 µg/ml), or BSA (5%) control. 3×10^5 cells were plated on day 0. On day 3, 5, 7, and 9, the cells were trypsinized and counted in triplicates (n = 3).

plates coated with BSA (5%), collagen (10 µg/ml), or periostin (5 µg/ml) prior to the scratch induced migration assay. Treated cells were scratch-wounded and allowed to migrate for 24 hours (Figure 24A). The rate of migration was based on the percent wound closure, evaluated after 24 hours.

Overall, our results show that periostin overexpression had no effect on the migration of primary tumor epithelium (Figure 24A). However, there was a significant increase in cell migration when uninfected cells were plated on collagen-coated plates ($P = 0.01$) (Figure 24A). But, the presence of BSA or periostin on plates did not affect the migration of uninfected mammary tumor epithelial cells *in vitro* compared to cells on non-coated plates. The efficiency of the periostin adenovirus infection used to overexpress periostin in mammary tumor epithelial cells was verified by Western blot analysis (Figure 24C). In contrast to our *in vivo* findings, these results suggest that periostin does not affect the growth or migration of primary mammary tumor epithelial cells overexpressing ErbB2/Neu *in vitro*. One possibility is that additional ECM proteins or growth factors are required.

A

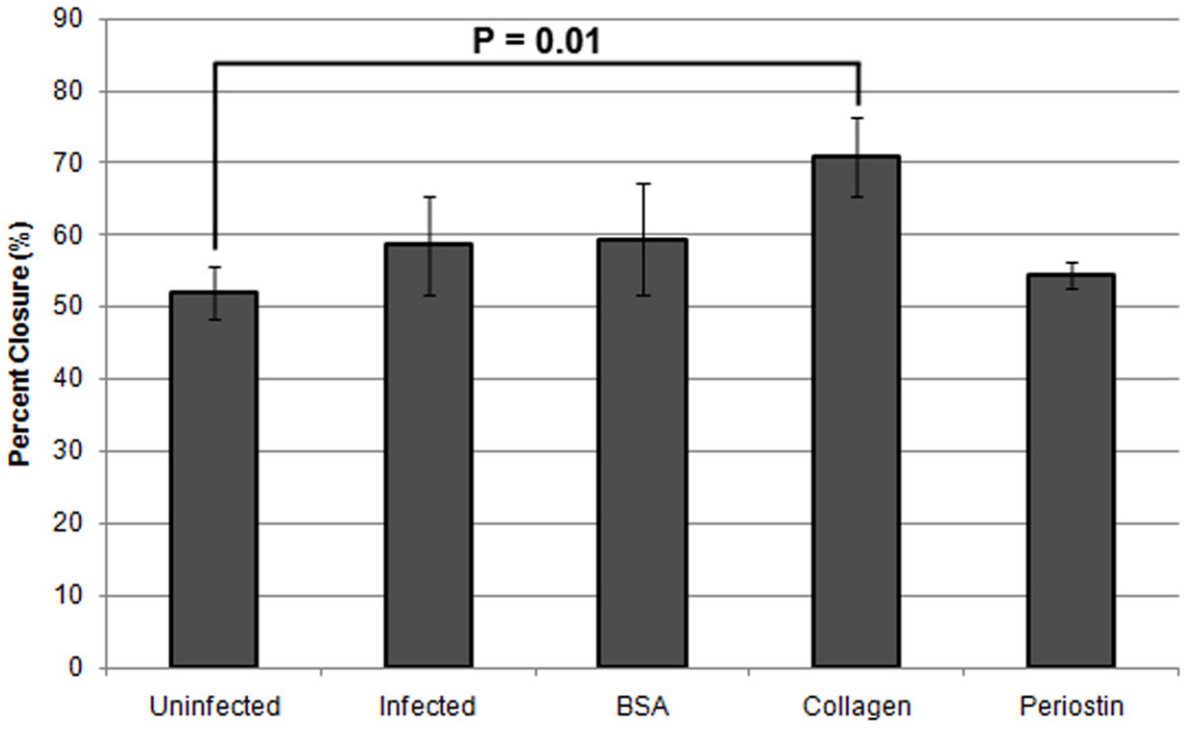
P = 0.01
Percent Closure (%)
90
80
70
60
50
40
30
20
10
0
Uninfected
Infected
BSA
Collagen
Periostin

B

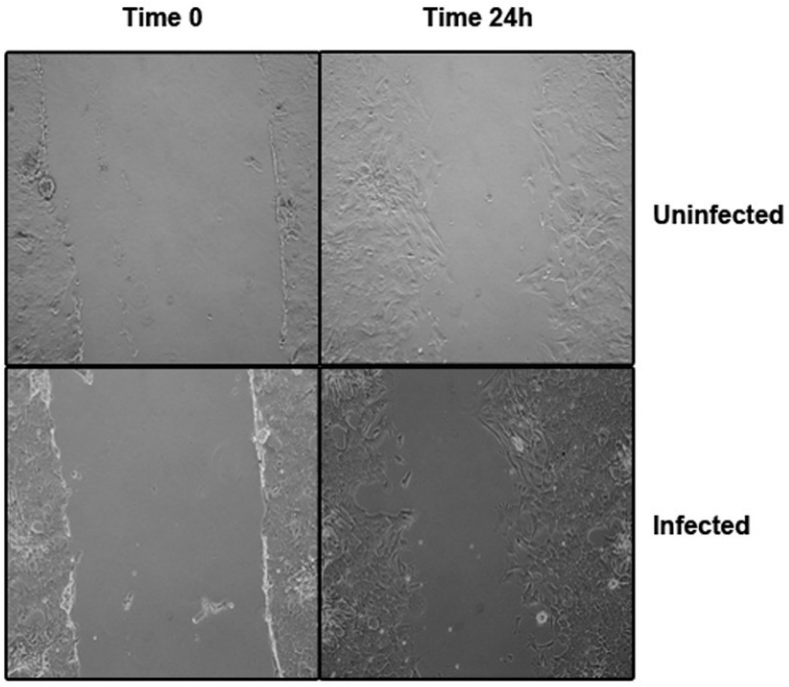
Time 0
Time 24h
Uninfected
Infected

C

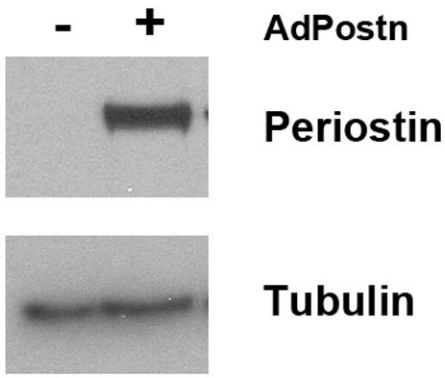
-
+
AdPostn
Periostin
Tubulin

Figure 24: Collagen but not periostin increases mammary tumor epithelial cell migration. A) Quantification of the *in vitro* scratch induced migration assay. *In vitro* migration assay of uninfected mammary tumor epithelial cells in the presence of 5% BSA-, 10 µg/ml collagen-, or 5 µg/ml periostin-coated cell culture plates when compared to uninfected mammary tumor epithelial cells and periostin adenovirus infected mammary tumor epithelial cells (n = 4). The rate of migration was based on the percent wound closure. B) Representative pictures from an inverted phase-contrast microscope of mammary tumor epithelial cells at time 0 and 24 h of an *in vitro* scratch induced migration assay. C) Western blot analysis of primary mammary tumor epithelial cells infected with and without periostin adenovirus prior to the migration assay. Note the increase in periostin expression in cells that were infected with the periostin adenovirus.

4. Discussion

4.1 Periostin is Dispensable for Mammary Ductal Outgrowth

The cell-cell and cell-microenvironment interactions modify the proliferation, survival, polarity, differentiation, and invasive capacity of mammary epithelial cells [133]. As an ECM protein, there is increasing evidence that periostin is involved in tumor progression, through evasion of apoptosis, induction of angiogenesis, as well as promotion of tumor invasion and metastasis [105, 117]. Since periostin has been shown to have a role in tumor progression, it was hypothesized that periostin ablation may influence breast cancer progression.

Periostin, a matricellular protein, has a functional role during bone, teeth, skin, and cardiac development. It also has a role in wound repair, such as after myocardial, vascular, and skeletal muscle injuries or bone fracture [104, 117]. Before testing the role of periostin in mammary tumorigenesis, it was imperative to determine its function in mammary gland development. In order to address this issue, $Postn^{-/-}$ mice in an inbred FVB background were generated by backcrossing periostin *lacZ* knock-in mice [114] in a C57Bl/6 background with pure FVB mice for five generations using MAX-BAX® analysis for FVB content. $Postn^{-/-}$ mice were analyzed by PCR, Western blot, and immunohistochemical analysis.

The mammary gland is composed of epithelium and stroma, a combination of multiple cell types that together form the complex interaction networks required for the proper development and functioning of the organ [133, 134]. In the mammary glands of $Postn^{+/+}$ and $Postn^{+/-}$ mice, periostin was expressed predominately in the stroma and absent in the epithelial cells. In the mammary glands of $Postn^{-/-}$ mice, it was undetectable. Since periostin is known to be a secreted cell adhesion protein, this suggests that it is produced by the stromal fibroblasts within the mammary gland. This may induce cell invasive activity through activation of EMT in the mammary gland of breast cancer patients.

The mammary gland is very unique because it is one of a few organs where major morphogenetic changes take place after birth, during puberty and pregnancy [135]. The rudimentary epithelial tree in the mammary fat pad remains quiescent until puberty onset, when ovarian steroid hormone production commences and induces ductal outgrowth [136]. At this time, bulbous structures on the tips of the ducts, known as the terminal end buds, are highly proliferative and penetrate into the fat pad as the ducts elongate [136]. They bifurcate and secondary branches form during this process, until the entire fat pad is filled with a network of branched ducts [136]. The huge amount of proliferation that accompanies this change occurs in a discrete and controlled fashion [136].

In the nulliparous Postn$^{+/+}$ mammary glands, these branching ducts were distinguished by an outer myoepithelial cell layer producing the basement membrane and an inner luminal epithelial cell layer. These structures were comparable in the Postn$^{+/-}$ and Postn$^{-/-}$ mammary glands, with no overt defects. The thin, branched epithelial ducts that are characteristic of non-pregnant mammary glands undergo dramatic alterations in pregnancy, when new types of epithelial structures, the milk-producing alveoli or lobules, emerge. These characteristics of mammary gland development were observed in the nulliparous and pregnant Postn$^{-/-}$ mice, respectively. Together, these results suggest that periostin, which is normally expressed in the stroma of the mammary gland, is not required for mammary ductal outgrowth during development or pregnancy. This would imply that female Postn$^{-/-}$ mice would be able to lactate normally and nurse their offspring.

Indeed, we observed that female FVB Postn$^{-/-}$ mice were able to produce viable litters through multiple rounds of pregnancy. Moreover, female FVB Postn$^{+/+}$, Postn$^{+/-}$, and Postn$^{-/-}$ mice had very similar weights when followed for 9 weeks, with no signs of growth retardation when compared to growth-impaired C57Bl/6 Postn$^{-/-}$ mice. An explanation for the differences in characteristics is likely their genetic background. The previous characterization of Postn$^{-/-}$ mice was in a pure C57Bl/6 background, whereas our Postn$^{-/-}$ mice were in a pure FVB background.

This suggests that the genetic background may contribute to the observed difference in phenotype due to the penetrance of periostin ablation in the different genetic backgrounds.

4.2 The Role of Periostin in Mammary Tumorigenesis

In the human population, genetic variation significantly influences susceptibility to disease. For example, genetic alterations such as overexpression of *HER2/ErbB2/Neu* can increase the incidence of breast cancer. Since the HER2/ErbB2/Neu proto-oncogene is amplified and overexpressed in 20-30% of human breast cancers [11], other modifier genes, as well as the environment, could influence disease penetrance. To affect disease penetrance, modifier genes may act by affecting breast tumor latency, multiplicity, and/or progression. It is difficult to evaluate the relative contributions of modifier genes in breast carcinogenesis because of the independent segregation of multiple alleles at multiple modifier loci.

However, inbred strains of model organisms such as the mouse have been used to control environmental influences, homogenize tumor histologies, and reduce the complexity of genetic backgrounds [137]. Inbred mice permit the assessment of disease phenotype in the presence of only a single allele at each modifier locus. This genetic uniformity is advantageous because it allows for precise characterization of tumor progression in individuals of identical genotypes. This advantage also applies to the study of mammary carcinogenesis in genetically engineered mice, in which the effect of oncogene or growth factor overexpression, or loss of tumor suppressor gene expression can be investigated in a uniform host population.

On the contrary, genetic uniformity can also be a disadvantage because extrapolation from models generated in only a single inbred mouse strain to the much more genetically variable human population will provide only a partial view of how breast carcinogenesis is influenced by modifier genes. In an outbred strain, individual genetic differences may affect transgene expression and consequent phenotype. In mice, as in humans, genotype can modify the phenotype associated with expression of cancer-related genes.

In transgenic animals, modifier genes can influence not only the downstream cellular and tissue responses to transgene expression, but also alter the temporal pattern and level of transgene expression, by way of their influence on gene regulatory sequences contained within the transgene construct. Transgenic mice have often been created in the inbred FVB strain due to its high fecundity and its susceptibility to breast cancer formation [138, 139]. Transgenic mouse models that develop spontaneous mammary carcinomas have proven valuable in revealing molecular mechanisms underlying tumorigenesis and metastasis [140, 141]. Specifically, the MMTV-based *Neu* transgenic mouse models, which have identified many target genes that control cell cycle and survival that function downstream of, or in concert with, HER2/ErbB2 to promote breast cancer progression [58].

The MMTV-*NeuNDL* mouse mammary tumor model was used to study the role of periostin in tumorigenesis. In the mixed FVB/C57 background, NeuNDL Postn$^{+/-}$ mice had a significant increase in tumor latency with very few hyperplastic lesions developing by 12 months of age. In the pure FVB background, NeuNDL Postn$^{+/+}$ and Postn$^{+/-}$ mice displayed tumor onset as early as 5 months of age with multiple hyperplastic lesions within their mammary glands. This resulted in tumorigenesis and shorter life span among the NeuNDL Postn$^{+/+}$ and Postn$^{+/-}$ mice in a FVB background compared to the NeuNDL Postn$^{+/-}$ mice in a mixed FVB/C57 background. One possibility is that *NDL* and/or *periostin* may have a higher penetrance in FVB mice compared to the mixed FVB/C57 background mice, allowing for more aggressive tumor progression in a shorter period of time. Therefore, the genetic make-up may influence the penetrance of *NDL* or *periostin* resulting in different phenotypes even with the same genotype.

To support this conclusion, different mouse strains have already been shown to affect transgene expression and phenotype due to strain-specific modifiers [130, 142, 143]. Numerous reports have documented strain-related differences in physiology and tumor pathogenesis for inbred mouse strains [130, 144]. For example, in transgenic mice that expresses TGF-α under the whey acidic protein promoter, mixed FVB/C57 background mice suppress mammary tumor

development when compared to those in the FVB background [129]. Also, the C57Bl/6 strain is more resistant while the FVB strain is more susceptible to PyMT mammary tumors [138, 145]. Furthermore, C57Bl/6 mice transgenic for the activated *Neu* proto-oncogene crossed into the BALB/c background showed a significant increase in tumor latency in the first five generations of backcrosses [146]. However, mixed FVB/C57 background versus pure FVB background did not show any significant differences in MMTV-*myc* and MMTV-*ras* induced mammary tumors, suggesting differential molecular pathways leading to tumorigenesis [147]. In general, C57Bl/6 mice seem to be less susceptible to transgene induced tumor development.

Most importantly, genetic modifiers have been shown to modulate mammary tumor latency in the MMTV-*Neu* mouse model of breast cancer. Mice in a mixed FVB/C57 background have increase latency for MMTV-*Neu* induced mammary tumors when compared to a pure FVB background [130]. Pure FVB MMTV-*Neu* female mice developed mammary tumors between 7 and 12 months of age, whereas mixed FVB/C57 MMTV-*Neu* mice had tumor latencies greater than 18 months [130]. This is consistent with our observations where FVB NeuNDL Postn$^{+/-}$ mice developed mammary tumors between 5 and 10 months of age, whereas mixed FVB/C57 NeuNDL Postn$^{+/-}$ mice had tumor latencies greater than 12 months. The early onset of tumorigenesis was correlated with an increase in hyperplastic lesions in the mammary glands and a shorter survival.

Strain-dependent modulation of mammary tumor latency in MMTV-*Neu* mice is likely influenced by discrete genetic susceptibility elements rather than modulation of transgene expression alone. C57Bl/6 mice may have genetic elements such as tumor suppressor genes that suppress the ability of mammary tumor induction in MMTV-*NeuNDL* transgenic mice. It is equally likely that FVB mice possess mutant or defective copies of tumor suppressor genes, thus allowing HER2/ErbB2-induced mammary tumor development to occur at a more rapid rate. Thus, different strain backgrounds display varying susceptibility to specific cancers. Therefore,

the importance of the strain background used in an experimental model is particularly relevant to genetically engineered mice.

4.3 Role of Periostin in Tumor Cell Proliferation

Collagen Type I is one of the main structural proteins of the ECM, responsible for the mechanical properties of fibrous connective tissues [91]. Collagen fibrillogenesis is a complex, multistep process which involves linear and accelerated growth followed by lateral growth and subsequent collagen fiber fusion [91]. It also requires the biosynthesis of pro-collagen, cross-linking of pro-collagen molecules, and excretion and fusion of collagen [148].

Periostin is predominately expressed in collagen-rich fibrous connective tissues that are subjected to high levels of mechanical loading, including blood vessels, heart valves, tendons, perichondrium, cornea, and periodontal ligaments (PDL) [91, 149]. It has been demonstrated that periostin is co-localized and directly binds collagen Type I in a specific protein-protein interaction [91]. In periostin knock-out mice, there is a reduction in collagen fibril diameters in skin dermis resulting in a decrease in overall stiffness, lower tensile strength, and decreased thickness of the collagenous dermal layer of the skin, which indicates aberrant collagen I fibrillogenesis [91]. By altering the collagen diameter, the structural and functional integrity of the connective tissue is compromised.

In addition, a lower collagen denaturing temperature in these mice reflects a reduced level of collagen cross-linking associated with improper collagen fibril formation [91]. The proper biomechanical function of connective tissues is dependent on collagen Type I and periostin interaction. Therefore, periostin can regulate collagen Type I fibrillogenesis and serve as an important mediator of the biomechanical properties of fibrous connective tissues [91].

Although periostin deletion does not seem to prevent the development of tumorigenesis as evidenced by the ability of NeuNDL Postn$^{+/-}$ and Postn$^{-/-}$ mice in a FVB background to form mammary tumors, there are obvious histological differences between these tumors. Cysts by

definition are pathologically dilated sacs lined by epithelium and containing fluid [150]. Cyst formation is one of the most common changes seen in breast tissue and is frequently present in combination with other benign lesions [150]. They are usually lined by a double cell layer, consisting of an inner epithelial layer and an outer myoepithelial layer, and the luminal epithelium frequently shows apocrine metaplasia [150]. However, cysts in malignant tumors are different from cysts in benign lesions. The lobule, together with its terminal duct, has been called the terminal duct lobular unit [150]. Most pathologic lesions arise from this area [150].

The tumors from the FVB NeuNDL Postn$^{+/-}$ and Postn$^{-/-}$ mice were considered intracystic/encapsulated papillary carcinomas or papillary intraduct carcinomas. These papillary carcinoma *in situ* show marked cystic expansion of the ductal lumen, which contains both solid and papillary components. Such lesions were present as a mass, as it should be.

In addition, the cysts in FVB NeuNDL Postn$^{+/-}$ and Postn$^{-/-}$ tumors were significantly more dilated along with more bleeding, representing shrinkage of tumor mass, when compared to the dense appearance of FVB NeuNDL Postn$^{+/+}$ tumors. This observation is correlated with a decrease in the tumor cellularity, Ki-67 positivity, and cyclin D1 expression within the tumors of FVB NeuNDL Postn$^{+/-}$ and Postn$^{-/-}$ mice compared to tumors of FVB NeuNDL Postn$^{+/+}$ mice. This suggests that periostin ablation decreases tumor cell proliferation *in vivo*.

Periostin has been shown to be down-regulated in periodontal ligaments of homozygous mice that underexpress fibrillin-1, which is essential for the formation of elastic fibers found in connective tissue [148, 151]. The capillaries in these mice were dilated and enlarged. They also displayed disorganized collagen fiber bundles with a thinner appearance compared with the well-organized collagen fiber bundles of wildtype mice [148]. Taken together, a decrease in or absence of periostin expression in FVB NeuNDL Postn$^{+/-}$ and Postn$^{-/-}$ mice, respectively, resulting in dilated and enlarged capillaries in the tumor, could also decrease the amount of collagen Type I and fibrillin-1 anchored to the basement membrane. This may disrupt blood vessel integrity within the mammary tumor and result in a dilated and cystic phenotype. It is

likely that reduced periostin expression may also contribute to the pathogenesis of the disorganized collagen fiber architecture, which affects the maintenance of the diameter and function of the blood vessel during tumorigenesis.

4.4 ErbB2/Neu Expression is Retained in Periostin-Deficient Mice

An alternate explanation for the increased tumor latencies observed in NeuNDL Postn$^{+/-}$ mice in a mixed FVB/C57 background is that these mice produce lower levels of *NDL* transgene compared to the NeuNDL Postn$^{+/-}$ mice in a pure FVB background. Strain-specific differences in regulation of promoter activity by methylation has been suggested [143]. If the MMTV promoter was less efficient at inducing gene expression in C57Bl/6 mice, then NeuNDL Postn$^{+/-}$ mice in a mixed FVB/C57 background should express lower levels of the Neu protein in their mammary glands and could be at lower risk for developing mammary tumors.

In support of this hypothesis, it has been reported that ras expression in MMTV-*ras* transgenic mice correlates with MMTV promoter methylation status, and that the long tumor latencies observed in these mice are associated with an age-dependant demethylation of this promoter [152]. Additional studies have demonstrated that mice have strain-specific modifiers of methylation and that C57Bl/6 mice are more efficient at methylating transgenic DNA than are SJL or DBA/2 strains of mice [142].

Unfortunately, without the appropriate quantification experiments we cannot say for certain that the MMTV promoter activity is decreased in NeuNDL Postn$^{+/-}$ mice in a mixed FVB/C57 background relative to the pure FVB background.

The present study demonstrates that ErbB2/Neu expression appears to be higher within the epithelial tumors than within the epithelial cells of the mammary glands by Western blot and immunohistochemical analyses. However, the level of the ErbB2/Neu protein is the same in FVB NeuNDL Postn$^{+/+}$, Postn$^{+/-}$, and Postn$^{-/-}$ tumors, as evidenced by ErbB2/Neu Western blot

analysis. This suggests that modulation of MMTV promoter activity is not affected by periostin ablation and that ErbB2/Neu expression is maintained in FVB periostin-deficient mice.

4.5 Periostin Does Not Increase Cell Proliferation or Migration *In Vitro*

Cell proliferation is strictly regulated by the concerted actions of both mitogenic growth signals and anti-proliferative signals that converge on regulators of the cell cycle [41]. Three engineered stable tumor cell lines that overexpress periostin, the human embryonic kidney cell 293T, the highly invasive mouse melanoma cell B16F1, and the metastatic human breast cancer cell MDA-MB-231, had noticeably slower proliferation rates than that of the control cells in culture [95]. However, these periostin-overexpressing tumor cell lines showed a phenotype of accelerated growth and angiogenesis when transplanted as xenografts into immunocompromised SCID-Beige mice [95].

ErbB2/Neu-overexpressing primary mammary tumor epithelial cell cultures from tumor-bearing FVB NeuNDL mice were generated. Our results show that primary mammary tumor epithelial cells do not express periostin and that overexpressing periostin through periostin adenovirus infection did not show increased cell proliferation when compared to controls. Taken together, this suggests that periostin does not promote proliferation of tumor cells *in vitro*. But, the role of periostin on cell proliferation has been known to be microenvironment dependent. Therefore, it is possible that when transplanted as xenografts in mice, a phenotype of accelerated growth may be observed *in vivo*. Since the activities of periostin, a mesenchyme-specific gene product, may not be exclusively associated with the promotion of cell proliferation, evaluation of the potential contribution of periostin to the progression of tumorigenesis must also be based on an assessment of its ability to promote tumorigenesis *in vivo*.

In pancreatic cancer cells, the $\alpha_6\beta_4$ integrin complex acts as the cell receptor for periostin, and this interaction promotes migration through FAK phosphorylation [102]. In addition, the induced expression of periostin in pancreatic cancer cells (to levels of 150 ng/ml)

inhibits EMT by changing them from mesenchymal to epithelial cells; this reduces cell migration *in vitro* as well as leads to the formation of smaller tumors and the suppression of metastasis *in vivo* [153]. On the other hand, a high concentration of recombinant periostin (1 μg/ml) promotes cell migration through AKT activation [153]. These findings suggest that periostin can have a biphasic effect on the migration of human pancreatic cancer cells [153].

Moreover, stable expression of periostin in tumorigenic, but non-metastatic, 293T cells induces those cells to undergo EMT and promotes cell migration, invasion, and adhesion [115]. In contrast, the migration assay with primary ErbB2/Neu-overexpressing mammary tumor epithelial cells demonstrated that cell migration did not differ between cells plated on periostin-coated cell culture plates and those plated on BSA-coated or plastic cell culture plates. Since periostin has a concentration-dependent effect on cell migration, it may not be surprising that we see no or very little effect of periostin in our *in vitro* migration assay. Different cell lines may also affect the periostin response to cell migration.

Another possibility is that periostin needs to act in the context with additional ECM proteins or growth factors and that periostin alone is not enough to increase cell proliferation or migration of ErbB2/Neu-overexpressing mammary tumor epithelial cells *in vitro*. The monolayer environment *in vitro* is very different than the 3-dimensional cell environment *in vivo*. As a result, these tumor epithelial cells may behave differently to the same treatment depending on the environment of the cells.

A better understanding of the molecular mechanisms involved in breast cancer progression in general is undoubtedly a major challenge in the development of new diagnostic and therapeutic approaches, underlying the necessity to identify new molecular targets. During the past decade, global gene expression profiling studies on various human cancer types, mainly relying on cDNA microarray technology, led to the identification of new candidate genes involved in cancer progression. In this study, we show that periostin is not required for mammary gland development. However, breast tumorigenesis seems to be affected. But, we

have yet to test its role on breast cancer metastasis. Studies are underway to determine the role of periostin in HER2/ErbB2-induced breast cancer invasion and spreading.

4.6 Conclusion

Our results show that periostin, a cell adhesion molecule, is expressed in the stroma and not the epithelial cells of the mammary gland. We observed that targeted ablation of periostin in the mouse mammary gland has no effect on mammary gland outgrowth during development or pregnancy nor on initiation of mammary tumorigenesis in FVB NeuNDL $Postn^{+/-}$ and $Postn^{-/-}$ mice. However, we observed an increase in tumor latency for NeuNDL $Postn^{+/-}$ mice in a mixed FVB/C57 background. Although, NeuNDL $Postn^{+/+}$, $Postn^{+/-}$, and $Postn^{-/-}$ mice in a FVB background all developed mammary gland tumors, there was a marked difference in histology, in which FVB NeuNDL $Postn^{+/-}$ and $Postn^{-/-}$ tumors were more cystic and had decreased cellularity of hyperplastic lesions and tumors *in vivo*. In addition, the proliferation index *in vivo* was decreased in the tumors of FVB NeuNDL $Postn^{+/-}$ and $Postn^{-/-}$ mice. In contrast, the presence of periostin did not increase cell proliferation or migration of ErbB2/Neu-overexpressing mammary tumor epithelial cells *in vitro*.

4.7 Future Experiments

In continuation of this research project, it will be of interest to determine if periostin has a more significant role during cancer progression *in vitro* and *in vivo*. Since periostin overexpression did not affect cell proliferation or migration of mammary tumor epithelial cells *in vitro*, we are interested in testing the effect of periostin in the presence of an additional matrix or growth factor like collagen I, HRGβ, or EGF. In addition, the effect of periostin on metastasis has yet to be addressed. Therefore, the injection of FVB tumor cells into the fat pad and tail vein of $Postn^{+/+}$, $Postn^{+/-}$, and $Postn^{-/-}$ mice in a FVB background will also be of great interest. Finally, the characterization of potential cell proliferation defects in FVB NeuNDL $Postn^{+/-}$ and $Postn^{-/-}$

tumors by gene array or biochemical approaches might reveal insights into the role of periostin in breast cancer progression.

References

1. Badache, A. and A. Goncalves, *The ErbB2 signaling network as a target for breast cancer therapy.* J Mammary Gland Biol Neoplasia, 2006. **11**(1): p. 13-25.
2. Sorlie, T., et al., *Gene expression patterns of breast carcinomas distinguish tumor subclasses with clinical implications.* Proc Natl Acad Sci U S A, 2001. **98**(19): p. 10869-74.
3. Rouzier, R., et al., *Breast cancer molecular subtypes respond differently to preoperative chemotherapy.* Clin Cancer Res, 2005. **11**(16): p. 5678-85.
4. Dinh, P., C. Sotiriou, and M.J. Piccart, *The evolution of treatment strategies: aiming at the target.* Breast, 2007. **16 Suppl 2**: p. S10-6.
5. Breastcancer.org, *Stages of Breast Cancer*. 2010.
6. Maughan, K.L., M.A. Lutterbie, and P.S. Ham, *Treatment of breast cancer.* Am Fam Physician. **81**(11): p. 1339-46.
7. Institute, N.C., *Tumor Grade: Questions and Answers*. 2004.
8. Institute, N.C., *Adjuvant and Neoadjuvant Therapy for Breast Cancer*. 2009.
9. Alvarez, R.H., V. Valero, and G.N. Hortobagyi, *Emerging targeted therapies for breast cancer.* J Clin Oncol. **28**(20): p. 3366-79.
10. Liang, X., et al., *Quantification of membrane and membrane-bound proteins in normal and malignant breast cancer cells isolated from the same patient with primary breast carcinoma.* J Proteome Res, 2006. **5**(10): p. 2632-41.
11. Eccles, S.A., *The role of c-erbB-2/HER2/neu in breast cancer progression and metastasis.* J Mammary Gland Biol Neoplasia, 2001. **6**(4): p. 393-406.
12. Andrechek, E.R., et al., *Amplification of the neu/erbB-2 oncogene in a mouse model of mammary tumorigenesis.* Proc Natl Acad Sci U S A, 2000. **97**(7): p. 3444-9.
13. Paterson, M.C., et al., *Correlation between c-erbB-2 amplification and risk of recurrent disease in node-negative breast cancer.* Cancer Res, 1991. **51**(2): p. 556-67.
14. Goldhirsch, A., et al., *Meeting highlights: international expert consensus on the primary therapy of early breast cancer 2005.* Ann Oncol, 2005. **16**(10): p. 1569-83.
15. Arteaga, C.L., *ErbB-targeted therapeutic approaches in human cancer.* Exp Cell Res, 2003. **284**(1): p. 122-30.
16. Holbro, T., G. Civenni, and N.E. Hynes, *The ErbB receptors and their role in cancer progression.* Exp Cell Res, 2003. **284**(1): p. 99-110.
17. Olayioye, M.A., *Update on HER-2 as a target for cancer therapy: intracellular signaling pathways of ErbB2/HER-2 and family members.* Breast Cancer Res, 2001. **3**(6): p. 385-9.
18. Stern, D.F., *ErbBs in mammary development.* Exp Cell Res, 2003. **284**(1): p. 89-98.
19. Lax, I., et al., *Localization of a major receptor-binding domain for epidermal growth factor by affinity labeling.* Mol Cell Biol, 1988. **8**(4): p. 1831-4.
20. Tai, W., R. Mahato, and K. Cheng, *The role of HER2 in cancer therapy and targeted drug delivery.* J Control Release. **146**(3): p. 264-75.
21. Pietras, R.J., et al., *HER-2 tyrosine kinase pathway targets estrogen receptor and promotes hormone-independent growth in human breast cancer cells.* Oncogene, 1995. **10**(12): p. 2435-46.
22. Schlessinger, J., *Cell signaling by receptor tyrosine kinases.* Cell, 2000. **103**(2): p. 211-25.
23. Tzahar, E., et al., *A hierarchical network of interreceptor interactions determines signal transduction by Neu differentiation factor/neuregulin and epidermal growth factor.* Mol Cell Biol, 1996. **16**(10): p. 5276-87.
24. Olayioye, M.A., et al., *The ErbB signaling network: receptor heterodimerization in development and cancer.* Embo J, 2000. **19**(13): p. 3159-67.
25. Riese, D.J., 2nd and D.F. Stern, *Specificity within the EGF family/ErbB receptor family signaling network.* Bioessays, 1998. **20**(1): p. 41-8.

26. Peles, E. and Y. Yarden, *Neu and its ligands: from an oncogene to neural factors.* Bioessays, 1993. **15**(12): p. 815-24.
27. Yarden, Y. and M.X. Sliwkowski, *Untangling the ErbB signalling network.* Nat Rev Mol Cell Biol, 2001. **2**(2): p. 127-37.
28. Guy, P.M., et al., *Insect cell-expressed p180erbB3 possesses an impaired tyrosine kinase activity.* Proc Natl Acad Sci U S A, 1994. **91**(17): p. 8132-6.
29. Graus-Porta, D., et al., *ErbB-2, the preferred heterodimerization partner of all ErbB receptors, is a mediator of lateral signaling.* Embo J, 1997. **16**(7): p. 1647-55.
30. Graus-Porta, D., R.R. Beerli, and N.E. Hynes, *Single-chain antibody-mediated intracellular retention of ErbB-2 impairs Neu differentiation factor and epidermal growth factor signaling.* Mol Cell Biol, 1995. **15**(3): p. 1182-91.
31. Beerli, R.R., et al., *Neu differentiation factor activation of ErbB-3 and ErbB-4 is cell specific and displays a differential requirement for ErbB-2.* Mol Cell Biol, 1995. **15**(12): p. 6496-505.
32. Hynes, N.E. and G. MacDonald, *ErbB receptors and signaling pathways in cancer.* Curr Opin Cell Biol, 2009. **21**(2): p. 177-84.
33. Di Fiore, P.P., et al., *EGF receptor and erbB-2 tyrosine kinase domains confer cell specificity for mitogenic signaling.* Science, 1990. **248**(4951): p. 79-83.
34. Prigent, S.A. and W.J. Gullick, *Identification of c-erbB-3 binding sites for phosphatidylinositol 3'-kinase and SHC using an EGF receptor/c-erbB-3 chimera.* Embo J, 1994. **13**(12): p. 2831-41.
35. Holbro, T., et al., *The ErbB2/ErbB3 heterodimer functions as an oncogenic unit: ErbB2 requires ErbB3 to drive breast tumor cell proliferation.* Proc Natl Acad Sci U S A, 2003. **100**(15): p. 8933-8.
36. Seluanov, A., et al., *Hypersensitivity to contact inhibition provides a clue to cancer resistance of naked mole-rat.* Proc Natl Acad Sci U S A, 2009. **106**(46): p. 19352-7.
37. Sasaki, H., et al., *Elevated serum periostin levels in patients with bone metastases from breast but not lung cancer.* Breast Cancer Res Treat, 2003. **77**(3): p. 245-52.
38. Slamon, D.J., et al., *Studies of the HER-2/neu proto-oncogene in human breast and ovarian cancer.* Science, 1989. **244**(4905): p. 707-12.
39. Sauter, G., et al., *Heterogeneity of erbB-2 gene amplification in bladder cancer.* Cancer Res, 1993. **53**(10 Suppl): p. 2199-203.
40. Lemoine, N.R., et al., *Amplification and overexpression of the EGF receptor and c-erbB-2 proto-oncogenes in human stomach cancer.* Br J Cancer, 1991. **64**(1): p. 79-83.
41. Hanahan, D. and R.A. Weinberg, *The hallmarks of cancer.* Cell, 2000. **100**(1): p. 57-70.
42. Goldman, C.K., et al., *Epidermal growth factor stimulates vascular endothelial growth factor production by human malignant glioma cells: a model of glioblastoma multiforme pathophysiology.* Mol Biol Cell, 1993. **4**(1): p. 121-33.
43. Yen, L., et al., *Heregulin selectively upregulates vascular endothelial growth factor secretion in cancer cells and stimulates angiogenesis.* Oncogene, 2000. **19**(31): p. 3460-9.
44. Xiong, S., et al., *Up-regulation of vascular endothelial growth factor in breast cancer cells by the heregulin-beta1-activated p38 signaling pathway enhances endothelial cell migration.* Cancer Res, 2001. **61**(4): p. 1727-32.
45. Yen, L., et al., *Differential regulation of tumor angiogenesis by distinct ErbB homo- and heterodimers.* Mol Biol Cell, 2002. **13**(11): p. 4029-44.
46. Izumi, Y., et al., *Tumour biology: herceptin acts as an anti-angiogenic cocktail.* Nature, 2002. **416**(6878): p. 279-80.
47. Spencer, K.S., et al., *ErbB2 is necessary for induction of carcinoma cell invasion by ErbB family receptor tyrosine kinases.* J Cell Biol, 2000. **148**(2): p. 385-97.
48. Khoury, H., et al., *HGF converts ErbB2/Neu epithelial morphogenesis to cell invasion.* Mol Biol Cell, 2005. **16**(2): p. 550-61.

49. Muraoka, R.S., et al., *Increased malignancy of Neu-induced mammary tumors overexpressing active transforming growth factor beta1.* Mol Cell Biol, 2003. **23**(23): p. 8691-703.
50. Siegel, P.M., et al., *Transforming growth factor beta signaling impairs Neu-induced mammary tumorigenesis while promoting pulmonary metastasis.* Proc Natl Acad Sci U S A, 2003. **100**(14): p. 8430-5.
51. Xu, F.J., et al., *Heregulin and agonistic anti-p185(c-erbB2) antibodies inhibit proliferation but increase invasiveness of breast cancer cells that overexpress p185(c-erbB2): increased invasiveness may contribute to poor prognosis.* Clin Cancer Res, 1997. **3**(9): p. 1629-34.
52. Mazumdar, A., et al., *Heregulin regulation of urokinase plasminogen activator and its receptor: human breast epithelial cell invasion.* Cancer Res, 2001. **61**(1): p. 400-5.
53. Voldborg, B.R., et al., *Epidermal growth factor receptor (EGFR) and EGFR mutations, function and possible role in clinical trials.* Ann Oncol, 1997. **8**(12): p. 1197-206.
54. Hsieh, E.T., F.A. Shepherd, and M.S. Tsao, *Co-expression of epidermal growth factor receptor and transforming growth factor-alpha is independent of ras mutations in lung adenocarcinoma.* Lung Cancer, 2000. **29**(2): p. 151-7.
55. Seth, D., et al., *Complex post-transcriptional regulation of EGF-receptor expression by EGF and TGF-alpha in human prostate cancer cells.* Br J Cancer, 1999. **80**(5-6): p. 657-69.
56. Cai, Y.C., et al., *Expression of transforming growth factor-alpha and epidermal growth factor receptor in gastrointestinal stromal tumours.* Virchows Arch, 1999. **435**(2): p. 112-5.
57. Umekita, Y., et al., *Co-expression of epidermal growth factor receptor and transforming growth factor-alpha predicts worse prognosis in breast-cancer patients.* Int J Cancer, 2000. **89**(6): p. 484-7.
58. Ursini-Siegel, J., et al., *Insights from transgenic mouse models of ERBB2-induced breast cancer.* Nat Rev Cancer, 2007. **7**(5): p. 389-97.
59. Brinster, R.L., et al., *Transgenic mice harboring SV40 T-antigen genes develop characteristic brain tumors.* Cell, 1984. **37**(2): p. 367-79.
60. Stewart, T.A., P.K. Pattengale, and P. Leder, *Spontaneous mammary adenocarcinomas in transgenic mice that carry and express MTV/myc fusion genes.* Cell, 1984. **38**(3): p. 627-37.
61. Adams, J.M., et al., *The c-myc oncogene driven by immunoglobulin enhancers induces lymphoid malignancy in transgenic mice.* Nature, 1985. **318**(6046): p. 533-8.
62. Hanahan, D., *Heritable formation of pancreatic beta-cell tumours in transgenic mice expressing recombinant insulin/simian virus 40 oncogenes.* Nature, 1985. **315**(6015): p. 115-22.
63. Sinn, E., et al., *Coexpression of MMTV/v-Ha-ras and MMTV/c-myc genes in transgenic mice: synergistic action of oncogenes in vivo.* Cell, 1987. **49**(4): p. 465-75.
64. Cardiff, R.D. and W.J. Muller, *Transgenic mouse models of mammary tumorigenesis.* Cancer Surv, 1993. **16**: p. 97-113.
65. Shih, C., et al., *Transforming genes of carcinomas and neuroblastomas introduced into mouse fibroblasts.* Nature, 1981. **290**(5803): p. 261-4.
66. Padhy, L.C., et al., *Identification of a phosphoprotein specifically induced by the transforming DNA of rat neuroblastomas.* Cell, 1982. **28**(4): p. 865-71.
67. Di Fiore, P.P., et al., *erbB-2 is a potent oncogene when overexpressed in NIH/3T3 cells.* Science, 1987. **237**(4811): p. 178-82.
68. Hudziak, R.M., J. Schlessinger, and A. Ullrich, *Increased expression of the putative growth factor receptor p185HER2 causes transformation and tumorigenesis of NIH 3T3 cells.* Proc Natl Acad Sci U S A, 1987. **84**(20): p. 7159-63.
69. Di Marco, E., et al., *Transformation of NIH 3T3 cells by overexpression of the normal coding sequence of the rat neu gene.* Mol Cell Biol, 1990. **10**(6): p. 3247-52.

70. Bargmann, C.I. and R.A. Weinberg, *Oncogenic activation of the neu-encoded receptor protein by point mutation and deletion.* Embo J, 1988. **7**(7): p. 2043-52.
71. Bargmann, C.I., M.C. Hung, and R.A. Weinberg, *The neu oncogene encodes an epidermal growth factor receptor-related protein.* Nature, 1986. **319**(6050): p. 226-30.
72. Bargmann, C.I., M.C. Hung, and R.A. Weinberg, *Multiple independent activations of the neu oncogene by a point mutation altering the transmembrane domain of p185.* Cell, 1986. **45**(5): p. 649-57.
73. Bargmann, C.I. and R.A. Weinberg, *Increased tyrosine kinase activity associated with the protein encoded by the activated neu oncogene.* Proc Natl Acad Sci U S A, 1988. **85**(15): p. 5394-8.
74. Stern, D.F., M.P. Kamps, and H. Cao, *Oncogenic activation of p185neu stimulates tyrosine phosphorylation in vivo.* Mol Cell Biol, 1988. **8**(9): p. 3969-73.
75. Weiner, D.B., et al., *Linkage of tyrosine kinase activity with transforming ability of the p185neu oncoprotein.* Oncogene, 1989. **4**(10): p. 1175-83.
76. Weiner, D.B., et al., *A point mutation in the neu oncogene mimics ligand induction of receptor aggregation.* Nature, 1989. **339**(6221): p. 230-1.
77. Bouchard, L., et al., *Stochastic appearance of mammary tumors in transgenic mice carrying the MMTV/c-neu oncogene.* Cell, 1989. **57**(6): p. 931-6.
78. Guy, C.T., et al., *Expression of the neu protooncogene in the mammary epithelium of transgenic mice induces metastatic disease.* Proc Natl Acad Sci U S A, 1992. **89**(22): p. 10578-82.
79. Guy, C.T., R.D. Cardiff, and W.J. Muller, *Activated neu induces rapid tumor progression.* J Biol Chem, 1996. **271**(13): p. 7673-8.
80. Muller, W.J., et al., *Single-step induction of mammary adenocarcinoma in transgenic mice bearing the activated c-neu oncogene.* Cell, 1988. **54**(1): p. 105-15.
81. Lucchini, F., et al., *Early and multifocal tumors in breast, salivary, harderian and epididymal tissues developed in MMTY-Neu transgenic mice.* Cancer Lett, 1992. **64**(3): p. 203-9.
82. Suda, Y., et al., *Induction of a variety of tumors by c-erbB2 and clonal nature of lymphomas even with the mutated gene (Val659----Glu659).* Embo J, 1990. **9**(1): p. 181-90.
83. Lemoine, N.R., et al., *Absence of activating transmembrane mutations in the c-erbB-2 proto-oncogene in human breast cancer.* Oncogene, 1990. **5**(2): p. 237-9.
84. Siegel, P.M., et al., *Novel activating mutations in the neu proto-oncogene involved in induction of mammary tumors.* Mol Cell Biol, 1994. **14**(11): p. 7068-77.
85. Siegel, P.M. and W.J. Muller, *Mutations affecting conserved cysteine residues within the extracellular domain of Neu promote receptor dimerization and activation.* Proc Natl Acad Sci U S A, 1996. **93**(17): p. 8878-83.
86. Siegel, P.M., et al., *Elevated expression of activated forms of Neu/ErbB-2 and ErbB-3 are involved in the induction of mammary tumors in transgenic mice: implications for human breast cancer.* Embo J, 1999. **18**(8): p. 2149-64.
87. Kwong, K.Y. and M.C. Hung, *A novel splice variant of HER2 with increased transformation activity.* Mol Carcinog, 1998. **23**(2): p. 62-8.
88. Naidu, R., et al., *Expression of c-erbB3 protein in primary breast carcinomas.* Br J Cancer, 1998. **78**(10): p. 1385-90.
89. Takeshita, S., et al., *Osteoblast-specific factor 2: cloning of a putative bone adhesion protein with homology with the insect protein fasciclin I.* Biochem J, 1993. **294 (Pt 1)**: p. 271-8.
90. Horiuchi, K., et al., *Identification and characterization of a novel protein, periostin, with restricted expression to periosteum and periodontal ligament and increased expression by transforming growth factor beta.* J Bone Miner Res, 1999. **14**(7): p. 1239-49.
91. Norris, R.A., et al., *Periostin regulates collagen fibrillogenesis and the biomechanical properties of connective tissues.* J Cell Biochem, 2007. **101**(3): p. 695-711.

92. Litvin, J., et al., *Expression and function of periostin-isoforms in bone.* J Cell Biochem, 2004. **92**(5): p. 1044-61.
93. Litvin, J., et al., *Periostin family of proteins: therapeutic targets for heart disease.* Anat Rec A Discov Mol Cell Evol Biol, 2005. **287**(2): p. 1205-12.
94. Tilman, G., et al., *Human periostin gene expression in normal tissues, tumors and melanoma: evidences for periostin production by both stromal and melanoma cells.* Mol Cancer, 2007. **6**: p. 80.
95. Shao, R., et al., *Acquired expression of periostin by human breast cancers promotes tumor angiogenesis through up-regulation of vascular endothelial growth factor receptor 2 expression.* Mol Cell Biol, 2004. **24**(9): p. 3992-4003.
96. Bao, S., et al., *Periostin potently promotes metastatic growth of colon cancer by augmenting cell survival via the Akt/PKB pathway.* Cancer Cell, 2004. **5**(4): p. 329-39.
97. Kudo, Y., et al., *Periostin promotes invasion and anchorage-independent growth in the metastatic process of head and neck cancer.* Cancer Res, 2006. **66**(14): p. 6928-35.
98. Chang, Y., et al., *Differential expression of osteoblast-specific factor 2 and polymeric immunoglobulin receptor genes in nasopharyngeal carcinoma.* Head Neck, 2005. **27**(10): p. 873-82.
99. Sasaki, H., et al., *Expression of the periostin mRNA level in neuroblastoma.* J Pediatr Surg, 2002. **37**(9): p. 1293-7.
100. Sasaki, H., et al., *Expression of Periostin, homologous with an insect cell adhesion molecule, as a prognostic marker in non-small cell lung cancers.* Jpn J Cancer Res, 2001. **92**(8): p. 869-73.
101. Gillan, L., et al., *Periostin secreted by epithelial ovarian carcinoma is a ligand for alpha(V)beta(3) and alpha(V)beta(5) integrins and promotes cell motility.* Cancer Res, 2002. **62**(18): p. 5358-64.
102. Baril, P., et al., *Periostin promotes invasiveness and resistance of pancreatic cancer cells to hypoxia-induced cell death: role of the beta4 integrin and the PI3k pathway.* Oncogene, 2007. **26**(14): p. 2082-94.
103. Fluge, O., et al., *Gene expression in poorly differentiated papillary thyroid carcinomas.* Thyroid, 2006. **16**(2): p. 161-75.
104. Hamilton, D.W., *Functional role of periostin in development and wound repair: implications for connective tissue disease.* J Cell Commun Signal, 2008. **2**(1-2): p. 9-17.
105. Kudo, Y., et al., *Periostin: novel diagnostic and therapeutic target for cancer.* Histol Histopathol, 2007. **22**(10): p. 1167-74.
106. Kuhn, B., et al., *Periostin induces proliferation of differentiated cardiomyocytes and promotes cardiac repair.* Nat Med, 2007. **13**(8): p. 962-9.
107. Zhou, H.M., et al., *Spatiotemporal expression of periostin during skin development and incisional wound healing: lessons for human fibrotic scar formation.* J Cell Commun Signal. **4**(2): p. 99-107.
108. Stanton, L.W., et al., *Altered patterns of gene expression in response to myocardial infarction.* Circ Res, 2000. **86**(9): p. 939-45.
109. Wang, D., et al., *Effects of pressure overload on extracellular matrix expression in the heart of the atrial natriuretic peptide-null mouse.* Hypertension, 2003. **42**(1): p. 88-95.
110. Lindner, V., et al., *Vascular injury induces expression of periostin: implications for vascular cell differentiation and migration.* Arterioscler Thromb Vasc Biol, 2005. **25**(1): p. 77-83.
111. Goetsch, S.C., et al., *Transcriptional profiling and regulation of the extracellular matrix during muscle regeneration.* Physiol Genomics, 2003. **14**(3): p. 261-71.
112. Nakazawa, T., et al., *Gene expression of periostin in the early stage of fracture healing detected by cDNA microarray analysis.* J Orthop Res, 2004. **22**(3): p. 520-5.
113. Takayama, I., I. Kii, and A. Kudo, *Expression, purification and characterization of soluble recombinant periostin protein produced by Escherichia coli.* J Biochem, 2009. **146**(5): p. 713-23.

114. Rios, H., et al., *periostin null mice exhibit dwarfism, incisor enamel defects, and an early-onset periodontal disease-like phenotype.* Mol Cell Biol, 2005. **25**(24): p. 11131-44.
115. Yan, W. and R. Shao, *Transduction of a mesenchyme-specific gene periostin into 293T cells induces cell invasive activity through epithelial-mesenchymal transformation.* J Biol Chem, 2006. **281**(28): p. 19700-8.
116. Elliott, R.L. and G.C. Blobe, *Role of transforming growth factor Beta in human cancer.* J Clin Oncol, 2005. **23**(9): p. 2078-93.
117. Ruan, K., S. Bao, and G. Ouyang, *The multifaceted role of periostin in tumorigenesis.* Cell Mol Life Sci, 2009. **66**(14): p. 2219-30.
118. Folkman, J., et al., *Induction of angiogenesis during the transition from hyperplasia to neoplasia.* Nature, 1989. **339**(6219): p. 58-61.
119. Yancopoulos, G.D., et al., *Vascular-specific growth factors and blood vessel formation.* Nature, 2000. **407**(6801): p. 242-8.
120. Hynes, R.O., *Integrins: versatility, modulation, and signaling in cell adhesion.* Cell, 1992. **69**(1): p. 11-25.
121. Lafrenie, R.M. and K.M. Yamada, *Integrin-dependent signal transduction.* J Cell Biochem, 1996. **61**(4): p. 543-53.
122. Schwartz, M.A., M.D. Schaller, and M.H. Ginsberg, *Integrins: emerging paradigms of signal transduction.* Annu Rev Cell Dev Biol, 1995. **11**: p. 549-99.
123. Desgrosellier, J.S. and D.A. Cheresh, *Integrins in cancer: biological implications and therapeutic opportunities.* Nat Rev Cancer. **10**(1): p. 9-22.
124. Yu, X., S. Miyamoto, and E. Mekada, *Integrin alpha 2 beta 1-dependent EGF receptor activation at cell-cell contact sites.* J Cell Sci, 2000. **113 (Pt 12)**: p. 2139-47.
125. Wang, F., et al., *Phenotypic reversion or death of cancer cells by altering signaling pathways in three-dimensional contexts.* J Natl Cancer Inst, 2002. **94**(19): p. 1494-503.
126. White, D.E., et al., *Targeted disruption of beta1-integrin in a transgenic mouse model of human breast cancer reveals an essential role in mammary tumor induction.* Cancer Cell, 2004. **6**(2): p. 159-70.
127. Guo, W., et al., *Beta 4 integrin amplifies ErbB2 signaling to promote mammary tumorigenesis.* Cell, 2006. **126**(3): p. 489-502.
128. Ng, P. and F.L. Graham, *Construction of first-generation adenoviral vectors.* Methods Mol Med, 2002. **69**: p. 389-414.
129. Rose-Hellekant, T.A., K. Gilchrist, and E.P. Sandgren, *Strain background alters mammary gland lesion phenotype in transforming growth factor-alpha transgenic mice.* Am J Pathol, 2002. **161**(4): p. 1439-47.
130. Rowse, G.J., S.R. Ritland, and S.J. Gendler, *Genetic modulation of neu proto-oncogene-induced mammary tumorigenesis.* Cancer Res, 1998. **58**(12): p. 2675-9.
131. Galderisi, U., F.P. Jori, and A. Giordano, *Cell cycle regulation and neural differentiation.* Oncogene, 2003. **22**(33): p. 5208-19.
132. Pardee, A.B., *A restriction point for control of normal animal cell proliferation.* Proc Natl Acad Sci U S A, 1974. **71**(4): p. 1286-90.
133. Polyak, K. and R. Kalluri, *The Role of the Microenvironment in Mammary Gland Development and Cancer.* Cold Spring Harb Perspect Biol.
134. Muschler, J. and C.H. Streuli, *Cell-matrix interactions in mammary gland development and breast cancer.* Cold Spring Harb Perspect Biol. **2**(10): p. a003202.
135. Citri, A., K.B. Skaria, and Y. Yarden, *The deaf and the dumb: the biology of ErbB-2 and ErbB-3.* Exp Cell Res, 2003. **284**(1): p. 54-65.

136. Hynes, N.E. and C.J. Watson, *Mammary gland growth factors: roles in normal development and in cancer.* Cold Spring Harb Perspect Biol. **2**(8): p. a003186.
137. Balmain, A., *Cancer as a complex genetic trait: tumor susceptibility in humans and mouse models.* Cell, 2002. **108**(2): p. 145-52.
138. Davie, S.A., et al., *Effects of FVB/NJ and C57Bl/6J strain backgrounds on mammary tumor phenotype in inducible nitric oxide synthase deficient mice.* Transgenic Res, 2007. **16**(2): p. 193-201.
139. Narko, K., et al., *COX-2 inhibitors and genetic background reduce mammary tumorigenesis in cyclooxygenase-2 transgenic mice.* Prostaglandins Other Lipid Mediat, 2005. **76**(1-4): p. 86-94.
140. Cardiff, R.D., *Mouse models of human breast cancer.* Comp Med, 2003. **53**(3): p. 250-3.
141. Fargiano, A.A., K.V. Desai, and J.E. Green, *Interrogating mouse mammary cancer models: insights from gene expression profiling.* J Mammary Gland Biol Neoplasia, 2003. **8**(3): p. 321-34.
142. Engler, P., et al., *A strain-specific modifier on mouse chromosome 4 controls the methylation of independent transgene loci.* Cell, 1991. **65**(6): p. 939-47.
143. Schumacher, A., et al., *Epigenetic and genotype-specific effects on the stability of de novo imposed methylation patterns in transgenic mice.* J Biol Chem, 2000. **275**(48): p. 37915-21.
144. Nielsen, L.L., et al., *In wap-ras transgenic mice, tumor phenotype but not cyclophosphamide-sensitivity is affected by genetic background.* Anticancer Res, 1995. **15**(2): p. 385-92.
145. Lifsted, T., et al., *Identification of inbred mouse strains harboring genetic modifiers of mammary tumor age of onset and metastatic progression.* Int J Cancer, 1998. **77**(4): p. 640-4.
146. Thomas, H., et al., *An inbred colony of oncogene transgenic mice: diversity of tumours and potential as a therapeutic model.* Br J Cancer, 1996. **73**(1): p. 65-72.
147. Hundley, J.E., et al., *Differential regulation of cell cycle characteristics and apoptosis in MMTV-myc and MMTV-ras mouse mammary tumors.* Cancer Res, 1997. **57**(4): p. 600-3.
148. Ganburged, G., et al., *Dilated capillaries, disorganized collagen fibers and differential gene expression in periodontal ligaments of hypomorphic fibrillin-1 mice.* Cell Tissue Res. **341**(3): p. 381-95.
149. Kruzynska-Frejtag, A., et al., *Periostin (an osteoblast-specific factor) is expressed within the embryonic mouse heart during valve formation.* Mech Dev, 2001. **103**(1-2): p. 183-8.
150. Sternberg, S.S., ed. *Diagnostic Surgical Pathology*. 3 ed. Vol. 1. 1999.
151. Kielty, C.M., et al., *Fibrillin: from microfibril assembly to biomechanical function.* Philos Trans R Soc Lond B Biol Sci, 2002. **357**(1418): p. 207-17.
152. Mangues, R., et al., *Promoter demethylation in MMTV/N-rasN transgenic mice required for transgene expression and tumorigenesis.* Mol Carcinog, 1995. **14**(2): p. 94-102.
153. Kanno, A., et al., *Periostin, secreted from stromal cells, has biphasic effect on cell migration and correlates with the epithelial to mesenchymal transition of human pancreatic cancer cells.* Int J Cancer, 2008. **122**(12): p. 2707-18.